LBL-1687

c.1

RECOIL TRITIUM REACTIONS WITH CYCLOHEXENE AND METHYLCYCLOHEXENE

Darrell Clark Fee
(Ph. D. Thesis)

June 1973

Prepared for the U.S. Atomic Energy Commission
under Contract W-7405-ENG-48

For Reference

Not to be taken from this room

LAWRENCE BERKELEY LABORATORY
UNIVERSITY OF CALIFORNIA
BERKELEY

LBL-1687

c.1

DISCLAIMER

This document was prepared as an account of work sponsored by the United States Government. While this document is believed to contain correct information, neither the United States Government nor any agency thereof, nor the Regents of the University of California, nor any of their employees, makes any warranty, express or implied, or assumes any legal responsibility for the accuracy, completeness, or usefulness of any information, apparatus, product, or process disclosed, or represents that its use would not infringe privately owned rights. Reference herein to any specific commercial product, process, or service by its trade name, trademark, manufacturer, or otherwise, does not necessarily constitute or imply its endorsement, recommendation, or favoring by the United States Government or any agency thereof, or the Regents of the University of California. The views and opinions of authors expressed herein do not necessarily state or reflect those of the United States Government or any agency thereof or the Regents of the University of California.

RECOIL TRITIUM REACTIONS WITH CYCLOHEXENE AND METHYLCYCLOHEXENE

Darrell Clark Fee

Lawrence Berkeley Laboratory
University of California
Berkeley, California 94720

June 1973

ABSTRACT

A study has been made of the reactions of recoil tritium atoms with cyclohexene (at 25°C and 135°C) and with methylcyclohexene (at 135°C). Principle attention was given to unimolecular decomposition processes following T-for-H substitution. T was produced by recoil in the $^3He(n,p)T$ reaction. The neutron irradiations at 25°C were in a standard Lazy Susan facility. Irradiations at 135°C were in a specially designed neutron irradiation container in which all samples received the same neutron dose and the temperature was controlled to ±0.5°C. The tritiated products were analyzed with a specially designed radio-gas-chromatographic system. Peaks were monitored at a constant flow rate in the same detector (a beta proportional counter) and the injection volume was large. A system of four columns used in series gave adequate resolution of more than twenty products from the whole sample. This system was a combination of (1) stop-flow, (2) center-cut, (3) recycle, (4) stepwise temperature programming, and (5) stepwise pressure programming techniques.

The comparative efficiency of SO_2 and O_2 as radical scavengers was determined in the T + cyclohexene, T + trans-2-butene, and T + n-butane gas phase system at 25°C. O_2, the only scavenger previously

in use in T + alkene systems, caused an anomalous increase in the butadiene-t yield from T + cyclohexene reactions. All other tritiated products from cyclohexene and trans-2-butene reactions showed similar scavenging trends. The use of SO_2 as a scavenger may be advantageous in some alkene systems although SO_2 fails to remove all thermal contributions to the HT yield in the T + n-butane system.

The anomalous increase in the butadiene-t yield (from T + cyclohexene reactions at 25°C) with O_2 scavenging was clarified by determining the comparative efficiency of H_2S, butadiene-d_6, O_2, and SO_2 as radical scavengers in the T + cyclohexene system at 25°C. Direct tritium substitution of cyclohexene yields cyclohexene-t which may undergo unimolecular decomposition to produce butadiene-t. In unscavenged samples butadiene-t is selectively depleted by reactions with H atoms produced by radiolysis. Neither SO_2 nor H_2S is sufficiently reactive with H atoms to protect butadiene-t from such depletion. The "hot" butadiene-t yield can only be determined by means of O_2 or butadiene-d_6 scavenging. All products except butadiene-t exhibit normal behavior with O_2, SO_2 or H_2S scavenging.

The pressure dependence (in the 300 to 1500 torr pressure range) of the products of recoil tritium reactions with cyclohexene was determined at 135°C. Both at 135°C and at 25°C roughly 85% of the T + cyclohexene reactions which gave gas phase products resulted from tritium atom abstraction to form HT, addition to form cyclohexyl-t radicals, or T-for-H substitution to form cyclohexene-t. The dependence of product yield on pressure showed that ethylene-t and butadiene-t

resulted from the unimolecular decomposition of excited cyclohexene-t (formed by T-for-H substitution). The apparent rate constant of cyclohexene-t unimolecular decomposition was determined as 5.1×10^6 sec^{-1}. The s parameter in the RRK (for Rice, Ramsperger and Kassel) treatment of the unimolecular decomposition of cyclohexene was determined as $s = 24$. Similarly, the pressure dependence of product yield showed that n-hexene-t, 1-butene-t and methane-t resulted from the unimolecular decomposition of cyclohexyl-t radical (formed by T addition to cyclohexene) with rate constants of 8×10^3 sec^{-1}, 3×10^4 sec^{-1}, and 5×10^2 sec^{-1}, respectively. The relative rate of abstraction versus addition of radicals in alkenes was determined from the scavenger dependence of the yields of products with a radical precursor.

The reactions of recoil tritium atoms with methylcyclohexene were also studied at 135°C. Roughly 90% of the T + methylcyclohexene reactions which gave gas phase products resulted from tritium atom abstraction to form HT, addition to form methylcyclohexyl-t radicals, or T-for-H substitution to form methylcyclohexene-t. The dependence of product yield on pressure (300 to 1200 torr pressure range) showed that excited 4-methylcyclohexene-t (formed by T-for-H substitution) decomposed unimolecularly to give propylene-t or butadiene-t with a rate constant of 1×10^7 sec^{-1} and that similarly excited 3-methylcyclohexene-t decomposed unimolecularly to give ethylene-t or pentadiene-t with a rate constant of 3×10^6 sec^{-1}.

A test was made of the RRK-RRKM assumption (M reflects the contribution of Marcus) of energy randomization prior to unimolecular

decomposition. The rates of unimolecular decomposition of cyclohexene-1-t and cyclohexene-3-t (formed by T-for-methyl substitution reactions of recoil tritium atoms with 1-methylcyclohexene and 3-methylcyclohexene, respectively) were compared. The rates of unimolecular decomposition of cyclohexene-1-t and cyclohexene-3-t were similar. Using the previously determined RRK parameter (s = 24) for the unimolecular decomposition of cyclohexene, the average energy of excitation deposited in cyclohexene-t by T-for-methyl substitution reactions with methylcyclohexene was estimated at 6.5 eV for both cyclohexene-1-t and cyclohexene-3-t. For the same energy of excitation, the probability of unimolecular decomposition was independent of the site of energy input.

It was concluded that the RRK-RRKM assumption of energy randomization prior to unimolecular decomposition is valid for the recoil tritium initiated unimolecular decomposition of cyclohexene.

RECOIL TRITIUM REACTIONS WITH CYCLOHEXENE AND METHYLCYCLOHEXENE

Contents

INTRODUCTION 1

1. Recoil Tritium Reactions 3

1.1 General Considerations 3

1.2 Observed Reactions 5

1.2.1 Addition 6

1.2.2 Abstraction 7

1.2.3 Substitution 8

1.3 Estrup-Wolfgang Kinetic Theory 9

1.3.1 Basic Theory 9

1.3.2 Practical Applications 12

2. Unimolecular Reactions 14

2.1 Basic Theories 14

2.1.1 Lindemann-Hinshelwood Theory 14

2.1.2 RRK Theory 17

2.1.3 RRKM Theory 18

2.1.4 Slater Theory 19

2.2 Comparison of Theory and Experiment: Fall-Off Data 20

2.3 Assumptions of Basic RRK-RRKM Theory 21

2.3.1 Energy Randomization Prior to Decomposition 21

2.3.2 Strong Collisions 23

3. The Aims and Scope of this Work 26

3.1 Project Definition 26

3.2 Assumptions 27

3.3 Project Summary 34

EXPERIMENTAL TECHNIQUES 35

4. Sample Preparation 36

4.1 Gas Phase - Parent Hydrocarbon C_4 or Less 36

4.2 Gas Phase - Parent Hydrocarbon C_5 or Greater 40

4.2.1 Pressure of Parent Hydrocarbon Sealed in Capsule $\leqslant$ Vapor Pressure at 25°C 40

4.2.2 Pressure of Parent Hydrocarbon in Sealed Capsule at 135°C > Vapor Pressure at 25°C 42

4.3 Liquid Phase 45

5. Sample Irradiation 47

5.1 Irradiations at 24°C 47

5.2 Irradiations at 135°C 48

5.2.1 Background 48

5.2.2 Apparatus 50

5.2.3 Illustration of Irradiation Container Use and Capability 55

6. Sample Analysis 56

6.1 Background to Radio-Gas-Chromatographic Analysis 56

6.2 Apparatus and Procedures 63

6.2.1 Pressure Control and Valve Arrangement 63

6.2.2 Columns 66

6.2.3 Counting and Data Reduction 67

6.2.4 Sample Preparation for the Illustrated Analysis . . 72

6.2.5 Sample Injector 72

6.2.6 Recovery and Analysis of High Molecular Weight Tritiated Products; "Polymer-t" 75

6.3 Illustration of Radio-Gas-Chromatographic System Use and Capability 76

6.4 Summary of Radio-Gas-Chromatographic Analysis System . . . 78

RESULTS AND DISCUSSION 80

7. Sulfur Dioxide as a Radical Scavenger in Alkene Systems: Anomalous Oxygen Scavenging Effect Discovered 81

7.1 Background to Scavenger Studies 81

7.2 Data and Discussion 82

8. Scavenger Effects in the Recoil Tritium Reactions of Cyclohexene: Anomalous Oxygen Scavenging Effect Explained . . 92

8.1 Further Background to Scavenger Studies 92

8.2 Data and Discussion 100

9. Recoil Tritium Reactions with Cyclohexene and Alkenes: Determination of Rate Parameters 108

9.1 Determination of the s Parameter in the RRK Treatment of Cyclohexene Unimolecular Decomposition 108

9.2 Determination of the Apparent Rate Constants for the Unimolecular Decomposition/Isomerization of Cyclohexyl Radicals 114

9.3 Determination of the Relative Rate of Abstraction versus Addition of Radicals in Alkenes 123

9.4 Summary and Conclusions 131

10. Recoil Tritium Reactions with Methylcyclohexene: Including a Test of the RRK-RRKM Assumption of Energy Randomization Prior to Unimolecular Decomposition 132

10.1 General Considerations in the T + Methylcyclohexene System 132

10.2 A Test of the RRK-RRKM Assumption of Energy Randomization Prior to Unimolecular Decomposition 143

10.3 Summary and Conclusions 147

11. Summary and Conclusions 148

Acknowledgements 152

Appendix 154

References 170

LIST OF FIGURES

Fig. 4.1 Vacuum Line 37

Fig. 5.1 Irradiation Container 51

Fig. 6.1 Schematic Diagram of Gas Chromatographic Flow Stream . . . 65

Fig. 6.2 Typical Proportional Counter Plateau 68

Fig. 6.3 Radio-Gas-Chromatogram of Recoil Tritium Reaction Products 70

Fig. 6.4 Sample Capsule Breaker 73

Fig. 7.1 Curves of T + Cyclohexene System Scavenged with SO_2 or O_2 84

Fig. 7.2 Curves of T + Trans-butene System Scavenged with SO_2 or O_2 86

Fig. 7.3 Curves of T + n-Butane System Scavenged with SO_2 or O_2 and Moderated with 86 Mole % Ne 89

Fig. 7.4 Curves of T + n-Butane System Scavenged with SO_2 or O_2 . . 90

Fig. 8.1 The Effects of O_2, SO_2, H_2S, and C_4D_6 on the Ethylene-t and the Cyclohexane-t Yield from T + Cyclohexene Reactions 101

Fig. 8.2 The Effects of O_2, SO_2, H_2S, C_4D_6, and C_4D_6 plus O_2, C_4D_6 plus SO_2, C_4D_6 plus H_2S on the Butadiene-t Yield from T + Cyclohexene Reactions 105

Fig. 9.1 The Unimolecular Decomposition of Cyclohexene-t to give Ethylene-t or Butadiene-t; Unscavenged Data at 135°C . . . 109

Fig. 9.2 The Unimolecular Decomposition of Cyclohexene-t to give Ethylene-t or Butadiene-t; "Scavenged" Data at 135°C . . . 111

Fig. 9.3 Moderator Effect of the Cyclohexane-t Yield at 25°C 115

Fig. 9.4 The Unimolecular Decomposition of Cyclohexyl-t Radicals to n-Hexene-t; H_2S Scavenged Data at 135°C 120

Fig. 9.5 The Unimolecular Decomposition of Cyclohexyl-t Radicals to 1-Butene-t; H_2S Scavenged Data at 135°C 121

Fig. 9.6 Unimolecular Decomposition of Cyclohexyl-t Radicals to Methane-t; H_2S Scavenged Data at 135°C 122

Fig. 10.1 The Unimolecular Decomposition of 4-Methylcyclohexene-t to give Propylene-t or Butadiene-t; Unscavenged Data at 135°C 138

Fig. 10.2 The Unimolecular Decomposition of 3-Methylcyclohexene-t to give Ethylene-t or Pentadiene-t; Unscavenged Data at 135°C 139

Fig. 10.3 The Unimolecular Decomposition of 4-Methylcyclohexene to give Propylene-t or Butadiene-t; "Scavenged" Data at 135°C 140

Fig. 10.4 The Unimolecular Decomposition of 3-Methylcyclohexene to give Ethylene-t or Pentadiene-t; "Scavenged" Data at 135°C 141

LIST OF TABLES

Table 4-1 Measured Vapor Pressures 43

Table 6-1 Sequence of Radio-Gas-Chromatographic Operations 71

Table 8-1 Hydrogen Atom Reaction Rate Constants at 25°C 96

Table 8-2 Methyl Radical Reaction Rate Constants at 25°C 98

Table 9-1 Abstraction/Addition Rate Constant Ratio of Tritiated Radicals at 25°C 129

Table 10-1 Rate Parameters from the Unimolecular Decomposition of Methylcyclohexene-t 142

APPENDIX

Table A-6-1 Calibrated Retention Data Using the Sequence of Operations given in Table 6-1 155

Table A-7-1 T + Cyclohexene Reaction Data (25°C) 156

Table A-7-2 T + Trans-2-butene Reaction Data (25°C) 157

Table A-7-3 Neon Moderated T + n-Butane Reaction Data (25°C) . . . 158

Table A-7-4 T + n-Butane Reaction Data (25°C) 159

Table A-8-1 T + Cyclohexene Reaction Data (25°C) 160

Table A-8-2 T + Cyclohexene Dual Scavenged Reaction Data (25°C) 161

Table A-9-1 T + Cyclohexene Reaction Data (unscavenged, 135°C) . . 162

Table A-9-2 Neon Moderated T + Cyclohexene Reaction Data (25°C) 163

Table A-9-3 T + Cyclohexene Reaction Data (H_2S scavenged, 135°C) 164

Table A-9-4 Abstraction/Addition Ratio Data (25°C) 165

Table A-9-5 Abstraction/Addition Ratio Data (25°C) 166

Table A-10-1 T + 4-Methylcyclohexene Reaction Data (135°C) 167

Table A-10-2 T + 3-Methylcyclohexene Reaction Data (135°C) 168

Table A-10-3 T + 1-Methylcyclohexene Reaction Data (135°C) 169

INTRODUCTION

Translational Excitation in Bimolecular Reactions

A Maxwell-Boltzmann distribution of the thermal energies of reactive species is a barrier to the study of high energy bimolecular reactions. Of two competing reactions, the reaction with the lower energy threshold tends to predominate simply because of the larger number of molecules with sufficient energy for reaction. For many years, the role of translational energy in promoting virtually all reactions has been emphasized. This suggests that the energy barrier to the study of high energy bimolecular reactions may be circumvented. One (or both) of the reactants could be a translationally excited species whose energy is not given by a Maxwell-Boltzmann distribution. The selection of reactants depends upon: (1) which reactants are "interesting" to study, (2) the relative difficulty of formation of the translationally excited reactant(s), (3) the relative ease of analysis of the predicted products. The large number of hydrocarbons in the environment focuses attention on reactions with hydrocarbons. The translationally excited reactant then logically becomes a hydrogen atom. Four methods have been used to produce translationally excited hydrogen: (1) Beams of hydrogen ions (H^+ and H_2^+ or the isotopic equivalent) with energies in the 1 to 200 eV range have been reacted with solid[1] and gaseous[2] hydrocarbons. (2) A beam of thermal hydrogen atoms has been reacted with alkenes.[3] (3) Translationally excited hydrogen atoms have been produced via photolytic decomposition and resulting recoil[4,5] and have been allowed to react with

gaseous alkanes. (4) Translationally excited ("hot") hydrogen atoms have been produced via nuclear reactions and resulting recoil and have been allowed to react with hydrocarbons in all phases.[6,7] The study of hydrogen atoms (tritium atoms) produced by nuclear reaction is called recoil tritium chemistry.

I am interested in the reactions of recoil tritium atoms with cyclohexene and methylcyclohexene. In particular, I am interested in unimolecular decomposition reactions which are often observed as secondary processes following T-for-H substitution in recoil tritium-hydrocarbon systems. I intend to use activation (energization) by recoil tritium atoms to test the assumption that excitation energy is randomly distributed in a molecule before the molecule undergoes unimolecular decomposition. Consequently, this Introduction will be divided into three sections: (1) a summary of recoil tritium reactions, (2) a general discussion of unimolecular reactions, (3) a more detailed definition and discussion of the aims and scope of this work.

1. RECOIL TRITIUM REACTIONS

1.1 General Considerations

Recoil tritium reaction studies began in the late 1950's as an effort to produce high specific activity tritium labeled compounds (the half life of tritium is 12.3 years) of biological interest such as glucose and galactose.[8,9] The tritium was produced by nuclear reaction. Nuclear reactions $^{6}Li(n,\alpha)T$ and $^{3}He(n,p)T$ liberate large amounts of energy which is shared (with conservation of momentum) amongst the products of the reaction. The energy which each particle receives in this manner is called its recoil energy. The recoiling tritium has an energy of 2.7 and 0.19 MeV, respectively, from these nuclear reactions. This excess energy is a driving force for the labeling reaction.

Subsequent studies of the recoil tritium labeling process (reviewed in Refs. 6 and 7) have yielded the following general scheme. The tritium is initially produced as an ion. The recoil triton (tritium ion) velocity is much faster than the velocity of an electron in the first Bohr orbit. The triton is produced with a recoil energy which is virtually infinite on the chemical scale. Carbon-carbon and carbon-hydrogen bond energies are 3 to 4 eV (one eV is 23 Kcal $mole^{-1}$). Thermal tritium atom energies are about 0.02 eV. The triton must undergo a series of energy-losing collisions with its environment until it reaches an energy below 20 eV where reactions which produce a stable tritium labeled species are thought to occur.

This energy degradation of the tritón <u>and</u> proton or alpha particle produces bulk radiation damage (radiolysis) of the hydrocarbon

system.[10] In the typical recoil tritium experiment 10^{18} to 10^{20} hydrocarbon molecules are placed in a glass capsule along with the appropriate source of tritium atoms (^{6}Li or ^{3}He). Neutron bombardment of the capsule is used to produce 10^{10} to 10^{12} tritium atoms. This number of tritium atoms is necessary to analyze the sample for tritium labeled products through separation of the products by gas chromatography and monitoring of the radioactive tritium by proportional beta counting. Production of 10^{10} to 10^{12} tritium atoms usually results in radiolysis damage of less than 1%. This ensures that the tritium atom is reacting with the parent hydrocarbon; not a radiolysis produced hydrocarbon fragment.

Although I have referred and will refer hereafter to the reactions of recoil tritium atoms, the charge state of the tritium (when it reacts to give the stable tritium labeled species) is a matter of some controversy. With each collision during the period of energy degradation the ion (or atom) could undergo charge exchange to give a possible T^{+} or T^{0} species. Detailed experimental determinations of the triton-tritium atom population in the 0.5 to 50 eV range have not been made. Arguments based on the adiabatic principle have been used to suggest that recoil tritons probably are[11] and later on, probably are not[12] completely neutralized in an environment containing a great deal of helium.

The general reaction scheme developed this far is of a highly energetic recoil triton being degraded in energy and ultimately reacting as an energetic tritium atom. Some of the tritium atoms may survive

collisions in the 20 to 0.02 eV range and ultimately react as thermal tritium atoms. But because all the reacting tritium atoms entered the reactive energy region from the high energy end, a study of high energy tritium atom reactions is possible. The fundamental limitation of recoil tritium studies is that the energy distribution of the reacting tritium atoms is not known. The energy distribution can, however, be modified. Consider gas phase recoil tritium reactions. Addition of a highly reactive substance (a scavenger) such as O_2 to the ^3He/hydrocarbon mixture removes (scavenges) all thermal tritium atoms and tritiated radical intermediates. All tritiated product yields which survive in the presence of a scavenger are thought to result from high energy tritium reactions. Conversely, addition of an inert species (a moderator) such as a noble gas to the ^3He/hydrocarbon mixture increases the number of energy losing but unproductive collisions which the tritium atoms may undergo. This increases the number of tritium atoms which survive throughout the entire reactive energy range to ultimately react as thermal tritium atoms. All tritiated product yields which increase with increasing concentration of moderator gas are thought to result from thermal tritium atom reactions. Scavenger and moderator studies have been used to determine the general reaction paths discussed in the next section.

1.2 Observed Reactions

The reactions of recoil tritium atoms, as observed from the study of reactions with more than one hundred parent compounds, follow three general reaction pathways.[6,7,13] The reaction paths are arranged in order of increasing threshold energy.

addition $T + R\text{-}CH{=}CH\text{-}R' \longrightarrow R\text{-}\overset{T}{\underset{H}{C}}\text{-}\overset{\cdot}{\underset{H}{C}}\text{-}R'$ 1-1

abstraction $T + R\text{-}H \longrightarrow H\text{-}T + R'$ 1-2

substitution $T + R\text{-}X \longrightarrow R\text{-}T + X'$ 1-3

$X = H$, alkyl, halogen, $-NH_2$, $-COOH$

1.2.1 Addition

Addition is the reaction with the lowest energy threshold in recoil tritium-alkene systems. Thermal studies show addition to have an activation energy of 2 to 4 Kcal $mole^{-1}$ and to be 30 to 40 Kcal $mole^{-1}$ exothermic.[14] Thermal H atom reaction rate constants for addition are usually an order of magnitude greater than for abstraction.[15] The addition of a tritium atom to the double bond forms a tritiated radical. This tritiated radical can undergo further reaction to: (a) abstract a hydrogen atom from the hydrocarbon system to form a tritiated alkane (which does not react further). The alkane-t species is monitored by radio-gas-chromatography. (b) undergo radical addition to an unlabeled parent hydrocarbon molecule initiating a radical chain. Tritiated dimers have been monitored by radio-gas-chromatography.[16,17] Higher tritiated polymers have been monitored by other means.[18] (c) be removed from the system by a scavenger. The ultimate fate of the scavenged species is, of course, dependent on the scavenger used. (d) decompose unimolecularly.

The observed unimolecular decomposition of tritiated radicals is pressure dependent in the expected manner. At higher hydrocarbon pressures more radicals are stabilized by collisions prior to

decomposition.[16] A comparison of the unimolecular reaction rate of tritiated radicals formed from recoil tritium reactions with known reaction rate parameters from thermal kinetics studies indicates that the average tritium atom addition reaction occurs at 0.1 eV above thermal energies.[16] The observed unimolecular decomposition of tritiated radicals is also temperature dependent in the expected manner. The decomposition of the tritiated radicals increases at higher temperatures. This increase in decomposition is consistent with an increase in excitation energy corresponding to the increased internal energy of the radical at the higher temperature.[19] The important thing to note in that the temperature dependent process is a secondary decomposition. No temperature effect has been observed in the primary addition, abstraction or substitution reactions of recoil tritium atoms.[19] This is consistent with recoil tritium reactions occurring at high energies.

1.2.2 Abstraction

Abstraction is the reaction with the lowest threshold in recoil tritium-alkane systems. Abstraction is observed in thermal kinetic studies with an activation energy of 7 to 8 Kcal $mole^{-1}$.[20] Abstraction is 1 to 20 Kcal $mole^{-1}$ exothermic depending upon the C-H bond site from which the H atom is abstracted.[21] This bond energy effect is important in recoil tritium atom abstraction reactions. The HT yield per C-H bond increases with decreasing bond energy. This can be explained by an energy cut-off model in which the weaker C-H bonds permit abstraction at lower energies. With a larger energy range of reaction, more tritium atoms are available for reaction. The probability per collision of an

abstraction reaction in the energy range available for reaction also increases with a decrease in C-H bond energy.[22] A primary isotope effect has been observed in recoil tritium atom abstraction reactions. At the tertiary C-H bond in isobutane, HT formation is favored over DT formation by 1.6 to 1.0.[23]

1.2.3 Substitution

Substitution is the reaction with the highest energy threshold of the three recoil tritium reactions listed above. Substitution is not observed in thermal systems. Although the reaction is thermoneutral, a threshold energy of 1.5 eV (in the lab frame, 1.3 eV in the center of mass frame) has been measured using photolytically produced tritium atoms.[24] The average substitution reaction, however, occurs at much higher energy. Comparison of the unimolecular decomposition of cyclobutane-t (following T-for-H substitution) with kinetic parameters known from thermal studies indicates that the average T-for-H substitution reaction leaves 5 eV of excitation energy in the cyclobutane-t molecule.[25,26] A similar analysis shows that T-for-CH_3 substitution reactions in 1,3 dimethyl cyclobutane leave an average of 6 to 7 eV of excitation energy in the methyl cyclobutane-t molecule.[27]

The substitution of T-for-H occurs with: (a) 99% retention of configuration (no Walden inversion) at asymmetric sp^3 sites[28] and 70% retention of configuration at sp^2 sites.[29] The retention of configuration at sp^3 sites is especially interesting since several theoretical trajectory studies indicate that T-for-H substitution <u>with</u> Walden inversion (and loss of configuration) should be an important reaction channel.[30,31]

(b) an isotope effect of 1.25 to 1.00 favoring T-for-H over T-for-D substitution.[23] (c) decreasing yield in CH_3X as the electronegativity of the X substituent increased.[32,33] This indicates that successful replacement of an H atom by a recoil T atom is facilitated by the presence of higher electron density in the C-H bond under attack.

The substitution of T-for-X, where X is not H, occurs with: (a) increasing yield in CH_3X as the C-X bond energy decreases.[32] The substitution of T for an alkyl group may also increase as the relevant C-C bond energy decreases. The evidence is scanty.[34] Electronegativity effects may also be important in alkyl substitution reactions.[35] (b) 85 to 95 per cent of the T being bonded at the position within the molecule recently occupied by the X species. This was shown by chemical degradation to determine the intramolecular tritium content.[36]

1.3 Estrup-Wolfgang Kinetic Theory

1.3.1 Basic Theory

The Estrup-Wolfgang kinetic theory of hot atom reactions[6,7,37-39] assumes that a tritium atom of energy E can react with a molecule to produce product i with probability $p_i(E)$. If there is a variety of possible high energy products produced by tritium atoms at different average energies, then the formation of the product from the reaction with the highest average energy will reduce the number of tritium atoms available to form the lower average energy product. The yield of high energy products will be enhanced. The yield of both high and low energy products will be reduced by the addition of inert moderator. The

relative yield of the low energy product will increase because there are fewer high energy collisions between tritium atoms and the hydrocarbon.

The effect of addition of an inert moderator upon the total yield of all high energy reactions (P) may be described by

$$P = 1 - \exp(-fI/\alpha) \qquad 1\text{-}4$$

f = mole fraction of reactive component corrected for collision cross section (S_j)

$$f_j = S_j X_j / \sum S_j X_j$$

S_j = collision cross section between T atom and reactive component

X_j = mole fraction of component j

$$I = \int_{E_1}^{E_2} \frac{\sum p_i(E)\, dE}{E} = \text{reactivity integral}$$

α = logarithmic energy loss parameter

$$\alpha = \sum f_j \alpha_j \qquad \alpha_j = -\ln \left\{ \frac{E_j \text{ (after collision)}}{E_j \text{ (before collision)}} \right\}$$

Let R be a single reactive substance and M be a single inert moderator. Then a graph of $[-\ln(1 - P)]^{-1}$ versus $(1 - f_R)/f_R$ should be a straight line with slope $\alpha(M)/I$ and intercept $\alpha(R)/I$. Such a graph has been called a plot of the "first kind". Although absolute values cannot be obtained, I and $\alpha(R)$ may be determined in terms of $\alpha(M)$. These may be used to construct a plot of the "second kind" for individual products.

$$(\alpha/f)P_i = I_i - (f/\alpha)K_i \qquad 1\text{-}5$$

$$I_i = \int_{E_1}^{E_2} \frac{p_i(E)}{E}\, dE \qquad 1\text{-}6$$

$$K_i = \int_{E_1}^{E_2} \frac{p_i(E)}{E} \left[\int_{E}^{E_2} \frac{p_i(E)}{E} \right] dE \qquad 1\text{-}7$$

A plot of $(\alpha/f)P_i$ versus (f/α) will give a straight line with slope K_i and intercept I_i. I_i, the reactivity integral, is the area under a plot of reaction probability versus the logarithm of tritium atom energy. K_i in the "energy shadowing" term which measures how much reaction has taken place at energies higher than the energy range for the production of product i.

The Estrup-Wolfgang Kinetic theory further assumes that: (1) the number of collisions in a reactive energy zone will be large. This justifies the use of an integral form. (2) the tritium atom population at energy E can be determined by subtracting out the reactions between limits E_2 and E itself (see Eq. (1-7)). (3) the value of α for the various components will be constant in the energy range considered. Despite the crudity of these assumptions, straight line relationships have been obtained.[6] However, recently it has been shown that straight line graphs can be obtained although many of the conditions of the theory have been violated.[40] In addition, refinement of the basic assumptions leads to non-linear predictions.[41,42] A straight line on an Estrup-Wolfgang graph may not signify much, certainly not as much as once thought.

1.3.2 Practical Applications

I have mentioned the Estrup-Wolfgang kinetic theory because it has served as a means of presenting experimental data. Note that it requires the "absolute yield" of each product, the fraction of the total tritium available for reaction which reacted to give product i. Often this is difficult to establish with certainty. The total amount of tritium produced N_t is given by

$$N_t \cong n\ f\ \sigma\ \tau \qquad 1\text{-}8$$

where n is the number of ^3He or ^6Li atoms in the sample, f is the flux of neutrons experienced by the sample in neutrons cm^{-2} sec^{-1}, σ is the cross section for the nuclear reaction in cm^2, and τ is the length of irradiation in sec. The length of irradiation can be accurately determined. The cross sections for the reactions are well known (5330 barns and 940 barns, respectively, for $^3He(n,p)T$ and $^6Li(n,\alpha)T$.[43] A barn is 10^{-24} cm^2.). The number of target atoms can be determined by weight for ^6Li or from the pressure of ^3He and volume of the capsule for ^3He. One problem lies in attenuation of the neutron flux by boron (the $^{10}B(n,\alpha)^7Li$ reaction cross section is 3840 barns[43]) in the wall of the glass capsule. Variations in the thickness of the capsule wall or the boron content of the glass from sample to sample could lead to spurious absolute yield measurements even though care is taken to ensure that each capsule receives the same total neutron dose. Another problem lies in determining the amount of tritium which is not "stopped" by the hydrocarbon but recoils into the

wall of the capsule*. Semi-empirical methods of determining the amount of this recoil loss may be ±10% in error.[44] The uncertainty induced by these two effects can be lessened by irradiation of a standard hydrocarbon sample with each sample batch and then normalizing all absolute yields to this standard yield.[39]

The alternate approach is to determine the yield of all observed products relative to one major product, usually the tritiated parent hydrocarbon. If the tritiated parent hydrocarbon is undergoing unimolecular decomposition then the sum of tritiated parent plus tritiated unimolecular decomposition products may be chosen as the relative standard.[26] The use of relative yield is advantageous because it is easier. Often only one method of reporting the results is used and then only a partial tabulation of product yields is found in the literature. Equally often the unreported data or alternate method of reporting the data is of subsequent interest, but unretrievable. Consequently, tables of the relative yields of all observed products in this work will be found in the Appendix. The information necessary to transform relative yields to absolute yields will also be included.

---

*For example, the recoil range of a 192 keV triton in 10 cm Hg pressure of methane gas is approximately 3 cm.[44]

2. UNIMOLECULAR REACTIONS

Unimolecular reactions have often been observed as a secondary process in recoil tritium-hydrocarbon systems. In this section, the study of unimolecular processes will be reviewed at the level necessary for the understanding of recoil tritium initiated unimolecular reactions. Much more detailed and comprehensive reviews of unimolecular reactions are available.[45-47]

2.1 Basic Theories

2.1.1 Lindemann-Hinshelwood Theory

The Lindemann-Hinshelwood theory is the basis for all modern theories of unimolecular reaction.[48,49] This theory considers the unimolecular reaction of molecule A to occur as three discrete processes:

(a) Activation. $$A + M \xrightarrow{k_1} A^* + M \qquad 2\text{-}1$$

A certain fraction of the A molecules become energized by collision to gain energy in excess of a critical energy E_o. The rate of the energization process depends on the rate of bimolecular collisions with M. M is another A molecule, an added "inert" gas molecule, or a product molecule. The energization process is considered to be largely one of translational-vibrational energy transfer. Vibrational energy is no doubt the major contribution in obtaining the critical energy, E_o. However, rotational energy may be important.[46]

In the Lindemann-Hinshelwood formulation k_1 is given by

$$k_1 = Z_1 \left[\left(\frac{E_o}{\underline{k}T}\right)^{s-1} \frac{1}{(s-1)!}\right] \exp(-E_o/\underline{k}T) \qquad 2\text{-}2$$

where Z_i is the collision number given by[50]

$$Z_i = (\sigma_d^2 N_A/R)(8\pi N_A \underline{k}/\mu)^{\frac{1}{2}}(1/T)^{\frac{1}{2}} \qquad 2\text{-}3$$

Z_i will be in $Torr^{-1}$ sec^{-1} (consistent with k_i in sec^{-1} and pressure in Torr) when: σ_d is the collision diameter in cm., μ is the reduced mass in g mol^{-1}, T is the temperature in degrees Kelvin, N_A is 6.023×10^{23} mol^{-1}, R is 6.236×10^4 cm^3 Torr $°K^{-1}$ mol^{-1}, and $\underline{k}$ is 1.3805×10^{-16} erg $°K^{-1}$, Boltzmann's constant.

The $\exp(-E_o/\underline{k}T)$ term of Eq. (2-2) represents the probability that two colliding molecules have relative translational energy $\geqslant E_o$ along their line of centers. The $\left[\left(\frac{E_o}{\underline{k}T}\right)^{s-1} \frac{1}{(s-1)!}\right]$ term of Eq. (2-2) represents the probability that molecule A would possess energy $\geqslant E_o$ in s classical degrees of internal freedom; that is, energy other than in the two classical degrees of freedom along the line of centers.

(b) <u>De-activation</u>. $\quad A^* + M \xrightarrow{k_2} A + M \qquad 2\text{-}4$

The energized molecules are de-energized by collision. This is the reverse of the process in Eq. (2-1). The rate constant, k_2, is taken as energy independent. Furthermore, k_2 is taken as the collision number, Z_2. The inherent assumption is that every collision of A^* with M leads to de-activation. This is known as the "strong collision" assumption and will be discussed later.

(c) <u>Decomposition (or isomerization)</u>. $\quad A^* \xrightarrow{k_3} B + C \qquad 2\text{-}5$

Decomposition or isomerization occurs with some time-lag after activation. In this early formulation, k_3 was independent of the energy content of A^*.

Application of the steady state hypothesis to the concentration of A^* gives

$$\frac{d[A^*]}{dt} = 0 = k_1[A][M] - k_2[A^*][M] - k_3[A^*] \qquad 2\text{-}6$$

solving for $[A^*]$ gives

$$[A^*] = \frac{k_1[A][M]}{k_3 + k_2[M]} \qquad 2\text{-}7$$

The overall rate of reaction, R, is given by

$$R = k_3[A^*] = \frac{k_3k_1[A][M]}{k_3 + k_2[M]} \qquad 2\text{-}8$$

At high pressures, $k_2[M] >> k_3$; so Eq. (2-8) becomes

$$R_\infty = (k_3k_1/k_2)[M] = k_\infty[M] \qquad 2\text{-}9$$

At low pressures, $k_2[M] << k_3$; so Eq. (2-8) becomes

$$R_{bim} = k_1[A][M] = k_{bim}[A][M] \qquad \text{(bim = bimolecular)} \qquad 2\text{-}10$$

At high pressures the reaction rate constant, k_∞, is a true constant independent of pressure. At low pressures the reaction rate constant is the second order rate constant for energization. The low pressure region is called the "fall-off" region. This is where k_{uni}

$$k_{uni} = \frac{1}{[A]}\left(-\frac{d[A]}{dt}\right) = \frac{k_3k_1[M]}{k_3 + k_2[M]} \qquad 2\text{-}11$$

(uni = unimolecular)

or k_{uni}/k_{∞} plotted as a function of pressure "falls off" from the high pressure k_{∞} value.

2.1.2 RRK Theory

Rice and Ramsperger[51,52] and Kassel[53,54] expanded the basic Lindemann-Hinshelwood scheme to include expressions for the energy dependence of k_3. In their formulation, known as RRK theory, k_3 becomes $k_a(E)$. The subscript, a, denotes the "apparent" rate constant for unimolecular decomposition. In RRK theory, the critical amount of energy, E_o, must be concentrated in one particular part of the molecule. The total energy, E, of the molecule is assumed to be rapidly and freely redistributed around the molecule. Thus, for any molecule with $E > E_o$, there is a finite statistical probability that energy E_o will be found in the relevant part of the molecule. For a molecule of s classical oscillators with total energy E, the probability of energy $\geqslant E_o$ being found in one oscillator is probability

$$(\text{energy} \geqslant E_o \text{ in one oscillator}) = \left(\frac{E - E_o}{E}\right)^{s-1} \qquad 2\text{-}12$$

Then

$$k_a(E) = A\left(\frac{E - E_o}{E}\right)^{s-1} \qquad 2\text{-}13$$

The A factor only becomes significant when Eq. (2-13) is combined with Eq. (2-2) and (2-9) and the equation is integrated over the entire range of activation energies $E \geqslant E_o$.

$$k_\infty = \int_{E=E_o}^{\infty} \left[A\left(\frac{E - E_o}{E}\right)^{s-1}\right] \left[\left(\frac{E}{\underline{k}T}\right)^{s-1} \frac{1}{(s-1)!} \exp(-E/\underline{k}T)\right] d(E/\underline{k}T) \qquad 2\text{-}14$$

Then

$$k_\infty = A \exp(-E/\underline{k}T) \qquad 2\text{-}15$$

which is the Arrhenius equation.[55] Similar derivation of k_{uni} allows "fall off" plots to be made from

$$\frac{k_{uni}}{k_\infty} = \frac{1}{(s-1)!} \int_{x=0}^{\infty} \frac{x^{s-1} \exp(-x)\, dx}{1 + (Ak_2^{-1}[M]^{-1})\{x/(x + E_o/\underline{k}T)\}^{s-1}} \qquad 2\text{-}16$$

This function has been well studied and tabulated.[56]

2.1.3 RRKM Theory

The extension of RRK theory by Marcus[57,58] is called RRKM theory. In RRKM theory: (a) k_1 is evaluated as a function of energy by a quantum-statistical-mechanical treatment as opposed to the classical treatment of RRK theory. (b) k_2 is still considered to be independent of energy. k_2 is equated with the collision number, Z_2, or λZ_2 where λ is a collisional de-activation efficiency factor. (c) The energized molecule A^* must achieve the precise quantum state (the necessary energy in the relevant vibrational mode of the molecule) before the reaction occurs. The energized molecules will not react instantaneously even when this rare quantum state is achieved. The vibrational modes will in general not be correctly phased at first. Thus, the energized molecules have

decomposition lifetimes which are long compared to vibrational periods. Furthermore, the energized molecule, A^*, must pass through an intermediate between A^* and product. This intermediate is known as the activated complex, $A^\dagger$.

$$A^*_{(E^*)} \xrightarrow{k_a(E^*)} A^\dagger \xrightarrow{k^\dagger} \text{products} \qquad 2\text{-}17$$

The activated complex is characterized by having a configuration corresponding to the top of the energy barrier between reactant and products. The activated complex is thus unstable to movement in either direction along the reaction coordinate (the site of bond breaking in unimolecular decomposition). In contrast to the energized molecule, the activated complex has no measurable lifetime. There will usually be more than one quantum state of $A^\dagger$ which can be formed from a given A^*, because of the different possible distributions of the energy between the reaction coordinate and the vibrational and rotational degrees of freedom of the complex. The rate constant, $k_a(E^*)$, will be evaluated from the various possible activated complexes. Methods of evaluating $k_a(E^*)$ are given in Ref. 45.

2.1.4 Slater Theory

Slater theory[59,60] is an extension of the Lindemann-Hinshelwood reaction scheme. The molecule undergoing reaction is pictured as an assembly of harmonic oscillators of particular amplitudes and phases. In the strictest formulation of Slater theory, the vibrational modes are entirely harmonic. There is no possible interchange of energy between

vibrational modes. If the energy input is not in the critical mode, regardless of E being greater than E_o, decomposition does not occur.

2.2 Comparison of Theory and Experiment: Fall-Off Data

Fall-off experiments have been used to test theories of unimolecular reaction. The experimental fall-off data on cyclopropane isomerization[61,62]

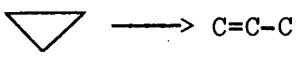

2-18

has been well reproduced by Slater theory,[63] RRK theory,[64] and RRKM theory.[64] Slater theory predicted drastic differences between the cyclopropane and cyclopropane-d_2 fall-off curves.[45-47] RRK and RRKM theories predicted little difference. The experimental results[65] showed little difference. Consequently, at present, Slater theory is little used. RRK and RRKM theoretical curves have closely fitted the experimental fall-off data in many cases. It should be noted that in applying RRK theory; s, the number of "active" vibrational modes, is an adjustable parameter. The energy, E, is freely interchanged among all s modes, but s is often less than the total number of vibrational modes, (3N - 6), when the A molecule is composed of N atoms. RRK theory is not predictive since it contains an adjustable parameter, s. However, RRK theory is much easier to apply than RRKM theory. Often "quickie" qualitative fall-off curves are calculated with RRK theory using s as 1/2 to 2/3 of (3N - 6). The average value[66] of s from a large number of experimental fits is $s = \frac{1}{2}(3N - 6)$.

2.3 Assumptions of Basic RRK-RRKM Theory

2.3.1 Energy Randomization Prior to Decomposition

RRK and RRKM theories assume that the non-fixed energy of the active vibrations and rotations is subject to rapid statistical redistribution. This means that every sufficiently energetic molecule will eventually be converted into products unless de-activated by collision. Often this assumption is stated as "the randomization of energy within the molecule prior to decomposition is rapid on the time scale of unimolecular decomposition". This does not mean that energy is interchanged among <u>all</u> degrees of freedom. Marcus[57] made provision of some of the degrees of freedom to be completely inactive. The energy in the inactive degrees of freedom cannot flow into the reaction coordinate. The energized molecule A^* is one with non-fixed energy greater than E_o in the active modes.

Tests of the randomization assumption have been made by chemical activation studies. Butler and Kistiakowsky[67] activated methylcyclopropane by the two different reactions shown in Eq. (2-19).

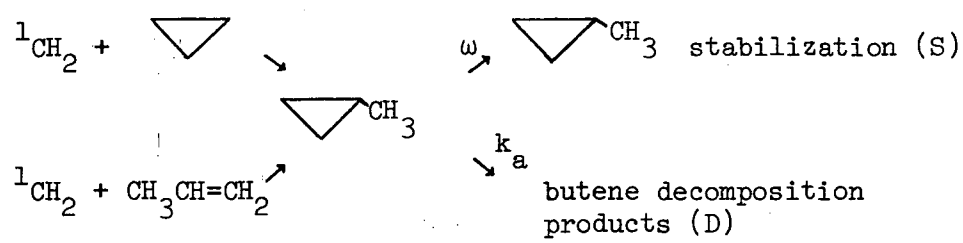

2-19

Excitation by the different reactions should result in energy input into characteristically different regions of the molecule. However, the

chemically activated species reacted at rates which were in accord with the expected difference based only on the ~ 7 Kcal $mole^{-1}$ differential in excitation energy.

The unimolecular rate constant, k_a, in chemical activation studies is determined from the decomposition (D) to stabilization (S) ratio. Assuming the only reaction of the excited species to be either decomposition or stabilization, then the D/S ratio is equal to the ratio of the rate constants k_a/ω. Using the strong collision assumption discussed later, ω is the collision frequency.

$$\omega = ZP \qquad 2\text{-}20$$

Note: Z is given by Eq. (2-3) and P is the pressure in Torr. This leads to

$$k_a = \omega(D/S) \qquad 2\text{-}21$$

The usual technique is to determine the pressure dependence of the D/S ratio.[68] The pressure at which D/S = 1 is determined from a plot of the D/S ratio versus pressure. The collision frequency at this pressure is k_a.

Similarly, sec-butyl radicals activated in the characteristically different ways shown in Eq. (2-22) decomposed with a difference in rates explainable by the energy differential.[69] Butane is formed

$$\begin{array}{lcl} CH_3CH_2CH{=}CH_2 + H\cdot & & \omega \nearrow \quad \text{butane (S)} \\ & \searrow \quad CH_3CH_2\text{-}\dot{C}HCH_3 & \\ CH_3CH{=}CHCH_3 + H\cdot & \nearrow & k_a \searrow \quad CH_3\cdot + [C{=}C\text{-}C\ (D)] \end{array} \qquad 2\text{-}22$$

when the stabilized sec-butyl radical abstracts a hydrogen atom.

Recently Rynbrandt and Rabinovitch[68] reported the first positive example of energy non-randomized unimolecular decomposition. The reaction sequence is shown in Eq. (2-23).

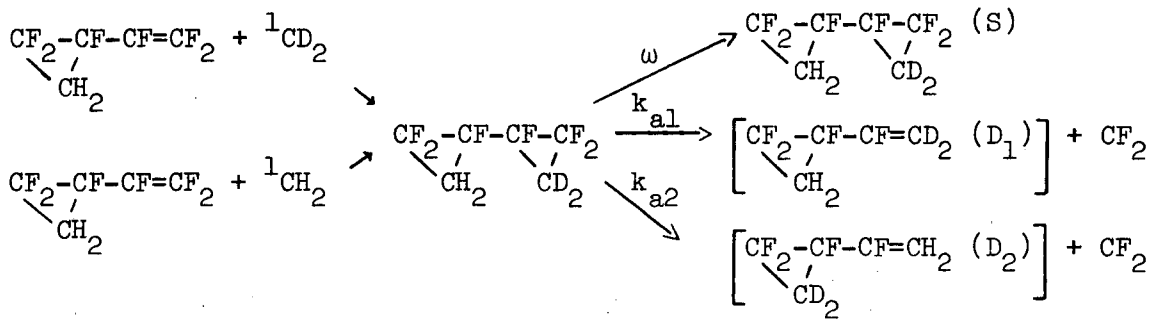

2-23

If energy was randomized prior to decomposition, $k_{a1} = k_{a2}$. However, analysis showed that regardless of the isotopic labeling of the added methylene, the newly formed ring was more probable to decompose. This non-random decomposition occurred in 3.5% of the total decompositions.

2.3.2 Strong Collisions

The assumption of strong collisions means that relatively large amounts of energy are transferred in molecular collisions. The RRK-RRKM model treats the processes of activation and de-activation as essentially single step processes. A strong collision is assumed to be so violent that the state of the molecule after collision is in no way dependent upon the state before collision. The final state is a random choice from all the available states with the appropriate energy.[70]

The strong collision assumption is reasonably realistic for thermal reactions in the temperature range of conventional kinetic studies. A constant limiting de-energizing efficiency of various gases

above a moderate size (C_3 or greater) is observed in the second order unimolecular decomposition region.[71] This limiting efficiency is presumed to be unity. These studies indicate that 5 Kcal $mole^{-1}$ or more of energy is transferred per collision. Because of this large energy transfer only a few collisions should be necessary to de-activate the majority of energized molecules. The average energy of excitation in thermal reactions is typically only 5 to 15 Kcal $mole^{-1}$ above the critical energy, E_o. For reaction systems with a low mole % of potentially activated large molecules in a bath of small inefficient de-activator molecules, crude allowance for limited energy transfer on collision may be made on a semi-empirical basis. Equation (2-21) becomes

$$k_a = \beta\omega\ (D/S) \qquad 2\text{-}24$$

where β is an experimentally determined collisional de-activation efficiency parameter. Tables of β values are derived from studies of collisional de-activation efficiencies in the second order region of unimolecular decomposition.[71] The β values for small inefficient deactivator molecules are less than unity. Combining Eqs. (2-20) and (2-24) and noting that Z is independent of the relative concentrations of potentially activated large molecules and bath gas gives Eq. (2-25).

$$k_a = z(\beta P)\ (D/S) \qquad 2\text{-}25$$

The term βP is the "effective pressure" of the reaction system.

The concept of effective pressure is best illustrated by example. Nitrogen has a β value of 0.27 relative to butene in Eq. (2-22).[71] For

a system of 10 Torr trans-2-butene, 0.1 Torr of a source of H-atoms, and no bath gas, k_a would be calculated using Eq. (2-21). For a system of 10 Torr trans-2-butene, 0.1 Torr of a source of H-atoms, and 10^5 Torr of N_2 bath gas, k_a would be calculated using Eq. (2-24). The "effective pressure" of the system would be $\beta P = 0.27 \times 10^5$ Torr. This means that the sec-butyl radicals were stabilized (S) by collisions as if the system were pure trans-2-butene at a pressure of 0.27×10^5 Torr. Eqs. (2-21) and (2-24) may be used to calculate k_a is systems composed of the extremes in concentration of potentially activated large hydrocarbon (HC) molecules relative to small inefficiently deactivating molecules of a bath gas (BG). For relative concentrations between the extremes a linear combination of Eqs. (2-21) and (2-24) may be used. This gives

$$k_a = Z\, P_{eff}\, (D/S) \qquad 2\text{-}26$$

with

$$P_{eff} = \text{effective pressure} = P_{HC} + \beta P_{BG} \qquad 2\text{-}27$$

The alternative to this single step de-activation process is a ladder-like process in which molecules lose their energy in a series of small steps. The ladder model requires detailed treatment of the energy levels of the excited molecule and the dynamics of the de-activating collisions.[72] The comparative simplicity of the strong-collision treatment is often the basis for use of the strong collision assumption.

3. THE AIMS AND SCOPE OF THIS WORK

3.1 Project Definition

This project was to test the energy randomization assumption of the RRK-RRKM theories of unimolecular reactions using activation by recoil tritium atoms. A priori consideration of T + methylcyclohexene reactions showed that one reaction channel was T-for-methyl substitution to give a labeled cyclohexene-t molecule. Cyclohexene-t molecules could be labeled at different sites by recoil tritium reactions with different methylcyclohexene isomers. The resultant activated (energized) cyclohexene-t molecules, regardless of the labeling site, were either: (a) stabilized (S) through collisions at rate ω, or (b) decomposed unimolecularly (D) to ethylene and butadiene (only one of which is T labeled) in a retro-Diels-Alder-reaction.[73] This reaction scheme is shown in Eqs. (3-1) to (3-3).

1-methyl cyclohexene

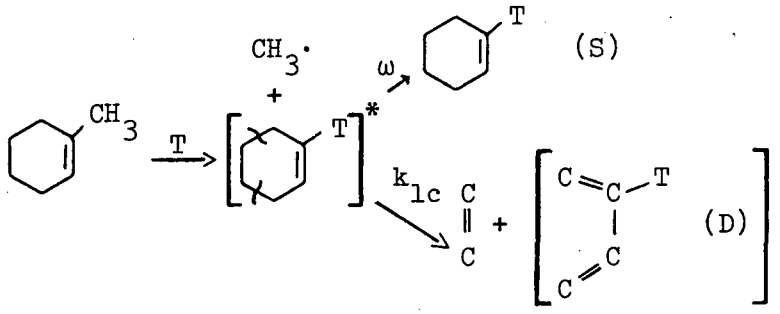

3-1

3-methyl cyclohexene

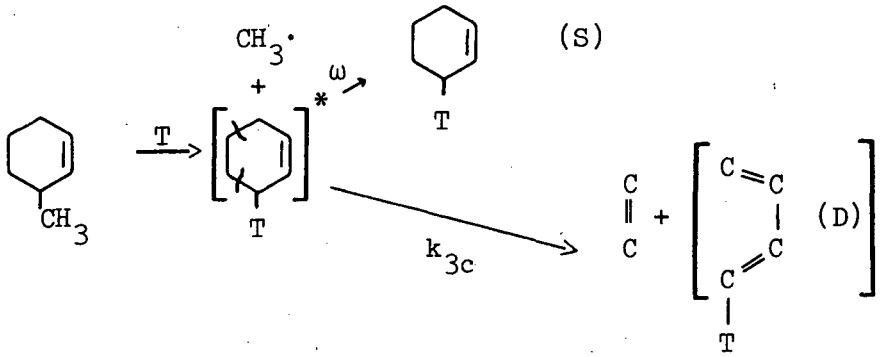

3-2

4-methyl cyclohexene

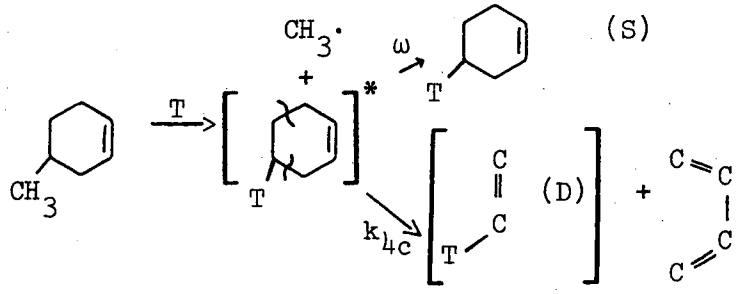

3-3

As shown in Sec. 2.3.1, the unimolecular rate constants, k_{1c}, k_{3c}, and k_{4c}, can be determined from the pressure dependence of the D/S ratio shown by the appropriate tritium labeled products of T + methylcyclohexene reactions. The rate of unimolecular decomposition of the excited cyclohexene-t molecule should, by RRK-RRKM theory, be independent of the site of the T label. Any difference in the three rate constants can be attributed to: (1) energy non-randomized decomposition of cyclohexene-t; that is, the breakdown of the RRK-RRKM assumption of energy randomization. (2) differences in the average energy of excitation of cyclohexene-1-t, cyclohexene-3-t, and/or cyclohexene-4-t molecules following T-for-methyl substitution. This will be developed further in Sec. 3.2.

3.2 Assumptions

In the postulation and discussion of the reaction scheme shown in Eqs. (3-1) to (3-3), there are several necessary assumptions:

(a) <u>T-for-methyl substitution occurs as indicated, without a</u> shift of the double bond. Evidence to support this assumption has been given in Sec. 1.2.3.

Test. The validity of this assumption could be checked by using established chemical degradation procedures[74,75] to determine the intramolecular tritium content of the (stabilized) cyclohexene-t molecules.

(b) The only reaction of excited cyclohexene-t molecules is either stabilization or retro-Diels-Alder cleavage as indicated to give ethylene-t or butadiene-t. The unimolecular decomposition of cyclohexene to give primarily ethylene and butadiene has been well established in pyrolysis,[74,76-80] shock tube,[81-83] photolysis,[84,85] and mercury sensitized photolysis[86] studies. Of the total unimolecular decompositions, 96% occur giving ethylene and butadiene, 3% occur by H_2 elimination to give cyclohexadienes and benzene, and the remaining 1% give C_5 and smaller hydrocarbons presumably through a free radical mechanism.[78,79,85] A possible radical contribution to the ethylene and butadiene yield has been proposed from cyclohexyl radicals via H-atom addition to cyclohexene.[81,82] However, addition of scavenger does not affect the ethylene and butadiene yield.[78,85,86] The unimolecular rate constant for cyclohexene decomposition

$$k_a = 10^{15.3} \exp(-66{,}900 \text{ cal}/\underline{k}T) \qquad 3\text{-}4$$

has been so well determined that cyclohexene is used as an internal standard in shock tube studies.[82,83]

Strong evidence for the retro-Diels-Alder cleavage of cyclohexene comes from the photolysis of cyclohexene-3,3,6,6-d_4. The photolysis

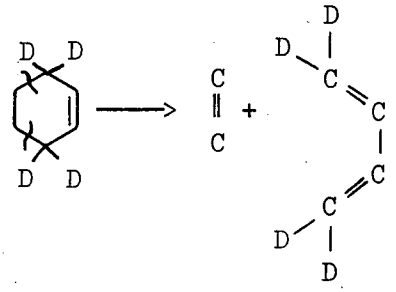

3-5

of cyclohexene-3,3,6,6-d_4 occured as shown in Eq. (3-5) to give C_2H_4 and $C_4H_2D_4$ in 98% of the decompositions at 4.9 eV photolysis energy and 86% of the decompositions at 8.4 eV photolysis energy. At 8.4 eV the remaining 14% of the decompositions gave $C_2H_2D_2$ and $C_4H_4D_2$ indicating cyclohexene cleavage as shown in Eq. (3-6).[85]

$$\longrightarrow C_2H_2D_2 + C_4H_4D_2 \qquad 3\text{-}6$$

Further evidence for the retro-Diels-Alder cleavage of cyclohexene comes from: (i) The pyrolysis of cyclohexene-1-t and cyclohexene-3-t to give primarily butadiene-t and the pyrolysis of cyclohexene-4-t to give primarily ethylene-t.[74]

(ii) The retro-Diels-Alder cleavage of substituted cyclohexenes as shown in Eqs. (3-7) to (3-11).

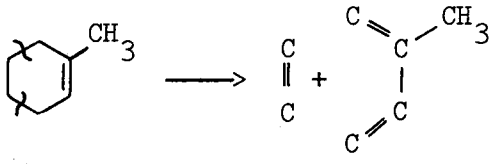

87,88 3-7

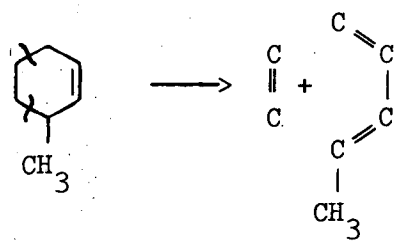

81,86,89 3-8

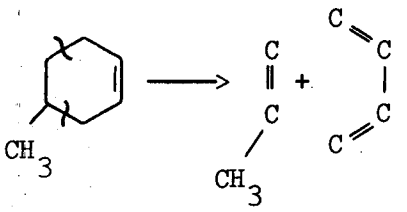

80,81,86 3-9

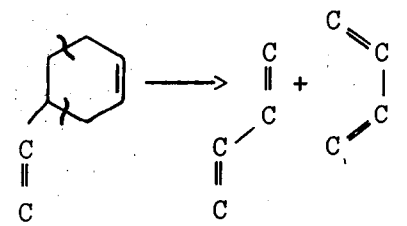

80,81,87 3-10

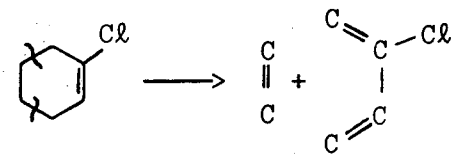

90 3-11

(iii) The retro-Diels-Alder cleavage observed in the mass spectral fragmentation patterns of cyclohexene[73,91,92] and substituted cyclohexenes.[73,93-96]

<u>Test</u>. The assumption of excited cyclohexene-t molecules reacting only by stabilization or retro-Diels-Alder cleavage appears to be strongly based on experimental evidence. The validity of this assumption could be checked by: (i) searching for cyclohexadiene-t formed by H_2

elimination. (ii) employing scavenger studies to attempt to determine (and eliminate) a possible radical precursor to the ethylene-t and butadiene-t yield. (iii) determining the deuterium content of the ethylene-t and butadiene-t from tritium atom reactions with 1- and 4-methylcyclohexene-3,3,6,6-d_4 and 3-methylcyclohexene-3,6,6-d_3. A T-for-methyl substitution reaction with these deuterated species would produce tritium labeled cyclohexene-3,3,6,6-d_4 (cyclohexene-3,6,6-d_3 from 3-methylcyclohexene-3,6,6-d_3). The cleavage patterns of cyclohexene-3,3,6,6-d_4 are established in Eqs. (3-5) and (3-6).

(c) <u>The reaction sequence shown in Eqs. (3-1) to (3-3) is the only</u> reaction channel leading to the formation of butadiene-t from T + 1-methylcyclohexene and T + 3-methylcyclohexene reactions and ethylene-t from T + 4-methylcyclohexene reactions. This assumption is supported by the retro-Diels-Alder cleavage of the methylcyclohexenes shown in Eqs. (3-7) to (3-9).

<u>Test</u>. Test (iii) of assumption (b) would also demonstrate the possibility of butadiene-t (or ethylene-t) coming from sources other than the retro-Diels-Alder cleavage of excited cyclohexene-t.

(d) <u>Ethylene-t and butadiene-t undergo no further reaction</u> following the retro-Diels-Alder cleavage of cyclohexene-t. This assumption is contrary to published data[76-86] on cyclohexene decomposition. This data shows that the butadiene yield is always less than the ethylene yield. Although stoichiometrically the yields should be equal, the butadiene yield is less by as much as 10%.[84] The discrepancy in the butadiene yield is larger than can be accounted for by further reaction

of butadiene via dimerization.[97] Further reaction of butadiene by secondary decomposition has been proposed.[85] The possibility of a discrepancy in the stoichiometry of the products of the retro-Diels-Alder cleavage of excited cyclohexene-t molecules may limit this test of the RRK-RRKM energy randomization assumption to a comparison of k_{1c} with k_{3c}. The determination of k_{1c} and k_{3c} both depend on measuring the butadiene-t to cyclohexene-t ratio. Thus, the determination of k_{1c} and k_{3c} is independent of any discrepancy in the ethylene/butadiene stoichiometry from the retro-Diels-Alder cleavage of cyclohexene. Assumption d may then be relaxed to: if the butadiene-t molecules from the retro-Diels-Alder cleavage of cyclohexene-t react further, this further decomposition or dimerization occurs at the same rate for butadiene-2-t as butadiene-1-t. This is tantamount to assuming energy randomization prior to decomposition for butadiene-t while testing energy randomization prior to decomposition for cyclohexene-t. It should be remembered, however, that for C_4 species energy non-randomized decomposition has not been observed (Sec. 2.2.1).

Test. The only way to test this relaxed assumption would be to discover and monitor a tritiated product known to result only from the secondary decomposition of butadiene-t.

(e) Corrections can be made for possible differences in the average energy of excitation of cyclohexene-1-t versus cyclohexene-3-t which are formed as shown in Eqs. (3-1) and (3-2). Implicit in this assumption are several corollaries, none of which can be tested:

(i) The average energy of the T atom initiating the T-for-methyl substitution is the same in the T + 1-methylcyclohexene and

T + 3-methylcyclohexene systems. Tabulated values of α, the logarithmic energy loss parameter (Sec. 1.3.1), show a strong dependence on carbon number. Changes in structure from 1-methylcyclohexene to 3-methylcyclohexene, however, should not drastically affect the tritium energy distribution.[6]

(ii) The energetics of the reaction are correctly given by the estimated ΔH values (Kcal mole^{-1}) shown in Eqs. (3-12) and (3-13).[21]

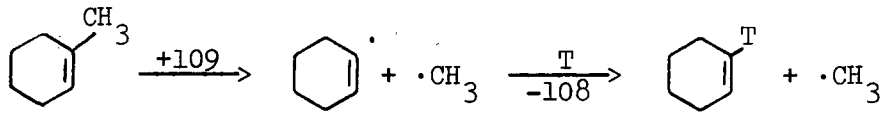

3-12

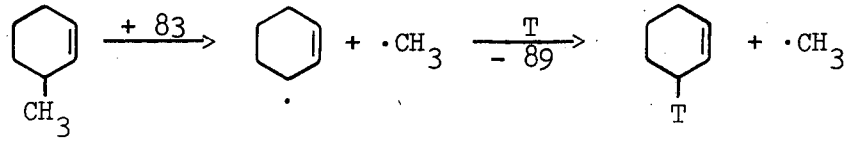

3-13

This shows that cyclohexene-3-t possesses an average of about 1 eV more excitation energy than cyclohexene-1-t if it is further assumed that

(iii) the methyl radical carries away the same average energy in the reactions shown in Eqs. (3-12) and (3-13).

(iv) This difference in excitation energy can be corrected for using RRK theory and Eq. (2-13) if the s parameter is known. An alternate route, of course, is to perform a complete RRKM calculation to determine the energy dependence of k_a for the unimolecular decomposition of cyclohexene.

(v) The s parameter of RRK theory in Eq. (2-13) may be determined for the retro-Diels-Alder unimolecular decomposition of cyclohexene by a

study of T + cyclohexene reactions. This will require a separate experiment to determine the pressure dependence of the D (ethylene-t plus butadiene-t)/S (cyclohexene-t) ratio from T + cyclohexene reactions. Working backwards through Eqs. (2-21), (2-20), and (2-3) to (2-13) with E set equal to 5 eV (the average energy of a T-for-H substitution reaction (Sec. 1.2.3)) will allow determination of the s parameter of RRK theory.

3.3 Project Summary

The first phase of this project will be to study T + cyclohexene reactions, to test as many as possible of the assumptions concerning the retro-Diels-Alder cleavage of cyclohexene-t, and to determine the s parameter in the RRK treatment of the unimolecular decomposition of cyclohexene. The second phase will be to study T + methylcyclohexene reactions, to test as many as possible of the assumptions listed in Sec. 3.2 (including the retro-Diels-Alder cleavage of methylcyclohexene) and to test the energy randomization assumption of the RRK-RRKM theories of unimolecular reaction by determining if the difference in the apparent rate constant of unimolecular decomposition between cyclohexene-1-t and cyclohexene-3-t can be attributed solely to the estimated 1 eV difference in average energy of excitation.

EXPERIMENTAL TECHNIQUES

The typical recoil tritium experiment involves:

(1) sample preparation - encapsulation of the potential source of recoil tritium with the hydrocarbon and moderator or scavenger of interest. (Discussed in Sec. 4.)

(2) sample irradiation - neutron irradiation of the sample to produce recoil tritium atoms from $^{3}He(n,p)T$ in the gas phase and $^{6}Li(n,\alpha)T$ in the liquid and solid phases. (Discussed in Sec. 5.)

(3) sample analysis - separation and counting of the gas phase tritium labeled products by radio-gas-chromatography and recovery and liquid scintillation counting of higher molecular weight tritium labeled products. (Discussed in Sec. 6.)

4. SAMPLE PREPARATION

4.1 Gas Phase - Parent Hydrocarbon C_4 or Less

The gas phase sample was placed in a 1720 Pyrex capsule. The 1720 Pyrex glass was chosen for two reasons: (1) HT cannot diffuse through the wall of a 1720 Pyrex capsule. HT has been observed to diffuse out of quartz capusles;[98] (2) Type 1720 Pyrex has desirable irradiation properties, chiefly low sodium content. The cylindrical body was 6.7±0.2 cm long, 2.17±0.03 cm o.d. with a 0.10±0.01 cm wall. The internal volume of the capsule (V_c) was 14.4±0.4 ml. These large dimensions were chosen to minimize loss of recoil tritons to the wall of the capsule.[44] One end of the capsule was hemispherical. The other end was a hemisphere with a tapered stem. This stem was used to connect the sample to the vacuum line.

The stem of the capsule was inserted through a one hole silicon rubber septum (Burrell fitting) in the end of a stopcock (K in Fig. 4.1) controlled inlet to the glass vacuum line. Of the four sample positions (stopcocks K_1, K_2, K_3, K_4) only one is shown in Fig. 4.1. Once the capsule was on the vacuum line, stopcock K would be opened and the capsule would be evacuated. The external wall of the capsule would be heated with the flame of a propane/oxygen torch to attempt to remove any material adsorbed to the interior capsule wall. Simultaneously the rest of the vacuum line shown in Fig. 4.1 would be evacuated. After several hours a vacuum on 5 micron Hg or less (shown on a NRC 801 thermocouple gauge from Norton Vacuum Equipment) could be maintained without pumping

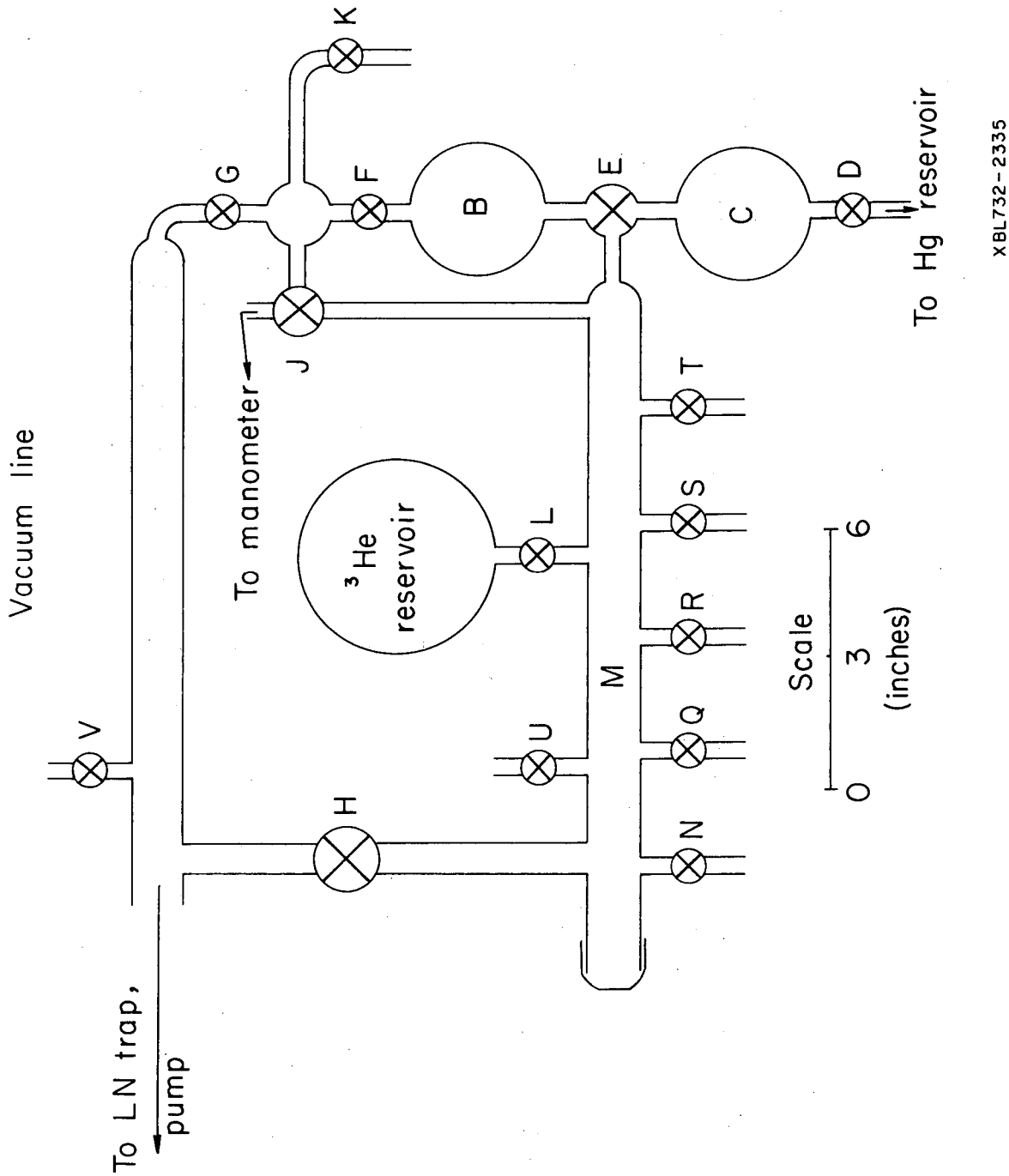

Fig. 4.1. Vacuum Line. Stopcocks Q, R, S, and T are inlets for scavengers, moderators and parent hydrocarbons C_4 or less. Stopcocks U and V are for vacuum gauges.

by the mercury diffusion pump (protected by liquid nitrogen (LN) traps) and a rotary oil pump. The capsule was now ready to be filled.

A three-way stopcock (E) connected a 300 ml bulb (C) to the manifold (M) or another 300 ml bulb (B). To initiate the sample filling, stopcock E was set to connect the manifold to bulb C and this volume isolated by closing stopcock H. Stopcock L was opened briefly and the desired pressure of ^{3}He admitted to the manifold (M) and bulb C*. This pressure was measured on a mercury manometer. (Stopcock J is another three-way stopcock which connects either the manifold to the manometer or bulb W to the manometer. In this case the manifold M is connected to the manometer.) Stopcock F would then be closed, isolating bulb B. Stopcock E was rotated to connect bulbs B and C. The air space above the mercury level in the mercury reservoir was opened to the atmosphere. Stopcock D was opened to the mercury reservoir. The mercury level rose in bulb C eventually forcing all the ^{3}He into bulb B. Bulbs C and B are the same size. This prevents condensation of low boiling hydrocarbons which could occur if the gas mixture was compressed. Then stopcock D was closed and stopcock E was rotated to connect the manifold M to bulb C now filled with mercury. Stopcock N was opened to the atmosphere and the air

---

*The ^{3}He (Mound Laboratories) was certified as 99.7 mole % ^{3}He with a tritium content of 1.0×10^{-11} mole %. A standard radio-gas-chromatographic analysis (Sec. 6) of an unirradiated aliquot of ^{3}He containing at least twice the moles normally sealed in the 1720 Pyrex capsules showed no measurable tritiated contaminent. The ^{3}He was used directly from the Mound Laboratories' container without further purification. All other materials used were research grade unless otherwise indicated.

space above the mercury in the mercury reservoir evacuated. When stopcock D was opened the mercury was forced out of bulb C and back into the reservoir. Stopcocks D and N were then closed, stopcock H opened, and the system evacuated.

This process could be repeated to place a known pressure of moderator or scavenger into bulb B. No ^3He is lost from bulb B when another gas is added. Opening stopcock E to connect bulb B (with ^3He) to bulb C (with moderator, for example) would allow both gases to equilibrate over bulbs B <u>and</u> C. The rising mercury level in bulb C forces all of the moderator and ^3He into bulb B. In this manner, sequential addition of gases to bulb B can be made without loss of any preceding gas. The final composition of the gas mixture in the bulb is thus well known. When the final gas was added to bulb B the mercury was not forced out of bulb C and into the reservoir. Instead stopcock J was rotated to connect bulb W to the manometer. The manometer, bulb W (65 ml) and the sample capsules were then evacuated. Stopcock G was then closed and stopcock F opened. The sample gas mixture in bulb B expanded into the manometer, bulb W and the sample capsules. The mercury level was then allowed to rise into bulb B until the pressure on the manometer was the sum of the pressures (P_i) sequentially measured into bulb C. Stopcock K was then closed isolating the gas mixture in the sample bulb. The composition of the gas in the sample was now well known assuming that the gases were independent and that the total pressure was the sum of the partial pressures of the components of the gas mixture.

The bottom end of the sample capsule was then cooled to LN temperature. This froze the parent hydrocarbon (and condensible

scavengers or moderators) on the bottom of the capsule and prevented gross sample decomposition by pyrolysis when the capsule was heat sealed. The entire capsule was then immersed in LN. The capsule was heat sealed (and removed from the vacuum line) by collapsing the wall of the stem near the hemispherical end to form a "break tip" sturdy enough to survive handling. An identifying number was scratched onto the side of the capsule. In determining the final pressure of the gases in the sealed capsule, corrections had to be made for the volume between the stopcock K and the sealoff point. This volume (V_a) was 1.8 ml. For condensibles the pressure (at 25°C) in the sealed capsule (P_f) was related to the partial pressure of that component in the final manometer reading (P_i) by

$$P_f = P_i \left(\frac{V_a + V_c}{V_c} \right) \qquad V_c = \text{capsule volume} \qquad 4\text{-}1$$

For noncondensibles the assumption of ideal gas behavior led to

$$P_f = P_i \left(\frac{T_1 (V_a + V_c)}{T_1 V_c + T_2 V_a} \right) \qquad \begin{array}{l} T_1 = 77\ ^\circ K \\ T_2 = 298\ ^\circ K \end{array} \qquad 4\text{-}2$$

4.2 Gas Phase - Parent Hydrocarbon C_5 or Greater

4.2.1 Pressure of Parent Hydrocarbon Sealed in Capsule $\leqslant$ Vapor Pressure at 25°C

Cyclohexene and the methylcyclohexenes were readily absorbed into Apiezon N vacuum grease. This absorption was so rapid that the vacuum could not be maintained long enough to seal the sample capsules. High-

vacuum silicon stopcock grease absorbed cyclohexene and the methylcyclohexenes at a slower but noticeable rate. After 5-10 minutes the silicon grease seemed to saturate. For example, 5 cm Hg of cyclohexene vapor were added to bulbs B and W and to the sample capsules and manometer. Ten minutes later only 3 cm Hg pressure was observed, but the 3 cm value did not change over the next half hour. In sealing cyclohexene and methylcyclohexene samples it was necessary to "pre-condition" the stopcock grease in stopcocks K, G, J, F, and E. A standard taper glass joint was added to one of the four sample positions. The cyclohexene (or methylcyclohexene) was inletted through stopcock K from a storage bulb placed on the standard taper joint. Stopcocks G and E were closed at this time. After ten minutes, the pressure of cyclohexene was measured on the manometer and stopcock B closed. Prior to the preconditioning the ^{3}He had been added to bulb C and isolated by closing stopcock E. The ^{3}He was now forced into bulb B (along with the cyclohexene) in the standard manner previously described. Stopcock J was then switched to connect the manometer to the manifold M. Evacuation of the manifold to a pressure of 5 micron Hg was now not possible due to outgassing of the cyclohexene absorbed in the stopcock grease of stopcock J. A pressure of 20 micron Hg could be obtained and scavengers or moderators added to bulb B in the standard manner. Note that the ^{3}He had been added to bulb C under 5 micron Hg pressure conditions. This was done to prevent contamination of the ^{3}He supply. Once the desired mixture was obtained in bulb B, stopcock J would be rotated to connect bulb W to the manometer. Then stopcock G was opened and the manometer, bulb W and the sample capsules evacuated (again to a pressure of 20 micron). Thereafter the procedure was the same as previously described.

4.2.2 Pressure of Parent Hydrocarbon in Sealed Capsule at 135°C > Vapor Pressure at 25°C

Capsules with cyclohexene and methylcyclohexene pressures of nearly two atmospheres at 135°C were also prepared on this vacuum line. The capsules were evacuated as described. Stopcock J would be rotated to connect bulb W to the manometer. Stopcocks K_2, K_3, K_4 were closed. Stopcocks G and F were also closed. Stopcock K_1 would be opened to allow a measured pressure of cyclohexene (or methylcyclohexene) into bulb W and the manometer. The sample capsule in position 2 (stopcock K_2) was cooled to LN temperature. Stopcock K_2 was then opened and all the cyclohexene in bulb W and the manometer was condensed into the capsule. Stopcock K_2 was then closed and the process of measuring the cyclohexene pressure into bulb W and then condensing the cyclohexene into capsule 2 was repeated as often as necessary to achieve the desired final pressure. Capsules 3 and 4 would be similarly filled. The calculated pressure (at 25°C) in the sealed capsule could be obtained using Eq. (4-1) with V_a equal to the volume of bulb W (V_w) plus the volume of the gas in the manometer (V_m). In actuality a liquid was observed in the bottom of the capsule at room temperature. When the capsule was placed in an oven at 135°C, no liquid was observed. This was expected from the data in Table 4-1.

Prior to introduction of cyclohexene to bulb W, ^3He had been introduced to bulbs B and C. ^3He is extremely expensive. The amount of ^3He used could be conserved by rotating stopcock E to alternately connect bulb C to the manifold M or to bulb B (with stopcock F closed). In this manner the ^3He pressure in the manifold M and bulbs B and C was

Table 4-1. Measured Vapor Pressures

Hydrocarbon	B.P. (°C) [Ref. 99]	Vapor Pressure (cm Hg) 25°C	135°C
Cyclohexene	83	7.1	> 150
1-methylcyclohexene	110	2.2	> 150
3-methylcyclohexene	104	3.2	> 150
4-methylcyclohexene	103	3.2	> 150

nearly equal. The ^3He in bulb C was then forced into bulb B by raising the mercury level. A noncondensible scavenger could then be added to the ^3He in the standard manner. (A condensible scavenger could be added to the sample capsule in the standard manner before the cyclohexene was introduced into bulb W. Condensing the scavenger in the capsule before stopcock K_2 was opened to admit the cyclohexene prevented loss of the scavenger.) Stopcock J was rotated to connect the manometer to bulb W. Stopcock G was opened for a final evacuation of the manometer and bulb W. Stopcock G was then closed and stopcock F opened. The mercury level in bulbs C and B was raised until the desired ^3He pressure (plus non-condensible scavenger, if used) was obtained on the manometer. Then stopcock F was closed. The capsule in position 2 was first cooled with LN on the bottom end to condense the cyclohexene (and condensible scavenger, if used), then the entire capsule was immersed in LN. Stopcock K_2 was then opened. The ^3He pressure on the manometer would drop and quickly stabilize at pressure P_{LN}. Stopcock K_2 was then closed and the capsule sealed and removed from the vacuum line as previously described. The ^3He pressure (and non-condensible scavenger pressure, if used) in the sealed capsule was calculated from the final ^3He pressure on the manometer P_{LN} and the volume of the capsule (V_c) using the ideal gas equation. Note that there was no loss of cyclohexene (and condensible scavenger, if used) because the cyclohexene was condensed when stopcock K_2 was opened to admit the ^3He. Stopcock F was opened and the mercury level was raised to obtain the same ^3He pressure initially obtained for the capsule in position 2. The ^3He filling process was repeated for samples in positions 3 and 4. In this manner sample capsules of known composition could be obtained.

4.3 Liquid Phase

Liquid phase samples were prepared in 7740 Pyrex capillary melting point tubes. One end of the tube was heat sealed. About 10 mg of LiF (enriched to 95% ^{6}Li) would be weighed into the capillary by difference in the capillary weight before and after addition of the LiF. The open end of the capillary was inserted into the Burrell fitting previously described. The capillary was then evacuated. The hydrocarbon of interest was then placed into bulb W in one of the previously described manners. Cooling the capillary in LN would condense to hydrocarbon into the capillary. Only one sample capillary would be open to bulb W at a time during this condensing. The condensing process could be repeated for other additives. The capillary was then sealed in a manner similar to that previously described. The sample was then placed in a labeled polyethylene bag for identification.

LiF is insoluble in most hydrocarbons. Consequently, the distribution of the hydrocarbon and the source of recoil tritium atoms (^{6}Li) was obviously non-homogeneous in liquid phase recoil tritium experiments. At the beginning of irradiation, the LiF was in the bottom of the capillary and the hydrocarbon above the LiF. After irradiation, some of the LiF was observed to be scattered along the walls of the capillary. Presumably this scattering resulted from tritons recoiling out of the LiF. Scattering of the LiF and diffusion of the hydrocarbon tends to reduce the possibility of recoil tritium atoms reacting principally with radiolysis produced hydrocarbon fragments whose concentration is greater near the LiF/hydrocarbon interface. As yet there

is no evidence to suggest the non-homogeneous distribution of LiF and hydrocarbon in the liquid phase (as compared to the homogeneous distribution of ^{3}He and hydrocarbon in the gas phase) has any effect on the course of recoil tritium reactions. Differences in the product distribution from T + hydrocarbon reactions between gas and liquid phases have been explained solely by the increase in collision frequency and the resultant increase in the S/D ratio from recoil tritium initiated unimolecular decompositions in the liquid phase.[6,7]

5. SAMPLE IRRADIATION

All irradiations were made in the Berkeley Campus Nuclear Reactor, a Mark III Triga pool type reactor facility. The irradiations were made in two locations; depending upon the temperature of irradiation.

5.1 Irradiations at 24°C

Irradiations of samples at 24±1°C were made in the Lazy Susan facility. The samples were loaded in the standard Lazy Susan polyethylene capsule. One gas phase capsule would fit snugly into each Lazy Susan capsule. Six liquid phase capillary tubes were placed in each Lazy Susan capsule. The liquid phase irradiations were made with the capillary in the identifying polyethylene bag. The Lazy Susan revolved around the reactor core with a period of two minutes during irradiation. This ensures that each gas phase sample received the same average flux hence the same total neutron dose. The irradiations were for 10 minutes at a flux of 3.80×10^{11} n cm^{-2} sec^{-1}. The flux was monitored by a cobalt foil ($^{59}Co(n,\gamma)^{60}Co$) and subsequent measurement of the ^{60}Co activity with a Na(I) counter. Comparison of foils placed inside a 1720 Pyrex gas phase capsule with one at the same distance from the core but between the 1720 Pyrex capsule and the internal wall of the Lazy Susan capsule showed that the flux was decreased by 12% through absorption in the 1720 Pyrex capsule wall.

5.2 Irradiations at 135°C*

5.2.1 Background

The temperature of the sample during irradiation is an important parameter in radiation chemistry[100] and hot atom chemistry.[6,7] The primary and secondary processes being studied may be temperature dependent. In addition, the phase (gas, liquid or solid) or the sample during irradiation is obviously temperature dependent. Temperature control during irradiation may be advantageous in activation analysis.[101] Numerous low temperature irradiation devices have been reported. Neutron irradiations using these cooling devices have been made at: liquid nitrogen[102] and liquid helium[103] temperatures, any temperature between 12 °K and 25 °K[104] and any temperature from 25°C down to -30°C[105] or - 75°C.[106] Gamma irradiations have been made at any temperature from 15°C to -196°C.[107] The same gamma irradiation container could have easily been adapted for use at higher than ambient temperatures (up to 150°C). High temperature neutron irradiations have also been made.[108,109] Temperature control in the 250°C to 800°C range has been achieved. A variable pressure gas gap around the sample controlled the rate of the loss of the heat that was generated in the sample by neutron absorption. The sample was essentially self-heated.

---

*The material in this section has been previously published as LBL-1264, Design of a High-Temperature Neutron Irradiation Container, by Darrell C. Fee and Samuel S. Markowitz and has been accepted for publication in Nuclear Instruments and Methods.

I am interested in hot-atom chemistry in general and recoil tritium reactions in particular. In hot-atom chemistry it is often desirable to irradiate many samples simultaneously. This ensures that all the samples in a series are irradiated under the same experimental conditions. The important experimental parameters during irradiation are temperature (as discussed previously) and total neutron dose. Inter-sample comparisons of absolute product yields can only be made if each sample receives the same neutron dose.[6,7,39] Furthermore, it is advantageous if these temperature and dose-controlled irradiations could be made in the most commonly available neutron irradiation facility, a pool type nuclear reactor. Dose-controlled hot-atom studies are easily made at pool temperatures using the "Lazy Susan" facility (see Sec. 5.1). Previously mentioned low temperature irradiation techniques are readily adapted to allow low temperature, dose-controlled hot-atom studies.[26] The high temperature irradiation techniques mentioned eariler cannot be adapted to hot-atom studies because little heat is generated in the hot-atom sample by neutron bombardment. Hot-atom studies have been made at temperatures higher than pool temperature. The irradiations were made with the samples in an oil bath on a hot plate in the dry irradiation facility (Hohlraum or exposure room) of the reactor. These studies were limited because the neutron does varied with sample position.[19] Reported here is the design and constructure of an irradiation container in which all samples receive the same total neutron dose and the temperature is controlled, to ±0.5°C in the 25°C to 200°C range.

5.2.2 Apparatus

The design concept was simple. The samples would be irradiated in a temperature-controlled oil bath placed in the Hohlraum of the reactor. The samples would be rotated so that each sample received the same neutron dose. The rotation could be achieved by directly coupling a motor to the sample rack. This would require neutron shielding to protect the motor. This is shown in Fig. 5.1.

Figure 5.1 is a cut-away side view of the apparatus. All materials are 1100 F aluminum (> 99% pure) unless stated otherwise. Constructing the irradiation container chiefly from 1100 F aluminum minimizes the potential radiation hazard. The $^{27}Al(n,\gamma)^{28}Al$ reaction during irradiation gives ^{28}Al with a 2.8 min half-life. After allowing the short-lived ^{28}Al to decay away, the sample capsules can be removed from the irradiation container. The 1/2 inch thick neutron shielding, A in Fig. 5.1, is composition 254 from Reactor Experiments, Inc. This thickness of shielding reduces the flux at the motor by a factor of 10^{-10}. The shielding protects the steel alloy Bodine motor which operates at 6 rpm. The motor is connected through a flexible rubber coupling (C) and Nylon shaft (G) to the sample rack (I). The sample rack is a right cylinder which rotates on the same axis as the Nylon shaft. A top view of the sample rack would show 24 slots for the standard 1720 Pyrex glass sample capsules (J). The sample slots are evenly spaced on a circle near the perimeter of the sample rack. If the period of irradiation is long compared to the period of rotation of the sample rack, each sample in the rack will receive the same neutron dose. The central shaft of the sample rack is threaded at the top. Unscrewing this shaft from the Nylon shaft

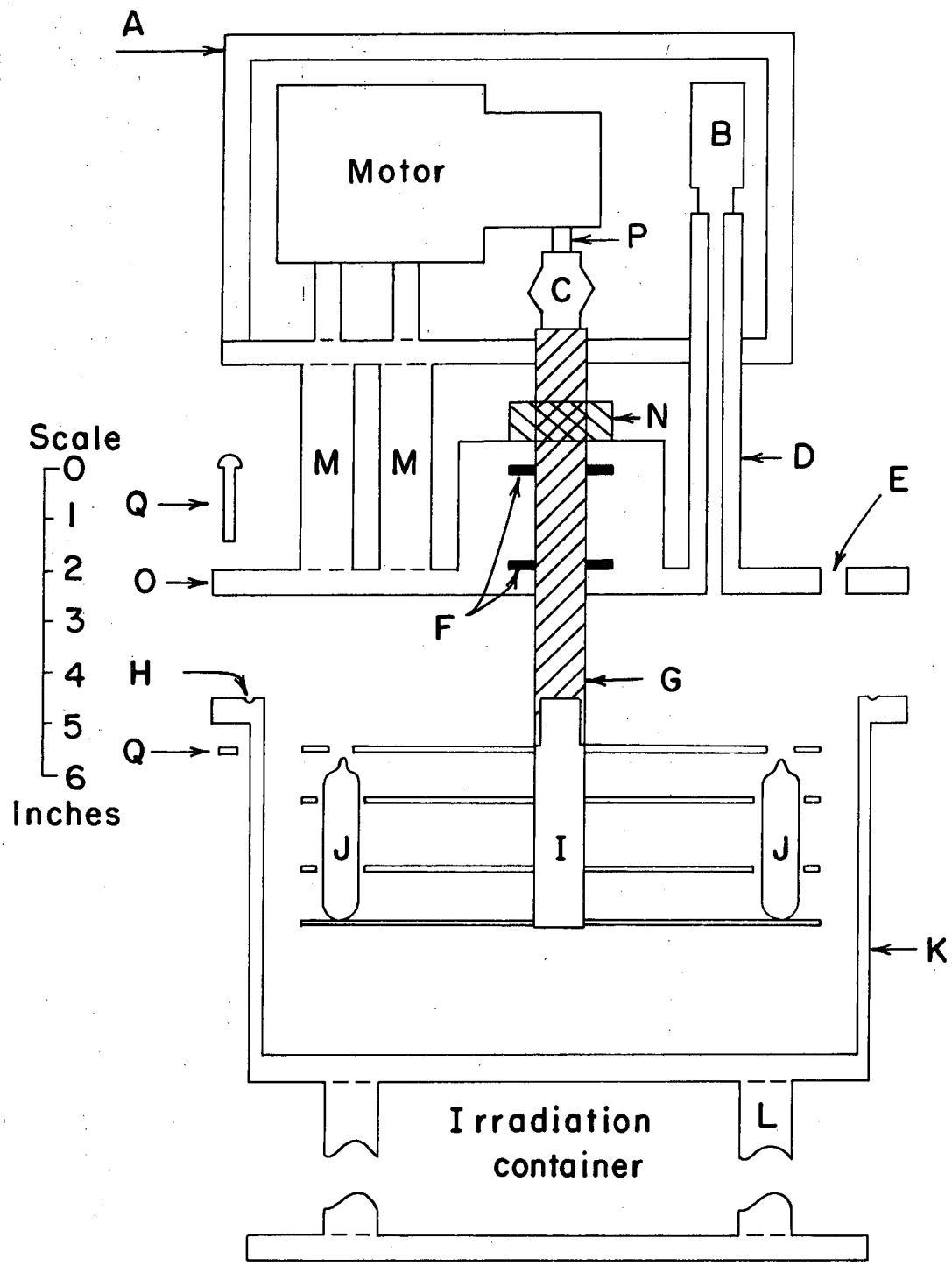

XBL 7210-4143

Fig. 5.1. Irradiation Container - The lid has been raised for purposes of illustration. Legend: A, neutron shield; B, brass pressure relief valve; C, flexible rubber coupling; D, pipe to pressure relief valve; E, hole for thermocouple lead plug; F, Teflon gaskets; G, Nylon shaft; H, O-ring groove; I, sample rack; J, sample capsule; K, oil bath container; L, 13" support leg; M, motor support leg; N, Nylon collar; O, lid; P, motor shaft; Q, Nylon bolt and nut.

allows the sample rack to be removed for sample changing. A slotted lid is shown in Fig. 1 as the uppermost part of the sample rack. This lid is to keep the sample capsules from floating out of the slots when the rack is immersed in the oil bath. The oil used is heavy mineral oil (B.P. 360°C - 390°C). This oil is housed in a cylindrical container (K). The axis of the container is the same axis as the Nylon shaft and sample rack. This container is supported on legs (13 inches long) (L) which raise the level of the samples to the center line of the Hohlraum. This puts the samples in the highest flux possible. The container is heated by winding three one inch by eight foot silicone-coated heating tapes around the sides of the cylinder. A fourth heating tape is looped back and forth on the bottom of the oil bath. Temperature control is maintained by operating three of these heating tapes via a rheostat at all times during irradiation. The rheostat would be adjusted so that the three tapes would maintain the temperature of the oil bath at 5 to 10°C less than the desired temperature. The fourth heating tape (controller tape) would be turned on and off by a temperature controller to maintain the desired temperature. The proportional temperature controller was located remote from the Hohlraum. The temperature probe used with the temperature controller was an iron-constantan thermocouple placed in the oil bath.

Other convenient construction features should be noted. The flexible rubber coupling (C) adjusts for small misalignment between the motor shaft (P) and the Nylon shaft. N is a Teflon collar attached to the Nylon shaft. This collar serves as the bearing on which the sample rack turns. The weight of the sample rack is suspended from this bearing, not the motor. M is just a support leg for the motor and neutron shield.

In addition to the neutron shielding, several safety features were incorporated in the design. (1) When the entire assembly shown in Fig. 5.1 was irradiated, it was placed in an oil drip pan. If the oil bath leaked, the oil would be caught in the drip pan. (2) A drastic oil leak could be remotely monitored and the irradiation stopped. A second thermocouple (safety thermocouple) was placed between the controller tape and the wall of the oil bath container. If a large leak occured, the oil level in the oil bath would drop below the controller thermocouple. The heat conduction between the wall and the controller thermocouple would be poor. Thus, the controller tape would be turned on all the time. The temperature monitored by the safety thermocouple would increase past a preset safety margin around the desired operating temperature. This would cause a remotely placed bell to ring, alerting the experimenter. (3) When the oil bath was filled with oil at room temperature, the oil level (including the samples and sample rack) was two inches below the top of the container. This margin would allow for expansion of the oil bath during heating.

(4) The oil was preheated in an open container for eight hours at 200°C before it was used for an irradiation. This would remove any significant low-boiling fraction. Nevertheless, oil vapors would be formed by the heating and irradiation. These vapors were not allowed to escape into the Hohlraum. The lid (O) of the oil bath was vapor sealed to the base (K) by a Teflon O-ring placed in groove H. The lid was held down by twenty 1/4-inch Nylon bolts (and nuts) (Q) which fastened the lid to the lip of the oil bath container. The thermocouple leads were

forced through tiny holes in a Teflon plug before they were welded into a thermocouple. This Teflon plug was screwed into a threaded hole in the lid (E) to make a pressure seal. Vapors could not escape around the Nylon shaft because of two Teflon gaskets (F). Pressure relief at 3 psi above atmospheric was provided by a brass pressure relief valve (B). The pressure relief valve was placed behind the neutron shielding but connected to the interior of the container by a pipe (D). The exhaust side was connected to the reactor facility vacuum exhaust system by 3/8" Nylon tubing. Any vapor which escaped around the lower gasket would presumably be exhausted before it escaped past the upper gasket and into the Hohlraum. The exhaust from the pressure relief valve and from the volume between the gaskets is not shown in Fig. 5.1.

(5) Also not shown in Fig. 5.1 is a microswitch which showed if the Nylon shaft was indeed rotating during irradiation. One side of the top of the Nylon shaft that projected into the neutron shielded region was flattened. The arm of the microswitch was placed against the side of the shaft so that as the shaft rotated the switch would be activated by the flattened side. This would occur once each revolution and could be remotely monitored.

(6) The temperature controller, the rheostat, the safety thermocouple alarm circuit, and the rotation sensor were all located external to the Hohlraum. The wires and the Nylon tubing were lead out of the Hohlraum through a beam port. A wooden beam port plug was made with one groove down the entire length for the nylon tubing and another groove for the wires. All wires except the thermocouple wires were fixed

with quick disconnects. The wires were fed through a pressure-tight cap at the external end of the beam port. This cap prevented escape of ^{41}Ar, from $^{40}Ar(n,\gamma)^{41}Ar$, formed in the Hohlraum during irradiation.

(7) The temperature monitored by the control thermocouple was also read out on a strip chart recorder. This gave a continuous record of the temperature control and would alert the experimenter to any failure. (8) In addition to ringing an alarm, the safety thermocouple also shut down all current to the irradiation container. (9) The total current to all four heating tapes is displayed on an ammeter.

5.2.3 Illustration of Irradiation Container Use and Capability

Excellent temperature control (±0.5°C) has been achieved at all temperatures in the 25°C - 200°C range in tests outside the reactor. Irradiations have been made for 24 hours at the Berkeley Campus Nuclear Reactor. Excellent temperature control was obtained at 135±0.5°C. The irradiation container was removed from the Hohlraum 40 hours after the end of bombardment. The observed gamma radiation was primarily from the heating tapes. The observed radiation two inches from the irradiation container and heating tapes (at the level of the sample capsules) was only 130 mR/hr on the side that was nearest the core and 70 mR/hr on the side that was farthest from the core. The flux on the side of the container at sample level was (in units of 10^8 n cm^{-2} sec^{-1}) 34.5 nearest the core, 10.3 farthest from the core and 3.90 in the sample position. The flux was monitored with cobalt foils. Na(I) counters were used to monitor the gamma radiation from ^{60}Co formed in the $^{59}Co(n,\gamma)^{60}Co$ reaction.

6. SAMPLE ANALYSIS*

6.1 Background to Radio-Gas-Chromatographic Analysis

Gas chromatography has been widely applied in the separation and analysis of multicomponent systems. If the components are radioactive, the effluent from a chromatographic column may be mixed with a counting gas and the radioactivity measured as the mixture flows through an internal proportional counter.[110] This immediate radio-assay is called radio-gas-chromatography. The radio-gas-chromatographic anslysis of tritium labeled hydrocarbons is of particular interest to me. I am studying the reactions of recoil tritium atoms.

There were several a priori considerations for the design of a general radio-gas-chromatographic analysis system for the products of recoil tritium reactions: (a) the expected (tritium labeled) products differed widely in boiling points and physico-chemical properties. The expected products ranged from HT and CH_3T to the tritiated parent hydrocarbon (I intended to eventually study the recoil tritium reactions of cyclohexene and methylcyclohexene) and included nearly every straight chain alkane-t and alkene-t species in between (for a review of recoil tritium reactions (see Refs. 6 and 7)). In addition, I wanted to

*The bulk of the material in this section (notable exceptions are Secs. 6.2.5 and 6.2.6) has been previously published as LBL-1249, Multicolumn Radio-Gas-Chromatographic Analysis of Recoil Tritium Reaction Products, by Darrell C. Fee and Samuel S. Markowitz and has been accepted for publication by Analytical Chemistry.

separate the methylcyclohexene-t isomers. (This would determine whether or not direct T-for-H substitution was accompanied by a shift of the double bond.[6,7,75] A normal "boiling point" column would not separate 3-methylcyclohexene-t from 4-methylcyclohexene-t. The three methylcyclohexene isomers had been individually resolved on a saturated silver nitrate/ethylene glycol column.[111] The methylcyclohexene-t isomers and the smaller tritiated alkenes from recoil tritium reactions would be individually resolved on a saturated silver nitrate/ethylene glycol column. However, all alkane-t species would emerge as one peak from such a column.[112] This suggested an aliquoting procedure. The tritiated alkenes and the methylcyclohexene-t isomers could be assayed using one aliquot. The tritiated alkanes could be assayed using another aliquot. Upon further consideration, I decided that no aliquoting procedure would be possible. Aliquoting might lead to unequal fractionation of low vapor pressure parent compounds. Consequently, I decided to inject the entire sample at once. The typical gaseous sample was contained in a glass capsule, 6 cm long with an internal diameter of 1.5 cm. (The dimensions of the capsule are fixed at such large values to minimize the loss of recoil tritons to the capsule wall following the $^{3}He(n,p)T$ reaction.[44]) The glass capsule would be mechanically crushed directly in the stream of the chromatograph.

This led to: (b) <u>a large sample injection volume</u>. The sample is initially distributed throughout the 20 cm^3 volume of the mechanical crusher. This sample volume is swept onto the gas chromatographic column in about 100 sec, assuming typical radio-gas-chromatographic

flow rates and pressure drops.[113] In contrast, the typical residence time in the 85 ml internal proportional counter is only 60 sec.[113] The residence time in the counter is smaller than the sample injection interval. Although the proportional counter has a large volume compared to conventional GC detectors, the volume of the counter is not a limiting factor. The large sample injection volume is the most important factor affecting peak resolution.

However, the use of the counter does add one limitation, namely, (c) the flow rate through the counter must remain constant. The flow rate, F (ml sec^{-1}), is related to the experimentally determined area of the ith radioactivity peak, A_i (counts) by

$$A_i = \lambda N_i E V F^{-1} \qquad 6\text{-}1$$

where λ is the decay constant of the radioactive nuclide (sec^{-1}), N_i is the number of radioactively labeled molecules of identity i, E is the detection efficiency of the counter for the nuclide of interest, and V is the active volume of the counter (ml).

The variable of experimental interest is N_i, the number of tritium labeled molecules in a peak whose identity is known from the retention time. N_i can easily be determined if the flow rate, F, is constant while a peak is being counted. The values for E and V can be experimentally determined. The value of λ is known from other sources.[43] In principle, N_i could be determined although the flow rate, F, varied drastically from one peak to another. The flow rate must only be known for each peak and constant during the counting of any given peak. In

practice, a peak to peak change in flow rate is virtually impossible. The measured flow rate, F, is really the combined flow rate of the helium carrier gas flowing through the chromatographic column, and the counting gas, usually propane. The helium flow rate and the propane flow rate can not be independently varied. A 1.8 to 1.0 propane to helium ratio gives the best counting characteristics.[113] An independent change of either the helium flow rate or the propane flow rate causes a shift in the plateau of the proportional counter. A plateau shift can change the detection efficiency, E. It is extremely difficult to make stepwise changes in both the helium and propane flow rates and to be sure that the combined flow rate has stabilized (at a 1.8 to 1.0 ratio) in the interval between peaks.

The limitation of a constant flow rate through the counter is, in practice, a limitation to a constant flow rate for the helium carrier gas. The helium flow rate is usually changed in programmed temperature gas chromatography[114] and in programmed pressure gas chromatography[115] and in sequential applications of the two techniques.[116] Consequently, these powerful techniques for gas chromatographic separations over a wide range of boiling points have not been used in radio-gas-chromatography. However, a stepwise change in column temperature accompanied by a stepwise change in column inlet pressure could be used in radio-gas-chromatography. The simultaneous change of two factors which affect the helium flow rate could be pre-calibrated so that the resultant helium flow rate is unchanged. The simultaneous stepwise change of both temperature and pressure could cause large perturbations in the helium flow rate. The

time interval between the radioactivity peaks would have to be large enough so that the helium flow rate was stabilized before the next peak was counted.

Another standard gas chromatographic technique which has not been used in radio-gas-chromatography is post-injector splitting of the helium flow stream.[117] With flow splitting, the effluent from each column must be individually monitored. This is often prohibitive in radio-gas-chromatography because it means duplication of relatively expensive counting equipment. (d) All counting of radioactivity must be done with only one counting system.

The four design criteria discussed above are not unique to the radio-gas-chromatographic analysis of recoil tritium reaction products. The same criteria are individually met elsewhere in the application of gas chromatography. Consequently, there remained three avenues of attack: a) Trapping and reinjecting. The disadvantages of trapping are the tedious procedure involved in the addition of non-radioactive carrier and the nagging worry about trapping efficiency.[118]

b) Backflushing.[119] Backflushing offers no advantage in the radio-gas-chromatographic analysis of recoil tritium reaction products. Although the parent hydrocarbon certainly makes up the bulk of the sample, there is no sharp break in the boiling points between the parent hydrocarbon and the other tritiated products. In addition, tritiated products of higher boiling point than the parent are formed.[16-18] Backflushing would not resolve these products from the parent hydrocarbon.

c) Multiple columns in series. Theoretically, the separating efficiency of each individual column may be reduced if the sample is

passed through more than one column before reaching the detector.[120] However, useable separations have been made with columns of different liquid phases in series. No one column completely resolved all the peaks. All peaks were resolved when the sample was passed through more than one column in series.[121] It is not feasible to pass all sample components through all columns if the sample components differ widely in boiling points and physico-chemical properties. The column in a series which gives good resolution of the low-boiling components gives unuseable peak shapes for the high-boiling components, and vice-versa. The obvious solution was to arrange the column in the series in the order: injector, high-boiling component column, low-boiling component column, detector. The trick was to pass the low-boiling components through both columns while passing the high-boiling components through the high-boiling column only. Three methods of solution have been developed: i) Rabinovitch and co-workers start with the columns in series but at the appropriate time during analysis change to have the columns in parallel.[122] This requires multiple detectors.

ii) Rowland and co-workers start with the columns in series but reverse the order of the columns at the appropriate time during the analysis.[123] Some or all of the low-boiling components pass through the high-boiling component column twice. This "recycling", using match columns, has been used to achieve difficult isotopic separations.[124] With the unmatched columns required in a general radio-gas-chromatographic analysis system, the recycled peaks and the high-boiling component peaks may overlap.

iii) Borfitz had discovered that the helium flow through a column may be stopped and peaks in that column may be "stored" for analysis at a later time.[125] The intuitive prediction is that the shape of the peaks would deteriorate rapidly once the flow through the column was stopped. In practice, useable peak shapes were obtained later when flow was routed through the column in the same direction as before the flow stoppage. Several authors[126-128] had applied the stop-flow technique to a series of multiple columns. In this multicolumn stop-flow method, the order of the columns remains unchanged.

The continuing interest in isotopic separations in general[118] and my specific interest in separating species which differ only by the position of the radioactive label (see Refs. 4 and 129) led me to create a multicolumn series with stop flow <u>and</u> recycle capability. I decided to maintain a constant flow rate through the detector in stop-flow applications by stepwise pressure programming instead of using preset needly valves (as in Refs. 122,126-128). A radio-gas-chromatographic system with stepwise pressure programming capability would also have stepwise temperature programming capability as discussed earlier. Later I was forced to develop the ability to remove and further separate unresolved peaks emerging in the middle of the analysis. This is known as taking a center cut. I am reporting a general radio-gas-chromatographic system which operates under the design criteria discussed earlier: (a) The components of the hydrocarbon mixture differ widely in boiling point and physico-chemical properties. (b) The sample injection volume is large; namely the whole sample. (c) The flow rate through the detector

is constant. (d) All peaks are monitored with the same detector (beta proportional counter). This system uses four columns in series and has the capability for (a) stop flow, (b) recycle, (c) center cut, (d) stepwise pressure programming, and (e) stepwise temperature programming applications.

6.2 Apparatus and Procedures

6.2.1 Pressure Control and Valve Arrangement

Pressure regulation of the helium carrier gas began at the commercially available tank with a standard two stage regulator. This regulator maintained a pressure of 100 psi in the ballast tank. The ballast tank was a common input to five single-stage regulators used for pressure programming. These single stage regulators each exhausted through a check valve (on/off) into a common manifold. Only one pressure regulator was open to the manifold at any time. That pressure regulator was preset for a specific series of columns. The preset pressure maintained a helium flow rate through the counter of 30 cc/min. Removing (or adding) a column from (or to) the series required a shift to a lower (or higher) preset pressure to maintain a 30 cc/min flow rate. The pressure in the manifold was changed by first shutting off the pressure regulator in current use. The manifold pressure was then bled off to the atmosphere. Following bleed-off, the new preset pressure regulator was opened to the manifold. This made a sharp pressure change. Reproducible flow rates were obtained with these "presettings" over long periods of time. During an analysis, the flow rate obtained through use of preset pressure regulators was more constant than the flow rate

obtained using a commercial constant flow controller (#63-BU-L, Moore Products Co.); particularly during stepwise temperature programming and reversing the order of the columns in the flow stream. This manifold was the beginning of the arrangement of columns and 4-way valves shown in Fig. 6.1.

The flow down stream from the manifold was through 1/6 inch o.d. stainless steel tubing. The 4-way valves were #P26-418 from Circle Seal Corp. The stainless steel tubing and 4-way valves were operated at 25°C. The exhaust from the buffer column passed through the detector side of a standard thermistor cell (plus power supply and bridge circuit) from Gow-Mac Corp. The thermistor detector was, of course, not sensitive enough to measure carrier-free amounts of tritium labeled hydrocarbons. The thermistor detector was used to determine retention times of standards and to monitor the parent hydrocarbon peak during an actual analysis. The thermistor response was printed out by one pen of a Leeds and Northrup 10 mV dual pen strip chart recorder. Following the thermistor the helium flow stream was mixed with propane in a standard 1/4 inch Swagelock Tee. The propane flow stream similarly consisted of a commercial tank, two-stage regulator, ballast tank, single-stage regulator, check valve, dummy column to give a useable pressure drop, then the mixing Tee. The combined helium and propane flow passed through the counter, through a soap bubble flow meter and was then exhausted into a hood. The combined flow rate was maintained at 83 cc/min, giving the desired 1.8/1.0 propane to helium mixture.[113] The propane pressure was not changed during an analysis.

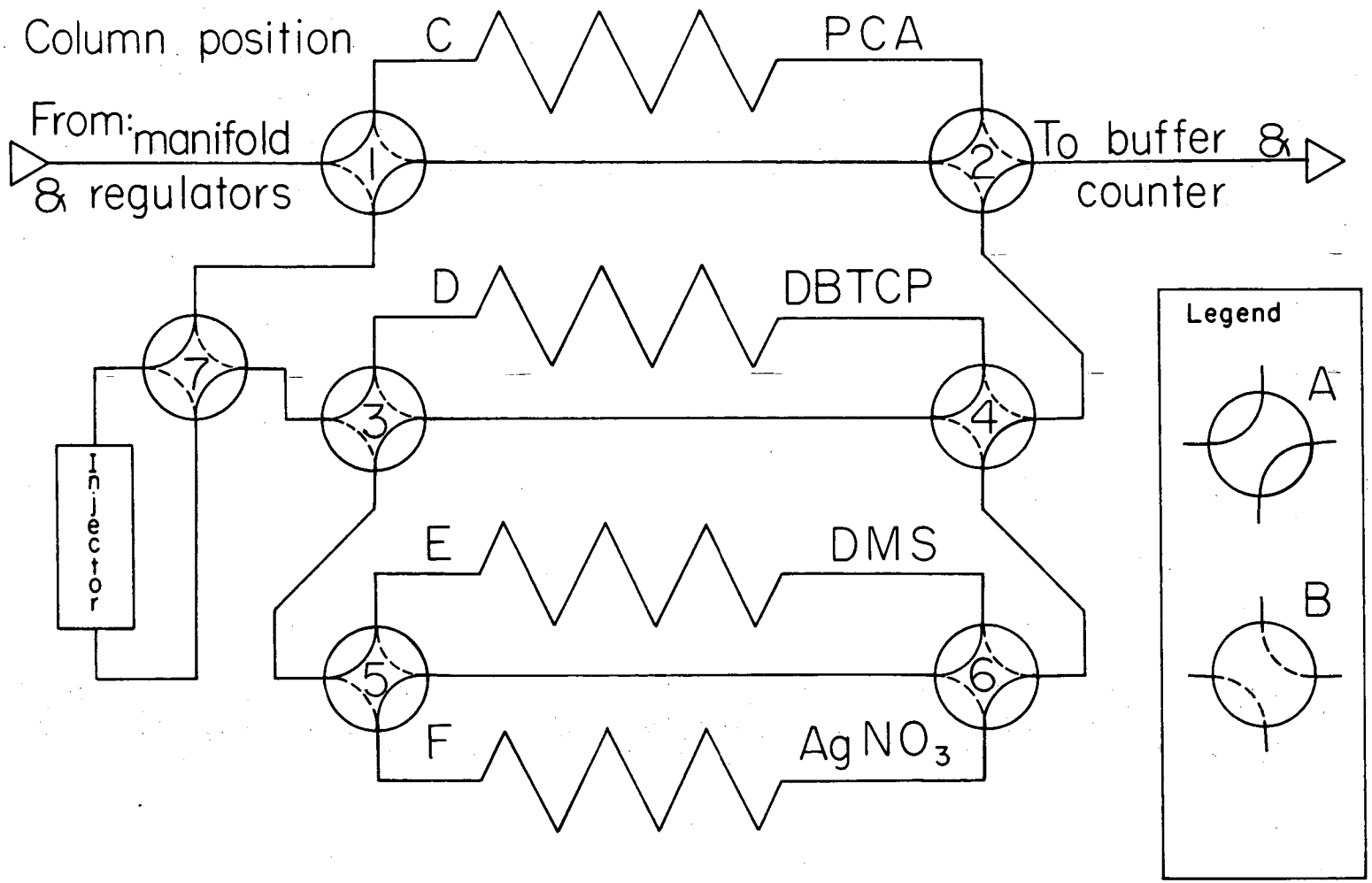

XBL729 - 4074

Fig. 6.1. Schematic diagram of gas chromatographic flow stream. The columns are defined in the text. The choice of columns is specific for this analysis. The recycle arrangement of 4-way valves with positions for four columns is presented as a general gas chromatographic system. The injector is discussed in Sec. 6.2.5 and illustrated in Fig. 6.4.

6.2.2 Columns

HT, CH_3T, ethane-t, and ethylene-t were resolved on a 50 ft. column of 10% propylene carbonate (PCA) on 60/70 mesh activated alumina F-1 in 1/4 inch o.d. copper tubing. The method of column preparation and typical retention times are given elsewhere.[130] This column was operated at two temperatures: -78°C, maintained by immersing the column in a dry ice-acetone slurry, and -8°C, maintained by immersing the column in an acetone bath inside a commercial freezer. The temperature change from -78°C to -8°C (or -8°C to -78°C) was made by physically removing the PCA column from one temperature bath and placing the column in the other temperature bath. Tritiated C_3 and C_4 hydrocarbons were resolved on a 50 ft. column of 25% 2,4-dimethyl sulfolane (DMS) on 30/60 mesh acid-washed Chromosorb P in 1/4 inch o.d. copper tubing. Typical retention data for this column are given in Ref. 131. This column was operated at room temperature. Tritiated C_5 - C_7 hydrocarbons were resolved on a 4.5 ft. column of 22% di-n-butyl tetrachlorophthalate (DBTCP) on 30/60 mesh acid-washed Chromosorb P in 1/4 inch o.d. copper tubing. Typical retention data for this column are given in Ref. 132. This column was operated at room temperature. During the course of this work, it became necessary to separate 1,3 butadiene-t from 1,3 butadiene-d_5t (see Secs. 7 and 8). This separation was done on a 25 ft. column of saturated silver nitrate/ethylene glycol ($AgNO_3$) on 30/60 mesh acid-washed Chromosorb P in 1/4 inch o.d. stainless steel tubing. The method of column preparation and typical retention data are given in Ref. 111. This column was operated at room temperature. A buffer column was placed

immediately before the counter to minimize the flow perturbations caused by changing the order of the columns in the series. The buffer column was 25 ft. of 60/80 mesh glass beads in 1/4 inch o.d. copper tubing and was operated at room temperature.

6.2.3 Counting and Data Reduction

The 85 ml proportional counter has been described.[113] A typical plateau of this counter is shown in Fig. 6.2. The efficiency of this counter, E in Eq. (6-1), for tritium was 99±1%. The high voltage on the centerwire of the counter was maintained by a 5 kV power supply. A pre-amplifier of my own design (schematics are available on request) was coupled to the counter. The pulses from the pre-amplifier went through a standard amplifier and single-channel analyzer, before passing through a standard anticoincidence network. An anticoincidence screen of plastic scintillator as well as an arrangement of lead bricks shielded the counter from background radiation. This lowered the background of the counter to typically 10 counts/min. The train of pulses emerging from the anticoincidence network was divided. One branch went to a rate meter. The rate meter response on a logarithmic scale was printed out on one pen of the dual pen recorder. During an actual analysis, this gave a continuous plot of the log of activity (monitored by the counter) versus time. The other branch passed through a variable time control unit and into a 1024-channel analyzer (Technical Measurements Corp.). The 1024-channel analyzer was used in the multiscaler mode. The length of the time during which the response of the counter was recorded in a single channel was set by the variable time controller unit. At the end of the preset

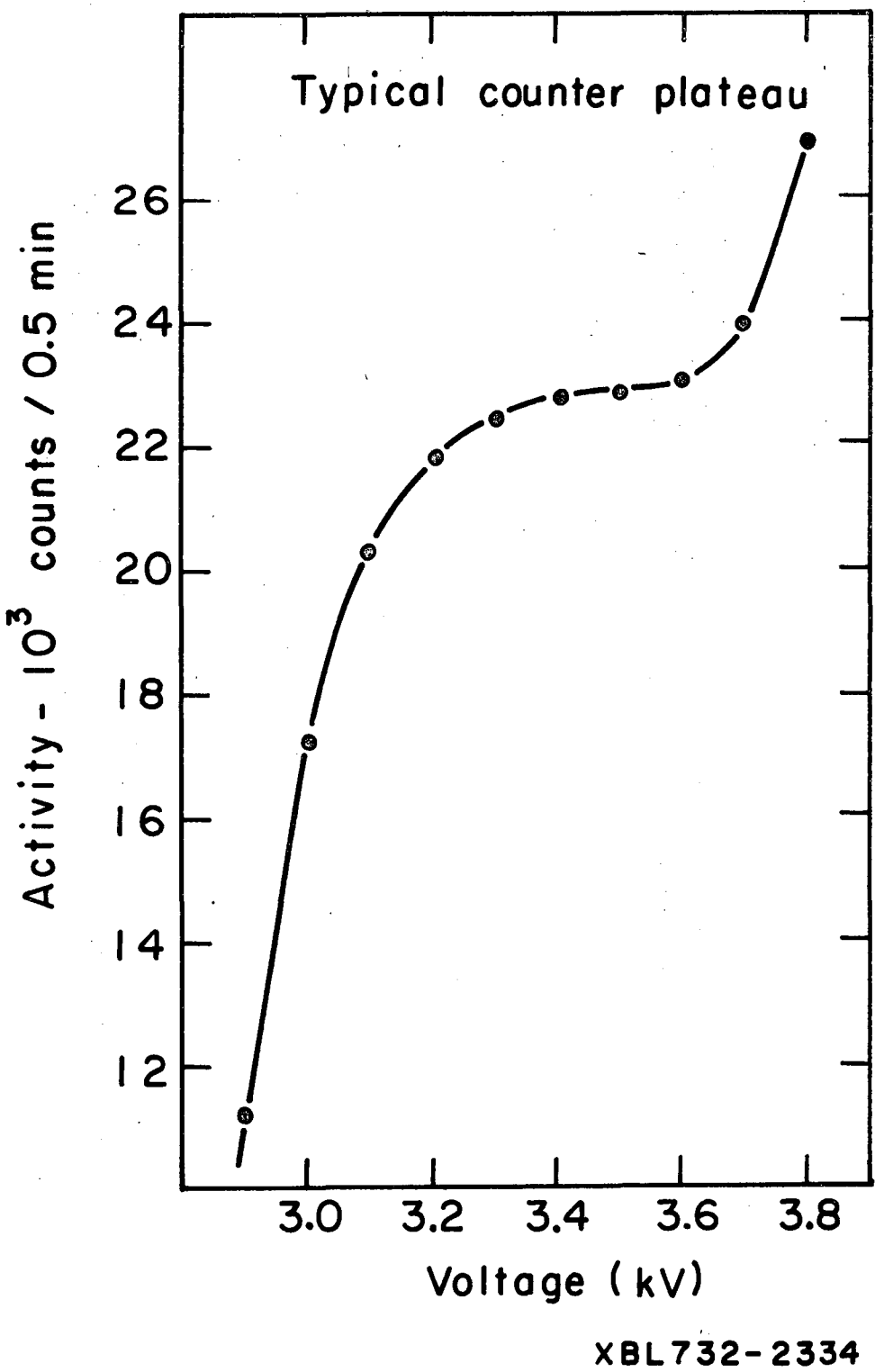

Fig. 6.2. Typical Proportional Counter Plateau. The data is taken counting a ^{60}Co source external to the counter.

length of time the controller unit advanced the counter response to the next channel. The controller was started when the sample was injected.

At the end of analysis the number of counts recorded in each channel had been stored in the memory of the analyzer. The memory could be printed out in both analog and digital fashion. Qualitative information could be obtained from the analog printout on a Hewlett-Packard X-Y plotter. The analog printout was a plot of counts (in each channel) versus channel number. The channel number could be converted to time from knowledge of the settings of the time controller. A typical radio-chromatogram is shown in Fig. 6.3. The sequence of operations used to obtain this radio-chromatogram is given in Table 6-1. (Calibrated retention data is given in the Appendix, Table A-6-1.)

Quantitative information could be obtained from the digital printout of a Hewlett-Packard model 562A printer. The digital printout could be obtained in two modes. Mode one gave the channel number and the counts recorded in that channel. Mode two gave the channel number and the sum of the counts in that channel and all preceding channels. A_i, the activity of the ith radio-activity peak (see Eq. (6-1)), could be easily obtained from this information. First the mode one printout was scanned. A channel number corresponding to the start of the ith peak selected. For this channel number the value of the running sum was determined from the mode two printout. Similarly, the value of the sum was determined for the channel corresponding to the end of the ith peak. The difference of these two sum values gave the gross area under the ith peak. A_i was this gross area less background contribution.

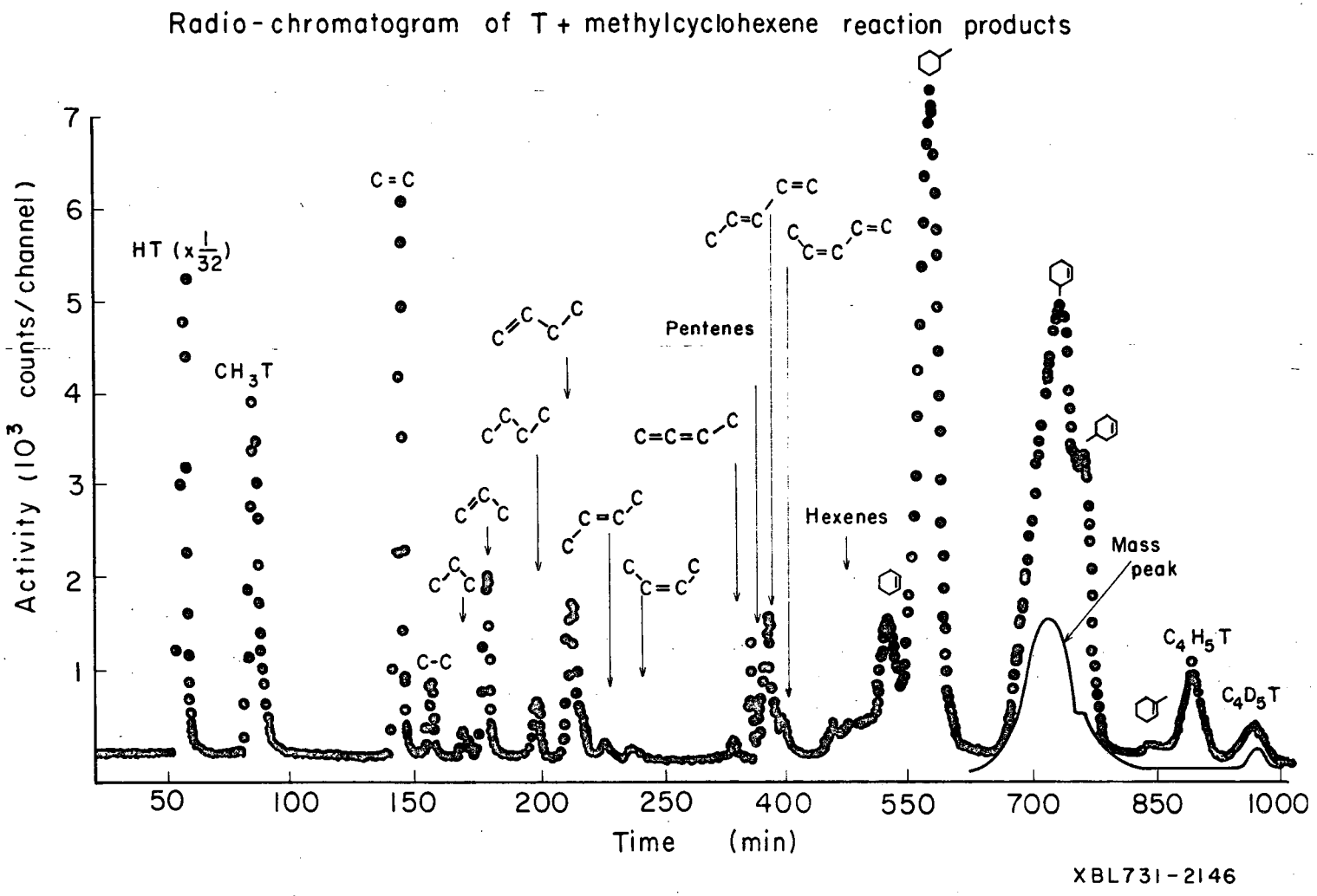

Fig. 6.3. Radio-gas-chromatogram of recoil tritium reaction products. Sample preparation is given in the text. The HT peak shown is 1/32 actual. Only the carbon skeleton is shown for the other radioactivity peaks. All mass peaks are shown on the same arbitrary scale. See Table 6-1 for an explanation of the time scale.

Table 6-1. Sequence of Radio-Gas-Chromatographic Operations

Time Min.	Manifold Pressure psi	Arrangement of Valves[a] 123 456 7	Column Order in Flow Stream[b]	Comment
-1	34.4	BBA AAB B	DBTCP, DMS, PCA-78	break capsule
0		BBA AAB A		inject sample; timing interval 0.5 min/channel
10		BBA AAB B		injector by passed
30	34.2	BBB AAB B	DMS, PCA-78	DBTCP by passed
38	28.0	ABB AAB B	PCA-78	DMS by passed
98	32.0		PCA-8	Temp. change -78°C to -8°C for PCA
162			PCA-78	Temp. change -8°C to -78°C for PCA
165	34.2	AAB AAB B	PCA-78, DMS	flow restarted in DMS
250				change timing interval to 1.5 min/channel
265	36.2	AAB AAA B	PCA-78, DMS, $AgNO_3$	$AgNO_3$ center cut of butadienes
320		AAB ABB B	PCA-78, $AgNO_3$, DMS	end center cut
375		AAB AAA B	PCA-78, DMS, $AgNO_3$	order switched
380		AAB BAA B	PCA-78, DMS, $AgNO_3$, DBTCP	flow restarted in DBTCP

[a]See Fig. 6.1.

[b]With valves as indicated and propylene carbonate column (PCA) in position C in Fig. 1, di-n-butyl tetrachlorophthalate column (DBTCP) in position D, 2,4-dimethyl sulfolane column (DMS) in position E, saturated silver nitrate/ethylene glycol column ($AgNO_3$) in position F.

6.2.4 Sample Preparation for the Illustrated Analysis

The procedure employed for sample preparation has been described previously (Sec. 4.2.2). The sample was a 1720 Pyrex capsule (14 ml internal volume) to which 8.5 cm 3-methylcyclohexene, 2.6 cm of 4-methylcyclohexene, 1.5 cm butadiene-d_6 and 30 cm of ^{3}He had been added (pressures corrected to 135°C). The irradiation was for 24 hours at a flux of 3.9×10^8 n cm^{-2} sec^{-1} in the Hohlraum of the Berkeley Campus Nuclear Reactor. The temperature of the sample during irradiation was maintained at 135.0±0.5°C by the specially designed irradiation container described in Sec. 5.2.

6.2.5 Sample Injector

A side view of the sample capsule breaker is shown in Fig. 6.4. The breaker is constructed from brass unless otherwise indicated. The direction of flow through the breaker is from right to left. The gas sample capsule is placed in the breaker at the right end. The gas tight seal is made by screwing the hex head bushing (B) in against the removable end plate (C) to compress the Viton o-ring (D). Helium flow comes into the breaker through 1/16 inch o.d. stainless steel tubing (A). The 1720 Pyrex capsule is crushed by depressing a spring loaded plunger (E). A gas tight seal around the plunger shaft is made by Viton o-rings (F). The gas phase tritium labeled products are liberated when the capsule is crushed. These products are carried out through the left end of the breaker by the helium flow stream. Another gas tight seal is made similar to the one at the right end.

The breaker was heated by wrapping it with heating tape. In general, for gas phase capsules the breaker was heated to the same

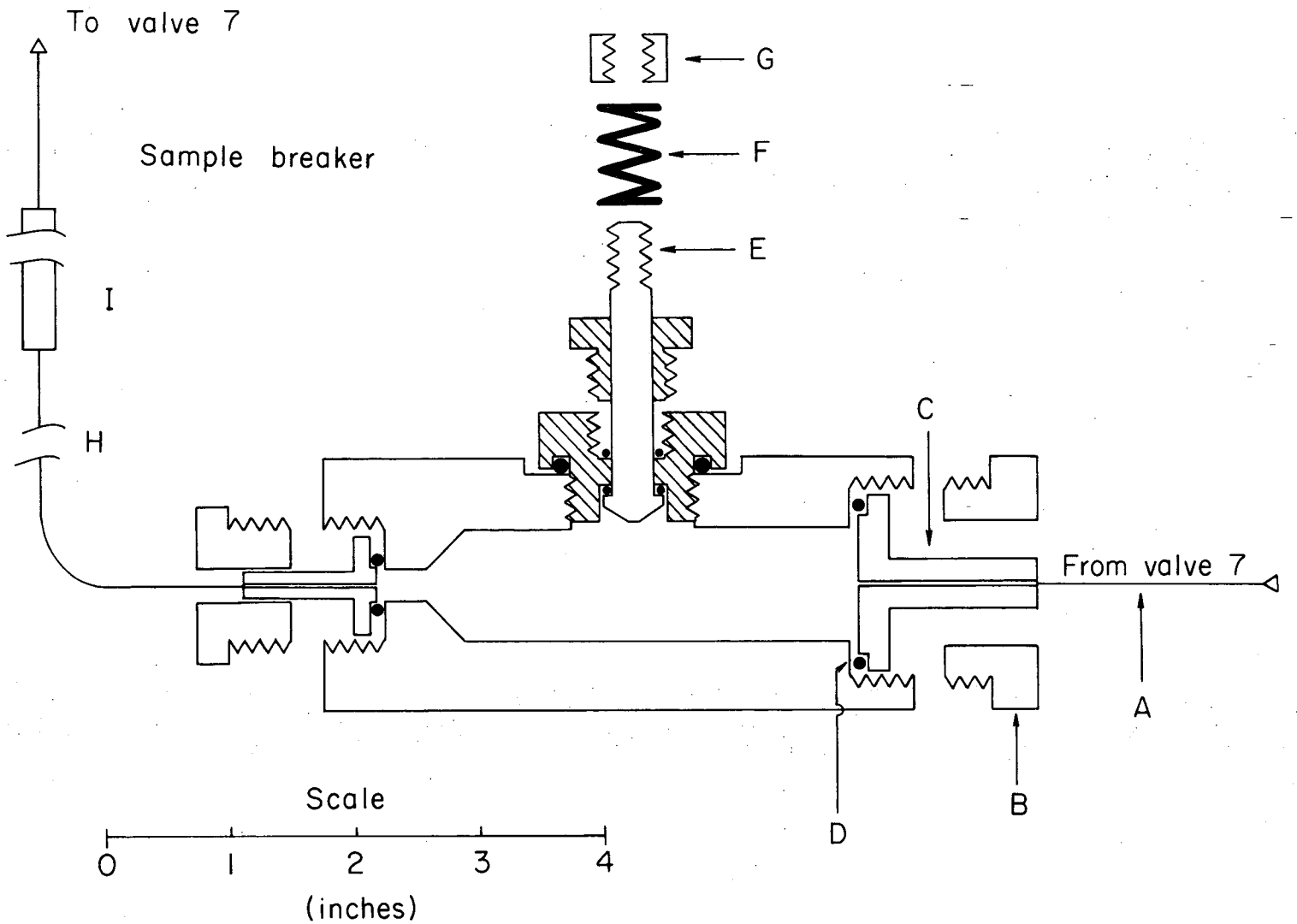

XBL732-2336

Fig. 6.4. Sample Capsule Breaker (Injector), side view. The helium flow stream is from right to left through the breaker. The labels "from valve 7" and "to valve 7" refer to valve 7 in Fig. 6.1.

temperature at which the irradiation was made. For liquid phase samples the breaker was heated to 135°C. For the samples in capillary tubing, a brass insert was made to hold the sample tube in position just below the plunger. The sample tube and insert would be placed in the breaker similar to a gas phase capsule.

The exhaust from the breaker passed through a ten foot section of 1/16 inch o.d. stainless steel tubing (G) called the cool tube (operated at 25°C at all times) and then through a six inch column of 60/80 mesh glass beads in 1/4 inch copper tubing. This small buffer column was called the plug and was operated at 25°C. The cool tube and plug will be discussed later.

Before being placed in the breaker the standard procedure for determining the internal volume of the gas phase capsule was initiated. The total volume displaced by the capsule (volume of glass (V_g) plus internal volume of the capsule (V_c)) was measured by placing the capsule in a standard volume measuring device of volume V_s. The remaining volume was filled with water from a buret. The volume of water required was $V_s - (V_g + V_c) = V_1$. The glass pieces from the capsule were collected after the capsule was broken. After the high molecular weight tritiated products had been extracted from these capsule pieces (see Sec. 6.2.6) the pieces were placed in the standard volume measuring device. Again the standard volume was filled with water. The volume of water required was $V_s - V_g = V_2$. The internal volume of the capsule is then given by $V_c = V_2 - V_1$.

6.2.6 Recovery and Analysis of High Molecular Weight Tritiated Products; "Polymer-t"

Tritium labeled products which are not eluted in the normal radio-gas-chromatographic analysis scheme discussed above are called "polymer-t". The recovery of "polymer-t" was similar to that previously described:[18] (a) Low (molecular weight) "polymer-t" is backflushed off the DBTCP column. In backflushing, flow is reversed in the column (after the radio-gas-chromatographic analysis) for 1.5 times the length of the forward flow. The "polymer-t" is collected in toluene when the reversed flow is bubbled through a toluene trap operated at 25°C. Backflushing of the DMS and PCA columns did not result in the recovery of any "polymer-t". All peaks stored in the DMS and PCA columns were apparently analyzed in the normal (forward flow) radio-gas-chromatographic analysis. Only the DBTCP column was routinely backflushed.

(b) Medium (molecular weight) "polymer-t" was washed with toluene from the cool tube and backflushed from the plug. The plug was used to prevent "creep" of medium "polymer-t" down the 1/16 inch stainless steel tubing and onto the DMS and PCA columns.

(c) High (molecular weight) "polymer-t" was washed with toluene from the internal walls of the sample breaker and soxhlet extracted with toluene from the wall of the broken sample capsule. The soxhlet extraction process was for 24 hours.

(d) The toluene fractions were collected in standard liquid scintillation vials to which a standard scintillator solution of 4 gm POP (2,5 diphenyloxazole) and 0.1 gm dimethyl POPOP {1,4-di-(2-[4-methyl-5-phenyloxazoyl]-benzene)} per liter of toluene. Corrections for the

quenching and determinations of the absolute counting efficiency were made by the external standard ratio method[133] using a Nuclear Chicago Mark II liquid scintillation spectrometer. This gave the number of tritium labeled species in each "polymer-t" category (low (L), medium (M), and high (H). This number could be compared to the radio-gas-chromatographic peaks by use of Eq. (6-1).

6.3 Illustration of Radio-Gas-Chromatographic System Use and Capability

A typical analysis of the products of recoil tritium reactions with methylcyclohexene is shown in Fig. 6.3. The sequence of operations used to obtain this radio-chromatogram is given in Table 6-1. This sequence of operations, with the exception of the center cut of butadienes (265 to 300 min), represents a general radio-gas-chromatographic analysis scheme and has been successfully employed in the analysis of the products of recoil tritium reactions with ethylene, propylene, butane, 1-butene, isobutene, cis- and trans-2-butene, butadiene, cyclohexane, and cyclohexene as well as the more difficult case of 3- and 4-methyl cyclohexene shown in Fig. 6.3. The timing of these operations is obviously specific for this choice of four columns. Table 6-1 and Fig. 6.3 are used to illustrate how the arrangement of 4-way valves shown in Fig. 6.1 may be employed to utilize the gas-chromatographic techniques discussed below. The techniques used in the analysis shown in Fig. 6.3 in the order of their appearance are:

(a) Stop flow. At 30 min, C_5 product peaks are just about to emerge from the DBTCP column. C_4 and lighter product peaks have already

emerged and are in the DMS and PCA columns. At 30 min, the C_5 and C_7 product peaks are "stored" in the DBTCP column for future analysis when flow in the DBTCP column is stopped. At 38 min, C_3 product peaks are just about to emerge from the DMS column. C_2 and lighter product peaks have already emerged and are in the PCA column. At 38 min, the C_3 and C_4 product peaks are "stored" in the DMS column for future analysis.

At 165 min, flow is restarted in the DMS column. While the flow through the DMS column was stopped, the pressure equilibrated over the entire column. In restarting the DMS column, this causes a flow surge which lasts for 3.5 min. The first C_3 product peak, propane-t, emerges and starts being counted 4 minutes after restarting. Consequently, the flow surge does not affect the analysis. Storage for a little over two hours has affected the peak shape. For example, the FWHM of a trans-2-butene mass peak increased by 10% because of peak storage. At 380 min, flow is similarly restarted in the DBTCP column. Again the flow surge does not affect the analysis. The FWHM of a cyclohexene mass peak increased by 15% because of peak storage in the DBTCP column for nearly six hours.

(b) Stepwise pressure programming. A constant helium flow rate through the detector was maintained when the DBTCP column and the DMS column were removed from the flow stream by decreasing the manifold pressure at 30 and 38 min, respectively. Similar use of the pressure "presettings" is made at later times in the analysis when columns are added to or removed from the flow stream.

(c) Stepwise temperature programming. At 98 min the operating temperature of the PCA column is changed from -78°C to -8°C. This

shortens the elution time of the ethylene-t peak by 400 min. The stepwise temperature change causes a perturbation in the helium flow rate. This perturbation does not affect the analysis because no peaks are being counted. At 162 min, the C_2 peaks in the PCA column have emerged and been counted. The temperature of the PCA column is then returned to -78°C to minimize the number of pressure regulators required for analysis.

(d) Center cut. It is known from calibration data that the unresolved butadiene-t and butadiene-d_5t peaks would have emerged from the DMS column and been counted at 275 to 290 minutes. The center cut of these peaks is made by placing the $AgNO_3$ column down stream from the DMS column during that interval.

(e) Recycle. The inherent recycle capability of this system is displayed in the permutations of the column order at 265, 300, and 375 minutes. A careful analysis of Fig. 1 will reveal a nested series of recycle loops. The recycle capability is used here to allow separation of the butadiene-t and butadiene-d_5t peaks to proceed simultaneously with the counting of peaks emerging from the DMS and DBTCP columns. The recycling of the butadiene-t and butadiene-d_5t peaks through the DBTCP column is unnecessary for the sake of resolution. However, this recycling is advantageous because after 380 min the analysis is automatic.

6.4 Summary of Radio-Gas-Chromatographic Analysis System

A general radio-gas-chromatographic analysis system has been developed for hydrogen and C_1 to C_7 alkanes and alkenes. Although all peaks had to be monitored at a constant flow rate in the same detector

and the injection volume was large, more than 20 peaks have been analyzed, with good resolution of most peaks, in a total time of 1000 minutes. I conclude that: (1) A recycle system of 4-way-valves and columns allows permutation to be made in the order of columns in a series. These permutations may be useful by themselves in addition to allowing peaks to be recycled and center cuts to be made. In addition, this system of 4-way-valves may shorten the time required for a particular analysis. (The long time required for the analysis shown here was due to the large injection volume.) (2) Stop flow chromatography is a useful technique if the accompanying increase in FWHM can be tolerated. (3) Stepwise inlet pressure programming can be used to maintain a constant flow rate through the detector when a column is removed from the series in stop-flow chromatography. Stepwise pressure programming is additionally advantageous because it allows utilization of powerful stepwise temperature programming techniques.

Therefore, I propose a new gas-chromatographic system that has broad application.

RESULTS AND DISCUSSION

As outlined in the project summary (Sec. 3.3), the first phase of this project was to study T + cyclohexene reactions. Scavenger studies of T + cyclohexene reactions are presented in Secs. 7 and 8. The next step, determining the value of the s parameter in the RRK treatment of the unimolecular decomposition of cyclohexene, is presented in Sec. 9. The study of T + methylcyclohexene reactions in order to test the energy randomization assumption of the RRK-RRKM theories of unimolecular reaction is presented in Sec. 10.

7. SULFUR DIOXIDE AS A RADICAL SCAVENGER IN ALKENE SYSTEMS: ANOMALOUS OXYGEN SCAVENGING EFFECT DISCOVERED*

7.1 Background to Scavenger Studies

Many recoil tritium experiments have used scavengers to remove thermalized tritium atoms and radical intermediates from the system before such species yield products which might be confused with high energy tritium reactions.[6,7] Oxygen,[39] iodine,[134] bromine,[134] deuterated ethylene,[135] nitric oxide,[136] and iodine halides[137] have been used in gas phase experiments. All of these satisfy some of the criteria for a good scavenger proposed by Hawke and Wolfgang,[137] namely

(a) <u>a scavenger must react avidly with the atoms and radicals to be</u> removed, preferably with a collision efficiency near unity. It may then be used in sufficiently low concentrations so as not to interfere with the hot or other primary processes being studied. I am interested in recoil tritium reactions with alkenes. Deuterated ethylene is thus eliminated by this criteria since its scavenging ability is of the same order of magnitude as other alkenes.[15]

(b) <u>a scavenger should be inert with respect to the bulk reagent</u>. For alkene systems, this eliminates iodine, bromine, and the iodine halides since they would undergo rapid addition to the double bond.

---

*The material in this section has been previously published as UCRL-20470, Sulfur Dioxide as a Radical Scavenger in Alkene Systems, by Darrell C. Fee and Samuel S. Markowitz and as Radiochimica Acta, <u>17</u>, 135 (1972).

(c) products of the scavenging reaction should not react further, or if they do, such reaction should be controllable. In the recoil tritium-trans-butene system, the presence of nitric oxide increased the 1-butene-t yield by 100%, presumably through a reversible reaction with sec-butyl-t radicals.[138] Thus, nitric oxide is an unreliable scavenger for alkenes.

(d) a gas phase scavenger must have an adequate vapor pressure at the temperature in question. Oxygen, the only reported scavenger left for alkene systems, readily satisfies this criterion.

(e) furthermore, it is highly desirable, but not always essential that the scavenged species be detectable. The peroxy radicals formed from

$$T + O_2 \rightarrow TO_2 \quad , \qquad 7\text{-}1$$

are not readily assayed in the conventional radio-gas-chromatographic methods used for recoil tritium experiments. In addition, the peroxy radicals may react further with either the bulk reagent or other radicals in the system. As yet, there is no evidence that such further reaction results in products which might be mistaken for the yield of a hot reaction.

7.2 Data and Discussion

I report here a comparison between oxygen and sulfur dioxide as scavengers for recoil tritium-alkene systems. Sulfur dioxide was selected since its reaction with radicals in other systems was known.[139] Radiation damage due to recoils following the $^3He(n,p)T$ reaction was less than 2%.

All data reported represents the average of the yields from two identical samples which agreed on major products to within 3% on the C_4 runs and to within 5% on C_6 runs. No correction has been made for "wall HT".[140,141] The irradiations were at 25°C.

The efficiency of a scavenger is determined by the dependence of various products on scavenger concentration. The yield of products formed solely by hot reactions will remain unchanged over a wide range of scavenger concentrations. The yield of products formed by both thermal and hot processes will decrease rapidly with the addition of scavenger until a plateau is reached where the yield is relatively insensitive to scavenger concentration. In this region, all thermal reactions, except with the scavenger, have presumably been suppressed and the yield is due entirely to hot reactions.[137]

In the T + cyclohexene system, the scavengeable thermal reaction product is cyclohexane-t which results largely from thermal addition of T to the double bond to form a cyclohexyl-t radical. This radical then abstracts a hydrogen from the bulk system to form cyclohexane-t. Ethylene-t and butadiene-t are high energy products from the unimolecular decomposition of excited cyclohexene-t formed by direct substitution.[142-144] The yields of these products for both O_2 and SO_2 scavenger are shown in Fig. 7.1. The sharp drop in cyclohexane-t yield is the same for both O_2 and SO_2. The small drop in the ethylene-t yield is the same for both O_2 and SO_2 and indicates a small thermal route in ethylene-t formation. The butadiene-t yield is constant with SO_2 scavenging but increases by 50% with O_2 scavenging! This anomalous increase in butadiene-t yield with O_2 scavenging is similar to an anomalous increase in the ethylene-t yield with O_2 scavenging that was reported by Urch and Welch in the T + ethane system.[134]

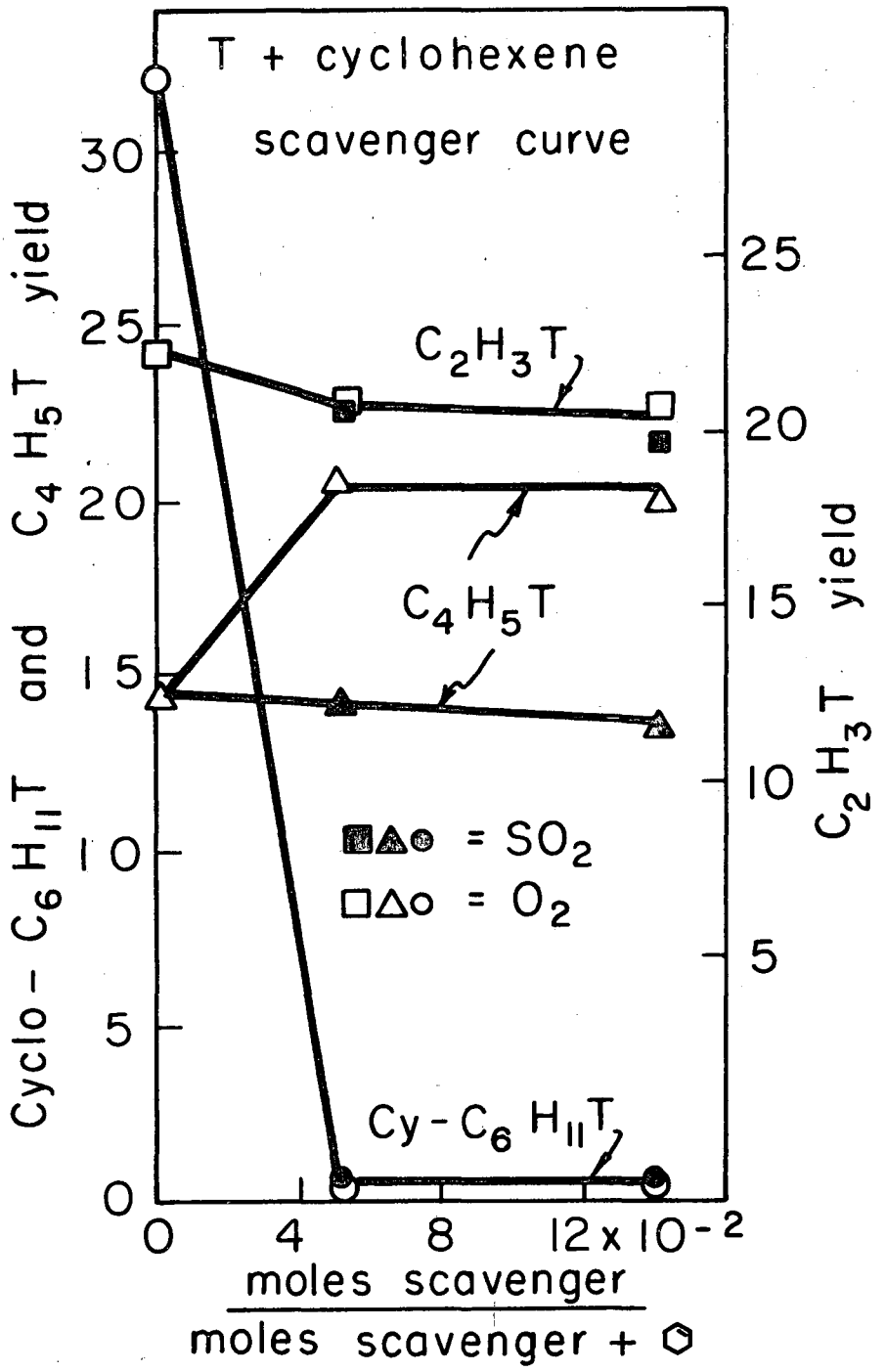

XBL729-4073

Fig. 7.1. Curves of T + cyclohexene system scavenged with SO_2 or O_2. Product yields are listed relative to cyclohexene-t yield as 100. The zero scavenger data point and the 5 mole % scavenger data point have been connected with a line for clarity. I do not mean to imply that the variation of yield with added scavenger is linear in this region. (Data in Appendix, Table A-7-1.)

This anomalous ethylene-t increase was explained by Baker and Wolfgang.[135] Apparently, in the absence of O_2, radiation produced H atoms were being scavenged by the ethylene-t formed by hot tritium reactions. This reduced the ethylene-t yield in unscavenged systems. When O_2 was added, the radiation-produced H atoms were scavenged by the more efficient O_2 and the ethylene-t yield rose to its "hot" value. A similar explanation is unfeasible here. The bulk of the system is cyclohexene which would scavenge any radiation produced H atoms.[145] Another anomalous effect in the cyclohexene + O_2 system is that when samples were irradiated and analyzed less than two weeks after they were prepared (as in data reported here) O_2 uniformly reduced the cyclohexane-t yield. However, oxygen was found to be an unreliable scavenger in samples which had been stored 3-4 months. Apparently oxygen failed due to reaction with cyclohexene. The rate of cyclohexene hydroperoxide formation is non-negligible at room temperature and increases with temperature. In addition, a Pyrex glass surface has a catalytic effect on the initial stages of the reaction.[146] This may rule out simultaneously raising the vapor pressure of cyclohexene by elevating the temperature and employing O_2 as a scavenger.

The comparison of O_2 and SO_2 was also made in the trans-butene + T system. As shown in Fig. 7.2, the yield of butane-t, a product analogous to cyclohexane-t, was sharply reduced on the addition of both O_2 and SO_2. All other products exhibited the same yields for both O_2 and SO_2 scavenging including a 50% decrease in the 1 butene-t yield. The anomalous increase in the 1 butene-t yield with NO as scavenger was duplicated in this laboratory.

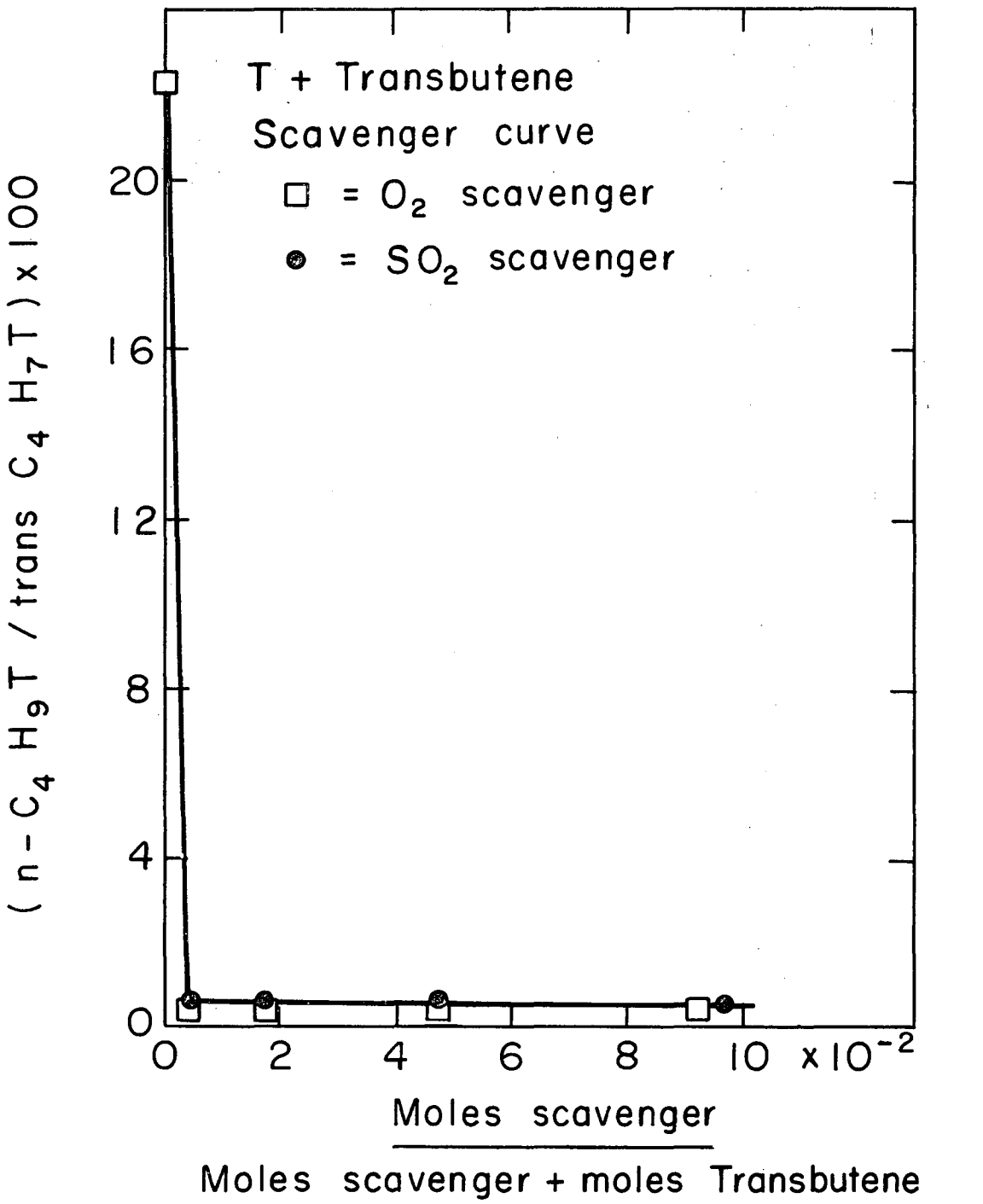

XBL714-3239

Fig. 7.2. Curves of T + trans-butene system scavenged with SO_2 or O_2. The ordinate gives the butane-t yield relative to the transbutene-t yield as 100. (Data in Appendix, Table A-7-2.)

Sulfur dioxide thus compares favorably with oxygen in some alkene systems and is superior in others. Sulfur dioxide has an adequate vapor pressure of over two atmospheres at room temperature.[147] Similar to oxygen scavenging, SO_2 scavenged species of the form $R\text{-}SO_2$ and HSO_2 are a) capable of further reaction. No problems of this sort are apparent in the SO_2 data to date. b) undetected in conventional analysis of gas phase products. While the "polymer-t" data does not indicate the chemical composition of the tritiated products, it does allow crude separation by volatility. Low (molecular weight) "polymer-t" is backflushed from the chromatographic columns. Medium "polymer-t" is washed from a 10 ft. cool tube connecting the sample breaker to the chromatographic columns. High "polymer-t" is washed from the walls of the capsule in which the recoil tritium reaction took place[18] (see Sec. 6.2.6). The relative abundance of activity in each volatility grouping changes with the scavenger employed. In the T + trans-butene system, for example, the "polymer-t" yield was distributed: 75% in the low and 18% in the high groupings for unscavenged samples; 65% in the low and 22% in the heavy groupings for O_2 scavenged samples; 4% in the low and 95% in the high groupings for the SO_2 scavenged samples. The lowered polymer-t volatility with SO_2 scavenging is consistent with the expected formation of scavenged species of higher molecular weight and/or lower volatility with SO_2 than O_2. No correction was necessary for ^{35}S activity (from the $^{34}S(n,\gamma)^{35}S$ reaction) which could be included in these measurements as $^{35}SO_2$ incorporated into the "polymer-t". Under the most extreme conditions, the total ^{35}S activity is less than 1% of the "polymer-t" activity.

I have also compared the scavenging ability of SO_2 and O_2 in an alkane system where hydrogen abstraction to form HT is the low energy reaction. The most stringent test of scavenging efficiency was conducted in a highly moderated system, where the chance of high energy tritium atom colliding with a reactant molecule at a given energy decreases. This results in an increased number of thermalized tritium atoms which would contribute to the yield of a given product. Consequently, the required level of scavenger efficiency is higher when moderator is present.[137] Figure 7.3 shows the effects of SO_2 and O_2 on the HT yield for on 86% Ne moderated T + n-butane system.

Oxygen scavenging of this system with 93% helium moderator has been previously reported by Rosenberg and Wolfgang.[39] My data reproduces the reported scavenging plateau, but shows a different HT/C_4H_9T ratio along the plateau and especially at the zero scavenger intercept. This difference can be attributed to the different moderators used. I selected Ne instead of He moderator to avoid complications from ion-molecule reactions which have been found in He moderated systems.[12,142] The SO_2 data points show no scavenger plateau. In addition, all of the thermal tritium atoms are not being removed by SO_2 since the HT yield is higher for the SO_2 than for the O_2 scavenged samples. These trends are also seen in the data from unmoderated T + n-butane reactions shown in Fig. 7.4. The difference in scavenging efficiency observed here can be attributed to the large difference in collisional efficiency between O_2 and SO_2 for reaction with thermal tritium atoms.

$$T + SO_2 \rightarrow TSO_2 \quad . \qquad 7\text{-}2$$

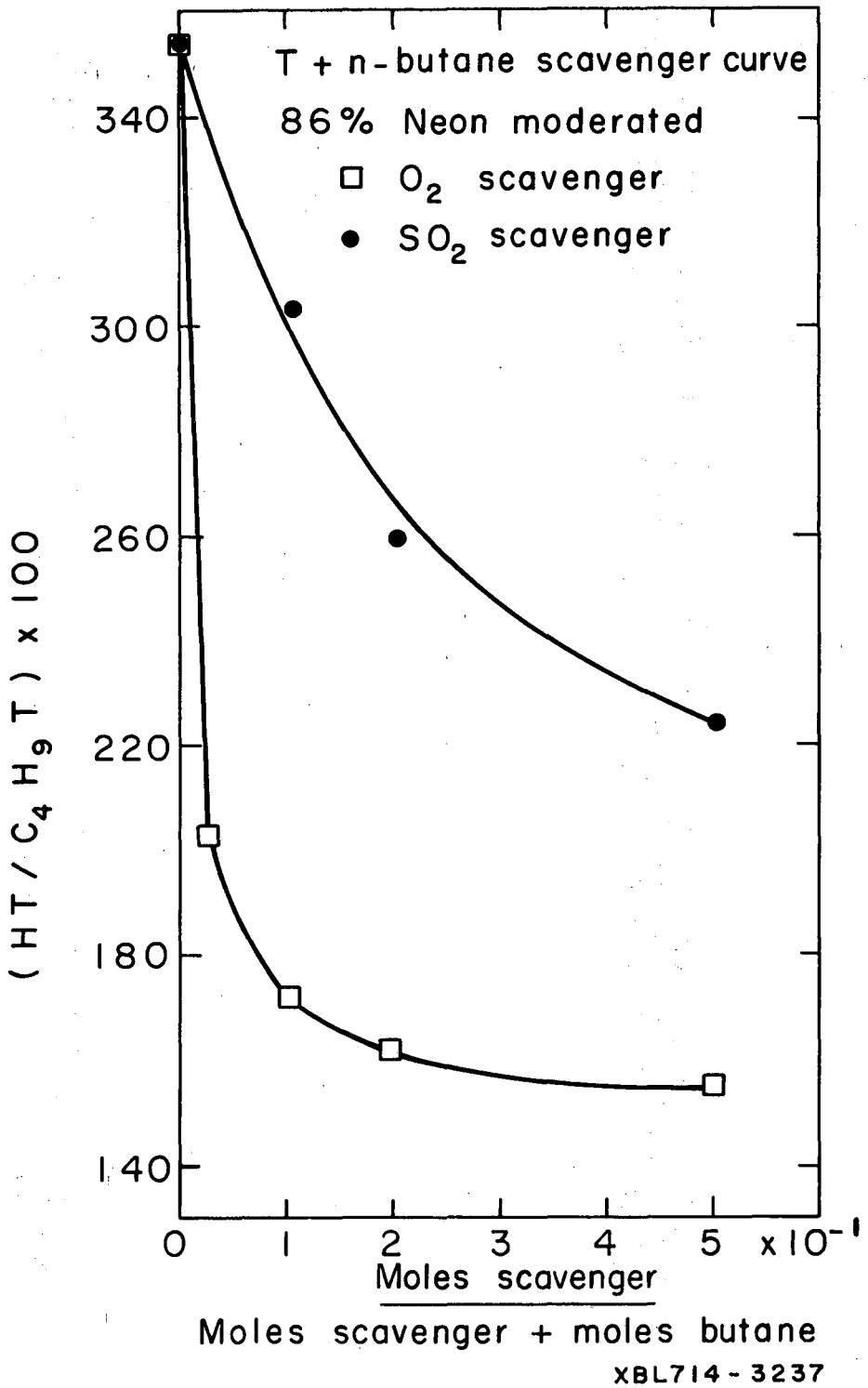

Fig. 7.3. Curves of T + n-butane system scavenged with SO_2 or O_2 and moderated with 86 mole % Ne. The ordinate gives the HT yield relative to the n-butane-t yield as 100. (Data in Appendix, Table A-7-3.)

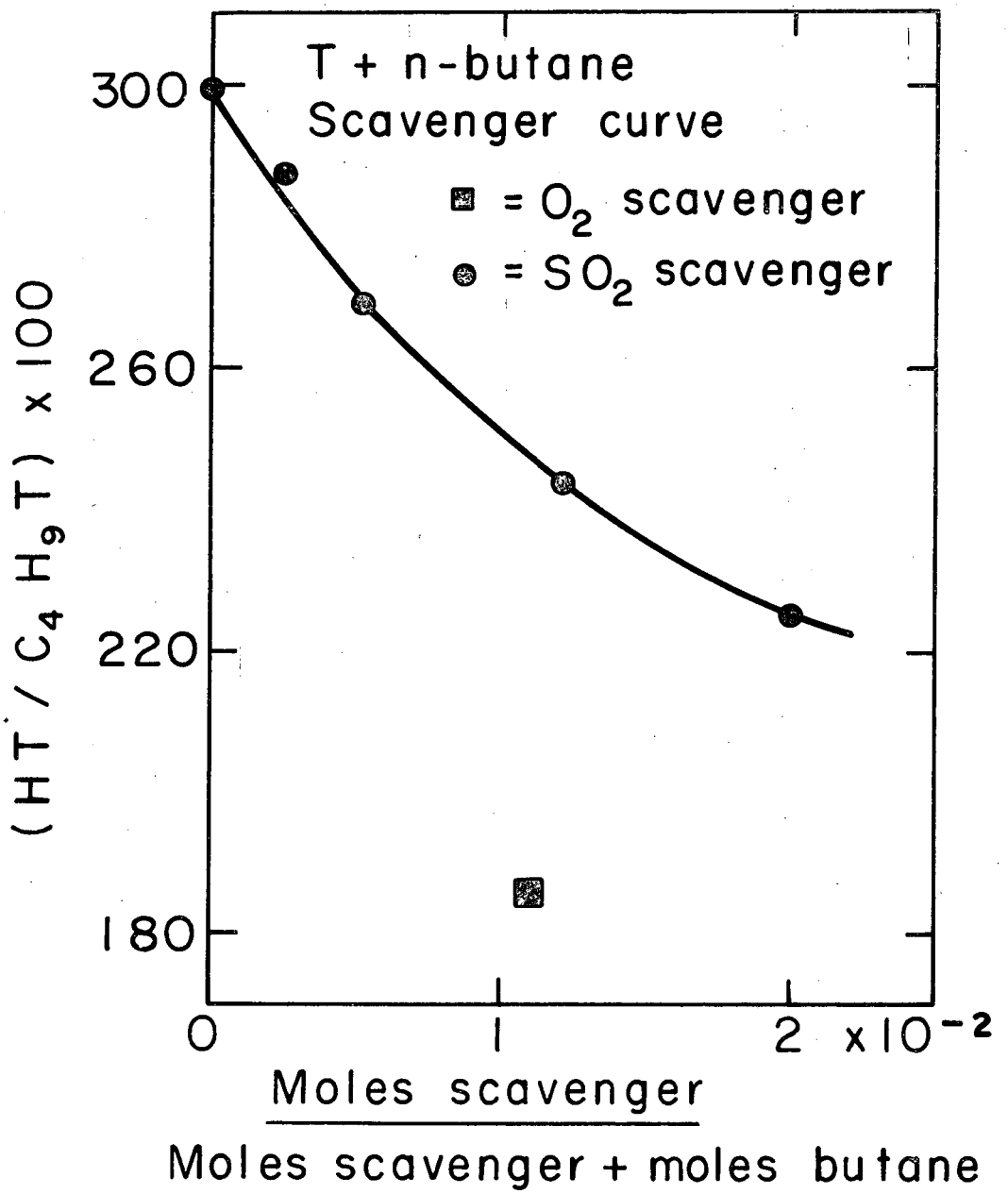

XBL714-3240

Fig. 7.4. Curves of T + n-butane system scavenged with SO_2 or O_2. The ordinate gives the HT yield relative to the n-butane-t yield as 100. (Data in Appendix, Table A-7-4.)

The measured rate constants for reactions 7-1[148,149] and 7-2[150] for protium in place of tritium show a 10^2 preference for O_2 over SO_2.

I conclude that while SO_2 is not a good scavenger in alkanes it compares favorably with O_2 as a scavenger for alkenes. The use of SO_2 as a scavenger may be advantageous in alkenes since O_2, the only other scavenger available, shows some anomalous effects in cyclohexene.

8. SCAVENGER EFFECTS IN THE RECOIL TRITIUM REACTIONS OF CYCLOHEXENE: ANOMALOUS OXYGEN SCAVENGING EFFECT EXPLAINED*

8.1 Further Background to Scavenger Studies

I was interested in explaining the anomalous oxygen scavenging effect shown in Sec. 7. I first reviewed the definition of a scavenger and the data that led to the discovery of the anomalous oxygen scavenging effect.

Many recoil tritium experiments have used scavengers to remove thermalized tritium atoms and radical intermediates from the system before such species can yield products which might be confused with high-energy tritium reactions.[6,7] The yield of products formed solely by high energy (hot) reactions will remain unchanged over a wide range of scavenger concentrations. The yield of products formed by both thermal and hot processes will decrease rapidly with the addition of scavenger until a plateau is reached where the yield becomes relatively insensitive to scavenger concentration. In this region all thermal reactions, except with the scavenger, have presumably been suppressed and the yield is due entirely to hot reactions.[137]

The comparative efficiency of sulfur dioxide and oxygen as radical scavengers was determined in the T + cyclohexene gas phase system

*The material in this section has been previously published as LBL-668, Scavenger Effects in the Recoil Tritium Reactions of Cyclohexene by Darrell C. Fee and Samuel S. Markowitz and accepted for publication by the Journal of Inorganic and Nuclear Chemistry.

(Sec. 7). In this system, one scavengeable thermal reaction product is cyclohexane-t which results largely from thermal addition of T to the double bond to form a cyclohexyl-t radical. This radical then abstracts a hydrogen atom from the bulk system for form cyclohexane-t. The cyclohexane-t yield exhibited identical scavenger plateaus with sulfur dioxide and oxygen scavenging. Ethylene-t and butadiene-t are primarily high energy products from the unimolecular decomposition of excited cyclohexene-t formed by direct substitution.[142-144] The ethylene-t yield exhibited identical scavenger plateaus with sulfur dioxide and oxygen scavenging. The butadiene-t yield was unaffected by sulfur dioxide scavenging but increased by nearly 50% with oxygen scavenging. This anomalous increase in the butadiene-t yield with oxygen scavenging is similar to an anomalous increase in the ethylene-t yield with O_2 scavenging that was reported by Urch and Welch in the T + ethane system.[134]

The anomalous ethylene-t increase in the T + ethane system was explained by Baker and Wolfgang.[135] Apparently, in the absence of O_2, radiation-produced H atoms were being scavenged by the ethylene-t formed by hot tritium reactions. This reduced the ethylene-t yield in unscavenged systems. When O_2 was added, the radiation-produced H atoms were scavenged by the more efficient O_2 and the ethylene-t yield increased from essentially zero to its "hot" value.

A similar explanation of the anomalous increase in the butadiene-t yield in the oxygen scavenged T + cyclohexene system was not intuitively obvious for two reasons: (a) In the T + ethane case, selective depletion of the ethylene-t molecules by H atoms may be solely dependent upon

ethylene-t being the only alkene in the system. The rate constant (at 25°C) for H atom addition to a double bond to form an alkyl radical is usually an order of magnitude greater than the rate constant of abstraction of a hydrogen atom to form H_2.[15,151,152] In the T + cyclohexene case, the butadiene-t molecules might be "protected" from radiation produced H atoms by the unlabeled cyclohexene molecules. The number of unlabeled cyclohexene molecules was larger than the number of butadiene-t molecules by a factor of 10^7 to 10^8. This should have made H-atom addition to cyclohexene the predominant reaction in the system even if the rate constant for H-atom addition to butadiene is larger than the rate constant for H atom addition to cyclohexene by a factor of 100. (b) SO_2 was as efficient as O_2 in scavenging products of thermalized radicals in the T + cyclohexene and T + trans-butene systems (Sec. 7). Sulfur dioxide was not as efficient as O_2 in removing thermalized tritium atoms. In the T + n-butane system, the thermal T atoms react by abstracting a hydrogen atom to form HT. The HT yield from tritium reactions with n-butane was decreased more with O_2 scavenging than with SO_2 scavenging. In addition, the HT yield exhibited a scavenger plateau with O_2 scavenging but no plateau with SO_2 scavenging. SO_2 removed some but not all of the thermal tritium atoms. SO_2 scavenging is thus expected to remove some but not all of the radiation produced H atoms in the T + cyclohexene system. If the butadiene-t yield in the T + cyclohexene system increases with O_2 scavenging due to removal of all radiation produced H atoms, the butadiene-t yield should increase to some extent with SO_2 scavenging. Because the butadiene-t yield did not increase with SO_2 scavenging, the hypothesis that the butadiene-t yield rises to its "hot" value only with O_2 scavenging was discredited.

I attempted to calculate the maximum effect of radiation produced H atoms on the butadiene-t yield in the T + cyclohexene system. The problem involves the competitive reactions with hydrogen atoms of butadiene-t vs. cyclohexene, cyclohexene plus O_2, and cyclohexene plus SO_2. The pertinent rate constants are shown in Table 8-1. The butadiene-t yield is extremely sensitive to the yield of H atoms from radiation damage. The "hot" butadiene-t yield is only reduced by about one third when the H atoms are not removed by O_2. The yield of H atoms simply cannot be estimated to the degree of certainty required to demonstrate convincingly that the butadiene-t yield is or is not reduced by H atom reactions. Similarly, an uncertain amount of unlabeled butadiene is also present in the system from radiation damage.[153] The unlabeled butadiene would also "protect" the butadiene-t yield by competing for H atoms with equal efficiency. Since the calculations were inconclusive and the preceding intuitive arguments actually depended upon the calculations, further experiments were necessary.

I decided to determine how the butadiene-t yield from T + cyclohexene reactions varied with scavenging by butadiene-d_6 and by hydrogen sulfide. Butadiene and butadiene/O_2 mixtures had been successfully employed as scavengers in recoil chlorine systems.[155,156] H_2S has been employed as a scavenger in radiolysis,[157] photolysis,[85] and recently in recoil tritium experiments.[16] A priori I compared O_2, SO_2, H_2S and butadiene-d_6 by the criteria for a good scavenger proposed by Hawke and Wolfgang,[137] namely:

Table 8-1. Hydrogen Atom Reaction Rate Constants at 25°C

Reactant	Addition [10^9 cm^3 $mole^{-1}$ sec^{-1}]	Abstraction [10^9 cm^3 $mole^{-1}$ sec^{-1}]
butadiene	1500 ref. [151,152]	22 [151,152]
cyclohexene	600 [154]	n.d.[a]
1-butene	320 [151,152]	30 [151,152]
O_2	300 [148,149]	–[b]
ethylene	200 [151,152]	13 [151,152]
trans-2-butene	180 [151,152]	21 [15]
H_2S	–	160 [151,152]
SO_2	6 [150]	–
NO (nitric oxide)	6 [169]	–
n-butane	–	0.6 [20]

[a]Not determined.

[b]Not applicable.

(a) A Scavenger Must React Avidly with the Atoms and Radicals to be Removed, Preferably with a Collision Efficiency Near Unity.

It may then be used in sufficiently low concentrations so as not to interfere with the hot or other primary processes being studied. The pertinent rate constants are shown in Table 8-1 and 8-2. I use methyl radicals as representative of all alkyl radicals; the rate constants of other alkyl radicals are not known for all potential scavengers. Abstraction is the reaction whose product is H_2 and CH_4 when hydrogen atoms and methyl radicals are respectively one of the reactants. Addition is the reaction which removes H-atoms or methyl radicals from the system by forming a new radical (via radical addition to the double bond of the scavenger) or by forming a stable molecule such as CH_3SO_2. From these tables, two things are clear: (i) Butadiene-t is the most reactive hydrocarbon in the T + cyclohexene system. It could be selectively depleted not only by hydrogen atoms but by also by radiolysis produced radicals. However, a "radical contribution" to the anomalous increase in the butadiene-t yield in the oxygen scavenged T + cyclohexene system can safely be neglected. Both O_2 and SO_2 are orders of magnitude more reactive with radicals than butadiene-t. (ii) Butadiene-d_6 is the most efficient of the four scavengers for removing H atoms. The effect of butadiene-d_6 scavenging on the butadiene-t yield should be unambiguous.

(b) A Scavenger Should be Inert with Respect to the Bulk Reagent.

Rapid cis-trans isomerization of either cis- or trans-2-butene is known to be catalyzed by H_2S and SO_2 in the presence of radiation.[163,164] Compensation can be made for the resultant cis/trans equilibrium mixture in recoil tritium studies of 2-butene with H_2S scavenging.[16] I have

Table 8-2. Methyl Radical Reaction Rate Constants at 25°C

Reactant	Addition [10^6 cm^3 $mole^{-1}$ sec^{-1}]	Abstraction [10^6 cm^3 $mole^{-1}$ sec^{-1}]
NO	2,400,000 [170]	—
O_2	300,000 [158]	—[b]
SO_2	5,000 [159]	—
H_2S	—	3,000 [160]
butadiene	160 [161]	n.d.[a]
ethylene	1.2 [161]	0.02 [161]
1-butene	1.0 [161]	0.36 [161]
trans-2-butene	0.3 [161]	0.2 [161]
cyclohexene	n.d.	n.d.
n-butane	—	0.004 [162]

[a]Not determined.

[b]Not applicable.

found that SO_2 catalyzes a 1% conversion of trans-2-butene to cis-2-butene in recoil tritium studies of trans-2-butene. This comparable to the radiolysis value.[164] The radiation-induced addition of H_2S to olefins is known to occur with enormous G values.[165,166] The resultant sulfur-containing species would not be eluted in the normal radio-gas-chromatographic analysis. Therefore, this effect cannot be directly measured in recoil tritium systems. I have monitored instead the area of the cyclohexene mass peak. This showed that within experimental error cyclohexene was not depleted by radiation-induced reactions with H_2S in the T + cyclohexene system. Similar measurements showed butadiene-d_6 to be unreactive with cyclohexene, as expected. Reactions of O_2 with the bulk cyclohexene system have been noted (Sec. 7).

(c) Products of the Scavenging Reaction Should not React Further, or if They Do, Such Reaction Should be Controllable.

No problems of this sort have been encountered previously with these scavengers.

(d) A Gas Phase Scavenger Must Have an Adequate Vapor Pressure at the Temperature in Question.

Oxygen easily satisfies this criteria. The vapor pressure at room temperature for SO_2 is more than two atmospheres, for H_2S more than twenty atmospheres; and for butadiene more than two atmospheres.[167]

(e) Furthermore, it is Highly Desirable but not Always Essential that the Scavenged Species be Detectable.

H_2S reacts with thermalized tritium atoms and alkyl and alkenyl radicals to form HT and the corresponding alkanes and alkenes, respectively. These species are readily detectable. The primary products of scavenging with butadiene-d_6 are tritiated alkenyl radicals. If these alkenyl

radicals abstract a hydrogen atom from the bulk system, the resultant alkene is readily assayed and identified as a scavenger product. However, if the alkenyl radical decomposes or begins a radical addition chain with the bulk system, a unique scavenger product cannot be determined. The primary products from O_2 and SO_2 scavenging are not readily assayed in the conventional radio-gas-chromatographic analysis used for recoil tritium experiments. In addition, these primary products may react further with the bulk system or other radicals. As yet, there is no evidence that such further reaction results in products which might be mistaken for the yield of a hot reaction.

8.2 Data and Discussion

The effect of the four scavengers on the cyclohexene-t yield is shown in Fig. 8.1. When butadiene-d_6 is used as a scavenger, butadiene-d_5T, DT and other deuterated tritium labeled hydrocarbons are formed from T + butadiene-d_6 reactions. In principle, the deuterated compounds could be separated from the protonated compounds by gas chromatography and the T + cyclohexene products could be unambiguously determined. In practice, this would be extremely difficult. I settled for separating butadiene-d_5T (C_4D_5T) from butadiene-t. For all other products with four or fewer carbon atoms, the sum of the contributions from T + cyclohexene and T + butadiene-d_6 reactions was determined. Cyclohexane-t and cyclohexene-t resulted only from T + cyclohexene reactions. All data reported represents the average of the yields of two identical samples that agreed to within 5% on major products. The irradiations were made at 25°C. The typical

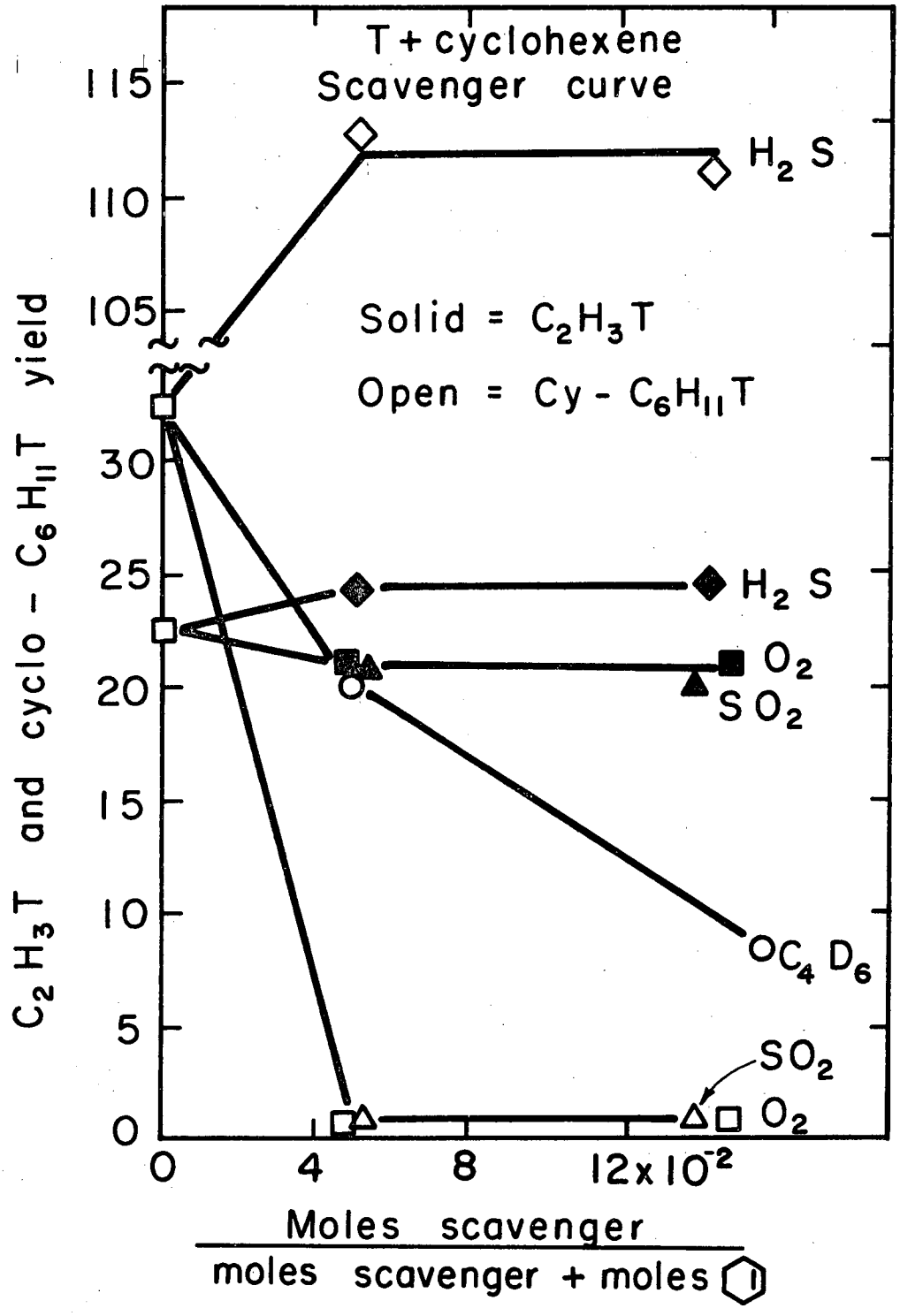

XBL726 - 3100

Fig. 8.1. The effects of O_2, SO_2, H_2S, and C_4D_6 on the ethylene-t and the cyclohexane-t yield from T + cyclohexene reactions. Product yields are listed relative to the cyclohexene-t yield as 100. The zero scavenger data point and the 5 mole % scavenger data point have been connected with a line for clarity. I do not imply that the variation with added scavenger is linear in this region. (Data in Appendix, Table A-8-1).

sample contained 5 cm Hg pressure of cyclohexene vapor. Radiation damage due to recoils following the $^3He(n,p)T$ reaction was less than 2%.

In Fig. 8.1, three trends should be noted: (a) The cyclohexane-t yield does not exhibit a scavenger plateau with butadiene-d_6 scavenging. Butadiene-d_6 is less efficient than O_2 and SO_2 in removing the cyclohexyl-t radicals. This is consistent with the trend of the rate constants in Table 8-2. (b) The ethylene-t yield increases slightly with H_2S scavenging. This confirms a small contribution to the ethylene-t from thermal or radical processes that is demonstrated by the decrease in ethylene-t yield with O_2 and SO_2 scavenging. The effect of butadiene-d_6 scavenging on the ethylene-t yield was not determined. The contribution to the ethylene-t yield from T + cyclohexene reactions was not separated from the contribution from T + butadiene-d_6 reactions. (c) The cyclohexane-t yield increases dramatically with H_2S scavenging. This confirms a cyclohexyl-t radical intermediate. As predicted by Table 8-2 abstraction of a hydrogen from H_2S is a faster reaction for cyclohexyl-t radicals than either the addition or abstraction reaction with cyclohexene. H_2S intercepts the cyclohexyl-t radicals before they react with cyclohexene to form tritiated hydrocarbons, C_{12} or greater, through radical chain addition. These species are counted as "polymer-t". While the "polymer-t" data do not indicate the chemical composition of the tritiated products, crude separations by volatility may be performed. Low (molecular weight) "polymer-t" is backflushed from the chromatographic columns. Medium "polymer-t" is washed from a 10 ft. stainless steel tube (1/16" o.d.) connecting the sample breaker to the chromatographic columns. High

"polymer-t" is washed from the walls of the capsule in which the recoil tritium reaction took place (Sec. 6.2.6). The relative abundance of activity in each volatility grouping changes with the scavenger employed. The "polymer-t" was distributed 20% in the medium and 70% in the heavy groupings for O_2 scavenged samples and 2% in the medium and 97% in the heavy groupings for SO_2 scavenged samples. The lowered "polymer-t" volatility with SO_2 scavenging is consistent with the expected formation of scavenged species of higher molecular weight and/or lower volatility with SO_2 than O_2. The total "polymer-t" yield decreased from 74 relative to cyclohexene-t as 100 for the unscavenged samples to 36 for H_2S scavenged samples. The cyclohexane-t yield increased from 32 to 112, and the yields of other minor products also increased with H_2S scavenging. This is surprising because the increase in cyclohexane-t yield should come at the expense of the "polymer-t" yield. This may indicate that recovery of "polymer-t" is not complete. No correction was necessary for ^{35}S activity (from the $^{34}S(n,\gamma)^{35}S$ reaction which could be included in our measurements as the ^{35}S was incorporated into the "polymer-t". Even with the highest SO_2 or H_2S pressures, the total ^{35}S activity is less than 1% of the "polymer-t" activity. The total "polymer-t" exhibits a scavenger plateau with O_2, SO_2 and H_2S scavenging. When butadiene-d_6 is used as a scavenger the total "polymer-t" yield increases with increasing butadiene-d_6 concentration. This is as expected because butadiene-d_6 is a major source of "polymer-t" and only the sum of the "polymer-t" from T + butadiene-d_6 and T + cyclohexene reactions could be determined.

Figure 8.2 shows that the butadiene-t yield increases with butadiene-d_6 scavenging. The scavenger plateau is identical to that obtained with O_2 scavenging. This supports the hypothesis that the butadiene-t yield is selectively depleted by radiolysis-produced H atoms in the absence of O_2. The butadiene-t yield decreases with H_2S scavenging. Table 8-1 shows that H_2S is inefficient as an H atom scavenger. But H_2S is a source of H atoms through radiolysis.[168] The increase in H atom concentration with no increase in the ability to scavenge H atoms (relative to butadiene-t) would further reduce the butadiene-t yield.

The hypothesis that butadiene-t is selectively depleted by reactions with H atoms from the radiolysis of H_2S and/or cyclohexene is supported by the dual scavenger data in Fig. 2. The solid data points show the effect on the butadiene-t yield when two scavengers are used simultaneously. All samples were scavenged by butadiene-d_6. The butadiene-d_6/(cyclohexene + butadiene-d_6) ratio was constant at 0.15. Varying amounts of H_2S, O_2 or SO_2 were added as indicated. The butadiene-t yield is the same for each of the combinations of scavengers and is slightly higher than for O_2 or butadiene-d_6 used solely*. When the

---

*With dual scavenging, the butadiene-t yield increases by at most ten percent over the yield for O_2 or butadiene-d_6 used solely. Because this is only twice the uncertainty of each individual data point, the increase may not be significant. It should be noted, however, that Baker and Wolfgang[135] reported a similar percent increase in the C_2H_3T yield (from T + ethane reactions) when O_2 and C_2D_4 were employed simultaneously as scavengers. If the increase is real it may indicate that the combination of scavengers is slightly more efficient in removing thermal H atoms than either scavenger used solely.

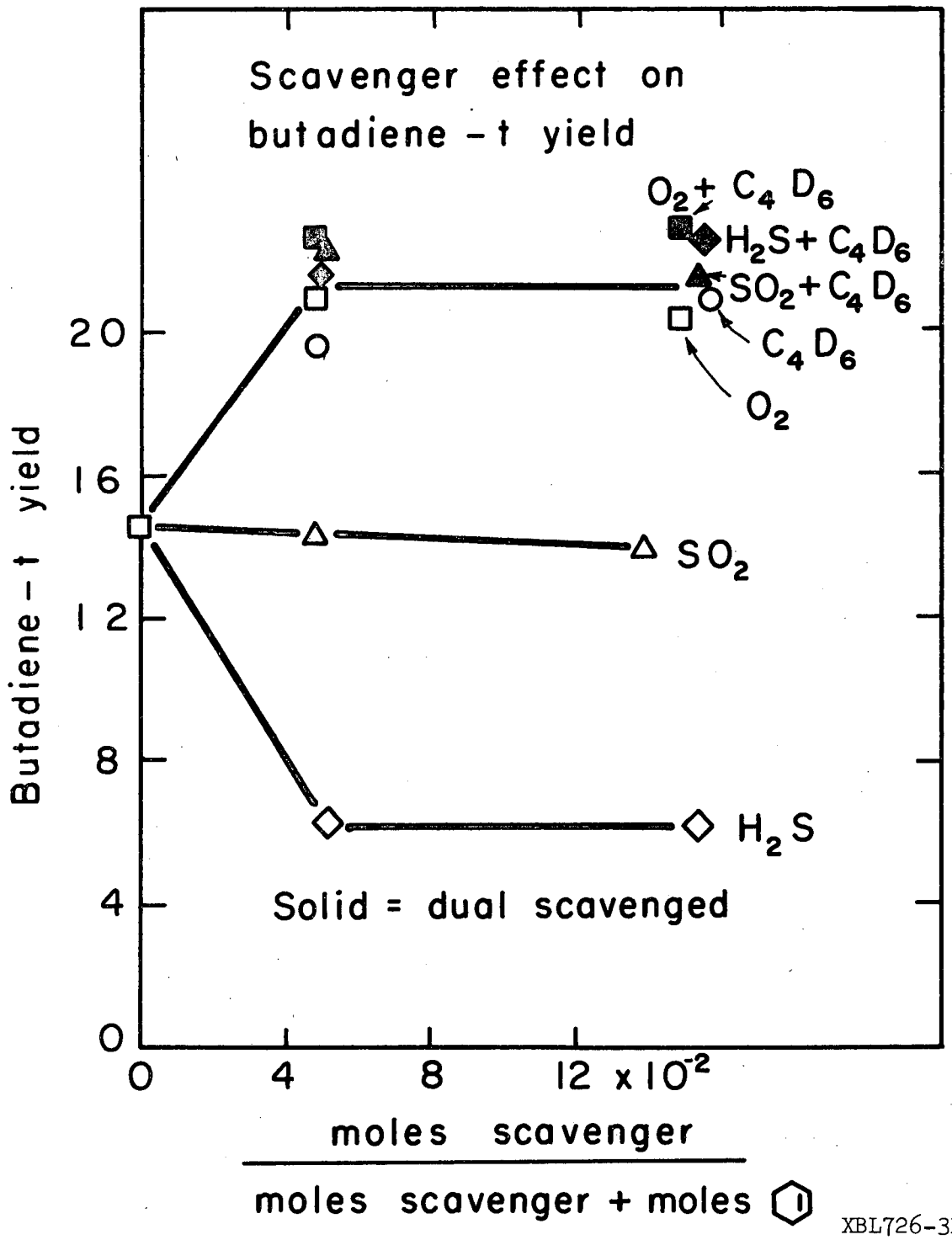

XBL726-3101

Fig. 8.2. The effects of O_2, SO_2, H_2S, C_4D_6, and C_4D_6 plus O_2, C_4D_6 plus SO_2 C_4D_6 plus H_2S on the butadiene-t yield from T + cyclohexene reactions. Product yields are listed relative to the cyclohexene-t yield as 100. The solid data points represent C_4D_6 plus another scavenger used jointly. The abscissa in this case does not include the moles of C_4D_6. The zero scavenger data point and the 5 mole % scavenger data point have been connected with a line for clarity. I do not imply that the variation of yield with added scavenger is linear in this region. (Data in Appendix, Table A-8-2.)

T + cyclohexene system is simultaneously scavenged by H_2S and butadiene-d_6, the butadiene-d_6 "protects" the butadiene-t from being selectively depleted by reactions with H atoms from H_2S and cyclohexene. The butadiene-t yield thus rises to its "hot" value. Except for butadiene-t, H_2S exhibits normal scavenger behavior in the T + cyclohexene system. The yield of products with a radical precursor increases with H_2S scavenging and a scavenger plateau is observed. When the T + cyclohexene system is simultaneously scavenged by SO_2 and butadiene-d_6, the butadiene-d_6 protects the butadiene-t from being selectively depleted by reactions with radiolysis-produced H atoms. Sulfur dioxide is not sufficiently reactive to protect butadiene-t from H atoms. However, SO_2 is sufficiently reactive to protect the less reactive unsaturated tritiated hydrocarbons. These yields are the same for both O_2 and SO_2 scavenging. Sulfur dioxide exhibits normal scavenger behavior in alkene systems for all products except butadiene-t. When O_2 and butadiene-d_6 are simultaneously used as scavengers in the T + cyclohexene system, both O_2 and butadiene-d_6 protect the butadiene-t yield from the radiolysis-produced H atoms. There is no anomalous behavior with O_2 scavenging.

I conclude that: (a) The "hot" butadiene-t value from T + cyclohexene reactions can only be determined with O_2 or butadiene-d_6 scavenging. Previous workers did not determine the "hot" butadiene-t yield.[142-144] (b) Oxygen is the most efficient single scavenger for both thermalized T (and H) atoms and tritiated radicals. Butadiene-d_6/SO_2 dual scavenging is nearly as efficient as O_2 for both radicals and H atoms. Although butadiene-d_6/SO_2 scavenging requires a more complex analytical scheme,

use of these scavengers may be preferable to O_2 in cases where O_2 reacts with the parent alkene. (c) Sulfur dioxide and hydrogen sulfide exhibit normal scavenger behavior in T + alkene systems for all products except butadiene-t. This may limit their use to systems where butadiene-t is not a major product.

9. RECOIL TRITIUM REACTIONS WITH CYCLOHEXENE AND ALKENES: DETERMINATION OF RATE PARAMETERS

9.1 Determination of the s Parameter in the RRK Treatment of Cyclohexene Unimolecular Decomposition

Scavenger studies of recoil tritium reactions with cyclohexene (Secs. 7 and 8) show that ethylene-t (C_2H_3T) and butadiene-t (C_4H_5T) are chiefly "hot" reaction products: (a) The ethylene-t yield is reduced by less than 10% with oxygen scavenging. (b) The "hot" butadiene-t yield could <u>only</u> be determined with oxygen or butadiene-d_6 scavenging.

Survival in the presence of oxygen scavenging is consistent with ethylene-t and butadiene-t resulting from unimolecular decomposition of cyclohexene-t formed via a T-for-H substitution reaction.

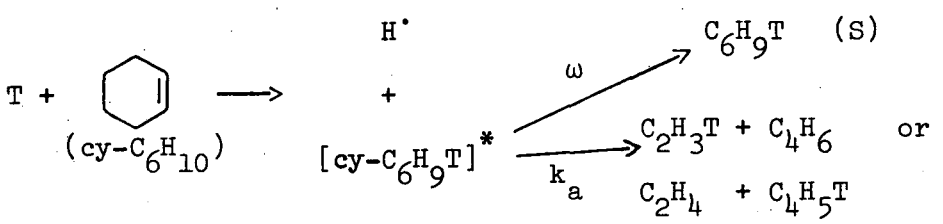

9-1

$$(D) = C_2H_3T + C_4H_5T$$

Ethylene-t and butadiene-t formation as shown in Eq. (9-1) was confirmed by determining the pressure dependence of the stabilization (S)/decomposition (D) ratio. This is shown in Fig. 9.1. Experiments at elevated temperature were required to obtain a larger pressure range than the (zero to) 7 cm Hg cyclohexene vapor pressure available at 25°C (Table 4-1). All samples were irradiated for eight hours at 135°C in the irradiation container described in Sec. 5.2.

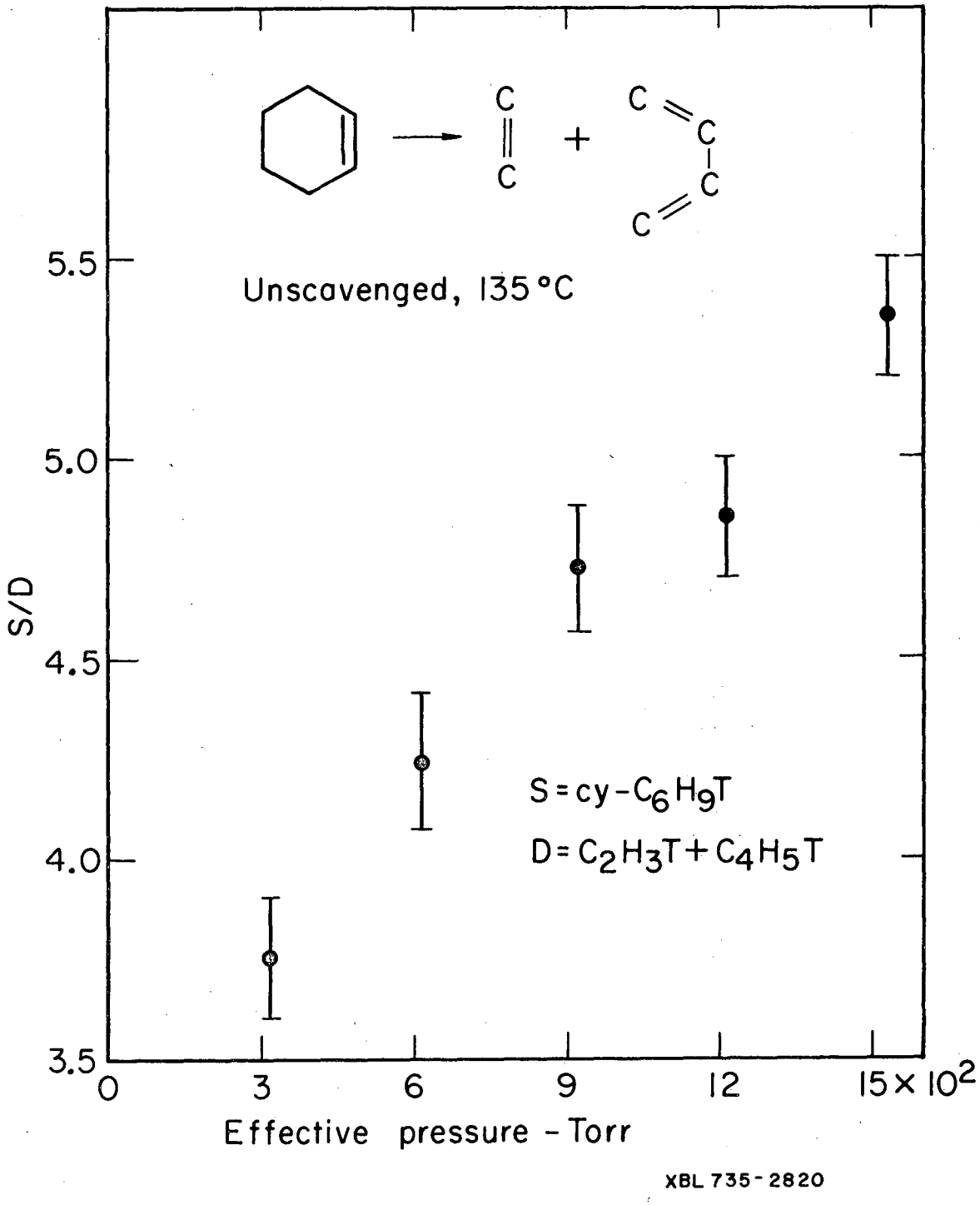

Fig. 9.1. The unimolecular decomposition of cyclohexene-t to give ethylene-t or butadiene-t; unscavenged data at 135°C. Activated cyclohexene-t molecules are formed by recoil T-for-H substitution. The abscissa is the effective collisional deactivation pressure (in the sample capsule) defined as effective pressure = cyclohexene pressure + 0.2 (helium-3 pressure). (Data in Appendix, Table A-9-1.)

In both Figs. 9.1 and 9.2, the pressure represents the total effective pressure in the sample capsule. The sample capsules contained a variable pressure of cyclohexene and a constant amount of ^3He (9.8 cm Hg at 135°C). The effective pressure was calculated using relative collisional deactivation efficiencies estimated from published sources[71] by the method developed in Eq. (2-27).

$$P_{effective} = P_{\bigcirc} + 0.2\ P_{^3He} \qquad 9\text{-}2$$

In both Figs. 9.1 and 9.2 the pressure dependence of the S/D ratio may be well represented by a line. This confirms the formation of ethylene-t and butadiene-t principally from the unimolecular decomposition of cyclohexene-t as shown in Eq. (9-1).

The data shown in Fig. 9.1 is for unscavenged samples. For both O_2 and SO_2 scavenger a scavenger/(scavenger + cyclohexene) ratio of 0.08 was insufficient to remove the cyclohexyl-t radical intermediate to the cyclohexane-t yield. At 25°C, this concentration of scavenger was sufficient to intercept cyclohexyl-t radicals (Fig. 7.1). The failure of both SO_2 and O_2 scavengers at 135°C may be due to macroscopic reactions between cyclohexene and the scavenger. The reaction of cyclohexene with oxygen scavenger has been discussed (Sec. 7). For oxygen scavenging, a scavenger/(scavenger + cyclohexene) ratio of o.14 was sufficient to intercept the cyclohexyl-t radicals. A comparison of O_2 scavenged and unscavenged samples showed that:

(a) The ethylene-t yield relative to the sum of yields from excited cyclohexene-t molecules (C_2H_3T + C_4H_5T + cy-C_6H_9T) was decreased by 9%

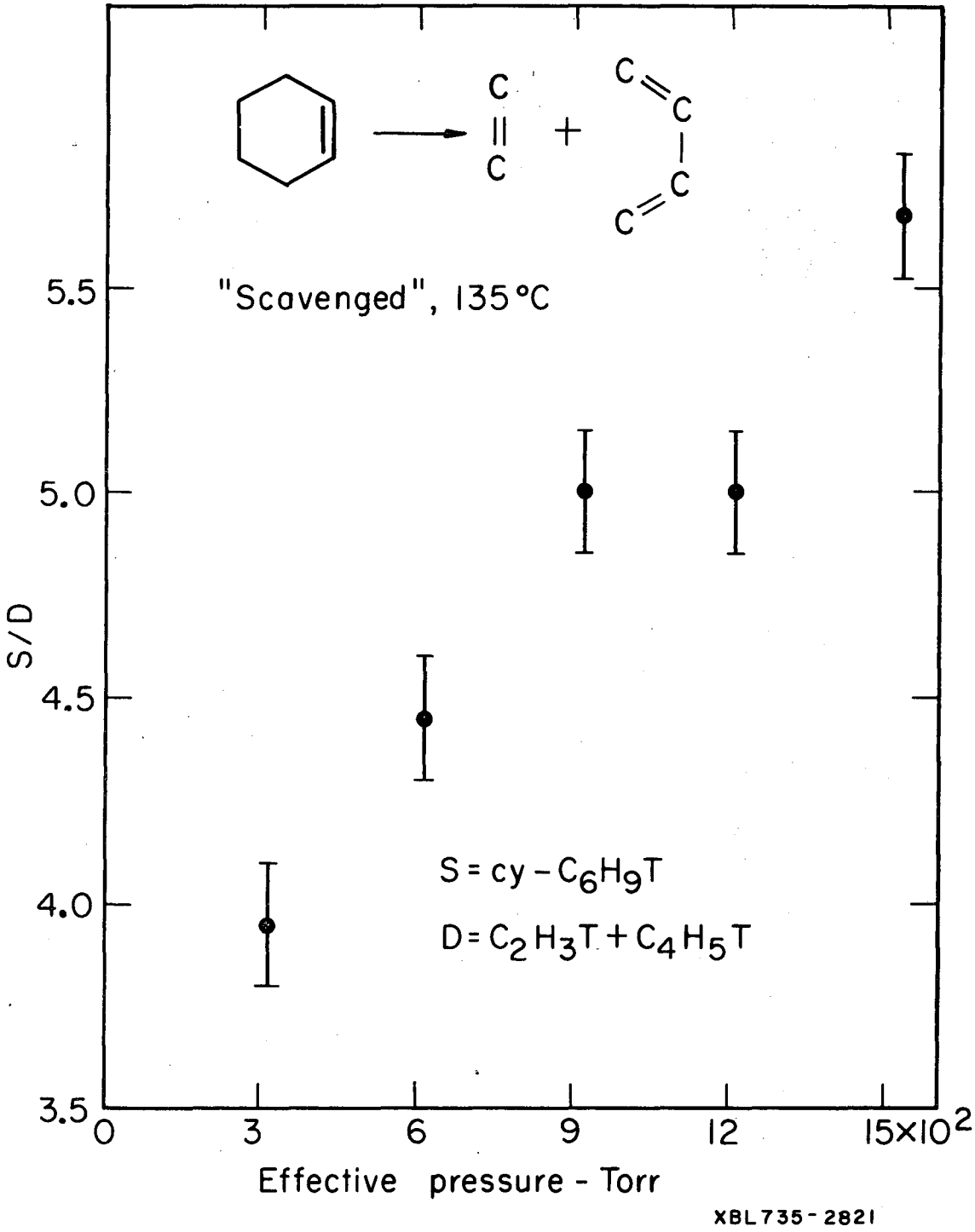

Fig. 9.2. The unimolecular decomposition of cyclohexene-t to give ethylene-t or butadiene-t; "scavenged" data at 135°C. Activated cyclohexene-t molecules are formed by recoil T-for-H substitution. The abscissa is the effective collisional deactivation pressure (in the sample capsule) defined as effective pressure = cyclohexene pressure + 0.2 (helium-3 pressure). The "scavenged" data represents the unscavenged experimental data in Fig. 9.1 from which a 9.2% radical contribution to the ethylene-t yield has been subtracted. (Data in Appendix, Table A-9-1.)

with O_2 scavenging. This indicates that at 135°C (as at 25°C) ethylene-t results largely from "hot" tritium atom reactions.

(b) The butadiene-t yield is the same in O_2 scavenged and unscavenged samples. The butadiene-t yield was also the same in butadiene-d_6 and unscavenged samples. Apparently the butadiene-t yield was not depleted by radiolysis produced H-atoms in unscavenged samples under these temperature and irradiation conditions. Similar numbers of recoil tritium atoms were produced in samples at 25°C and 135°C. In addition, the pressures of cyclohexene parent hydrocarbon were the same in this case at 25°C and 135°C. Thus, the total radiolysis damage in the samples at 135°C was similar to samples at 25°C. The temperature effect on H-atom depletion of the butadiene-t yield cannot be calculated because the pertinate rate constants are not known at the desired temperatures. The crudely estimated temperature effect is slight. The lack of butadiene-t being depleted by radiolysis produced H-atoms is consistent with a decreased steady-state concentration of H-atoms during irradiations with the lower tritium atom production rate that existed at 135°C (versus 25°C).

In the data shown in Fig. 9.2 the scavengeable portion of the ethylene-t yield has been subtracted off. This is reflected in the upward shift of the S/D ratio. This data is from unscavenged samples shown in Fig. 9.1. The ethylene-t/(C_2H_4T + C_4H_5T + cy-C_6H_9T) relative yield ratio for the lowest cyclohexene pressure point was multiplied by 0.09 to correct for the 9% scavengeable ethylene-t yield observed at low cyclohexene pressures. This value of the ethylene-t relative yield ratio was subtracted from the ethylene-t relative yield ratios at all pressures of

unscavenged samples. This assumes that the scavengeable ethylene-t yield is relatively constant at all pressures. The correction is small at any rate. The resultant corrected S/D ratios are listed in Fig. 9.2 as resulting from "scavenged" samples.

The least-squares fitted line of the S/D ratio versus pressure [actually log $(\frac{S}{D})$ versus log (pressure)] was extrapolated to S/D = 1.0. The pressure at which S/D was 1.0 was 0.50 Torr from Fig. 9.1 and 0.33 Torr from Fig. 9.2. A previous determination by Weeks and Garland of the pressure at which the S/D ratio from the recoil tritium initiated unimolecular decomposition of cyclohexene equalled 1.0 gave a pressure of 0.2 Torr. However, in these previous experiments, the temperature ranged from 25°C for the lowest pressure unscavenged sample to 135°C for the highest pressure unscavenged sample.[143]

From Eq. (2-21) and (2-20) $k_a = \omega = Z\,P$ at the pressure where S/D = 1.0. Z was calculated using Eq. (2-3) with T = 408 °K (135°C) and $\sigma_d = 5.47 \times 10^{-8}$ cm. The σ_d value for cyclohexene was estimated from published values.[71] This gave an apparent rate constant for the unscavenged unimolecular decomposition of cyclohexene to ethylene and butadiene of 5.1×10^6 sec^{-1}. Using this value of k_a in Eq. (2.13) with parameters from other sources, namely: $A = 2 \times 10^{15}$ sec^{-1}, $E_o = 2.90$ eV,[82] E = 5.0 eV, the average energy of excitation resulting from a T-for-H substitution (Sec. 1.2.3);[25,26] the s parameter in the RRK treatment of the unimolecular decomposition of cyclohexene was determined as s = 24. For $s = \frac{1}{2}(3N-6) = 21$, E was 4.6 eV. For $s = (2/3)(3N-6) = 28$, E was 5.6 eV. For $s = 32 \cong (3/4)(3N-6)$, E was 6.2 eV.

9.2 Determination of the Apparent Rate Constants of the Unimolecular Decomposition/Isomerization of Cyclohexyl Radicals

As demonstrated in Secs. 7 and 8, the cyclohexane-t yield in T + cyclohexene reactions appears to have a radical precursor. The cyclohexane-t yield: (a) decreases to nearly zero with O_2 or SO_2 scavenging. (b) decreases with butadiene-d_6 scavenging. (c) increases with H_2S scavenging. All of these trends indicate a radical precursor. The proposed mechanism of cyclohexane-t formation was tritium atom addition to the double bond of cyclohexene to form a cyclohexyl-t radical. The cyclohexyl-t radical could then abstract a hydrogen atom from the bulk system to form cyclohexane-t. Addition of a moderator should increase the number of tritium atoms which survive collisions in the 20 to 0.02 eV energy range and ultimately react as thermal tritium atoms. The lowest activation energy process for tritium atoms is addition to the double bond. The expected increase in cyclohexane-t yield with increasing neon moderator is shown in Fig. 9.3. Similar monotonic increases in the cyclohexane-t yield (from T + cyclohexene reactions) with increasing moderation has been observed with helium,[142] krypton,[142] and nitrogen[144] as moderators. The yield of "polymer-t" also increased with increasing moderation. "Polymer-t" may result from the addition of cyclohexyl-t radicals to the double bond of cyclohexene initiating a radical chain. All this indicates the presence of relatively large amount of cyclohexyl-t radical in the T + cyclohexene system. Cyclohexane-t is a major product.

As indicated in Sec. 1.2.1, cyclohexyl-t radicals are capable of further reaction. By analogy to other kinetic studies[171-177] the

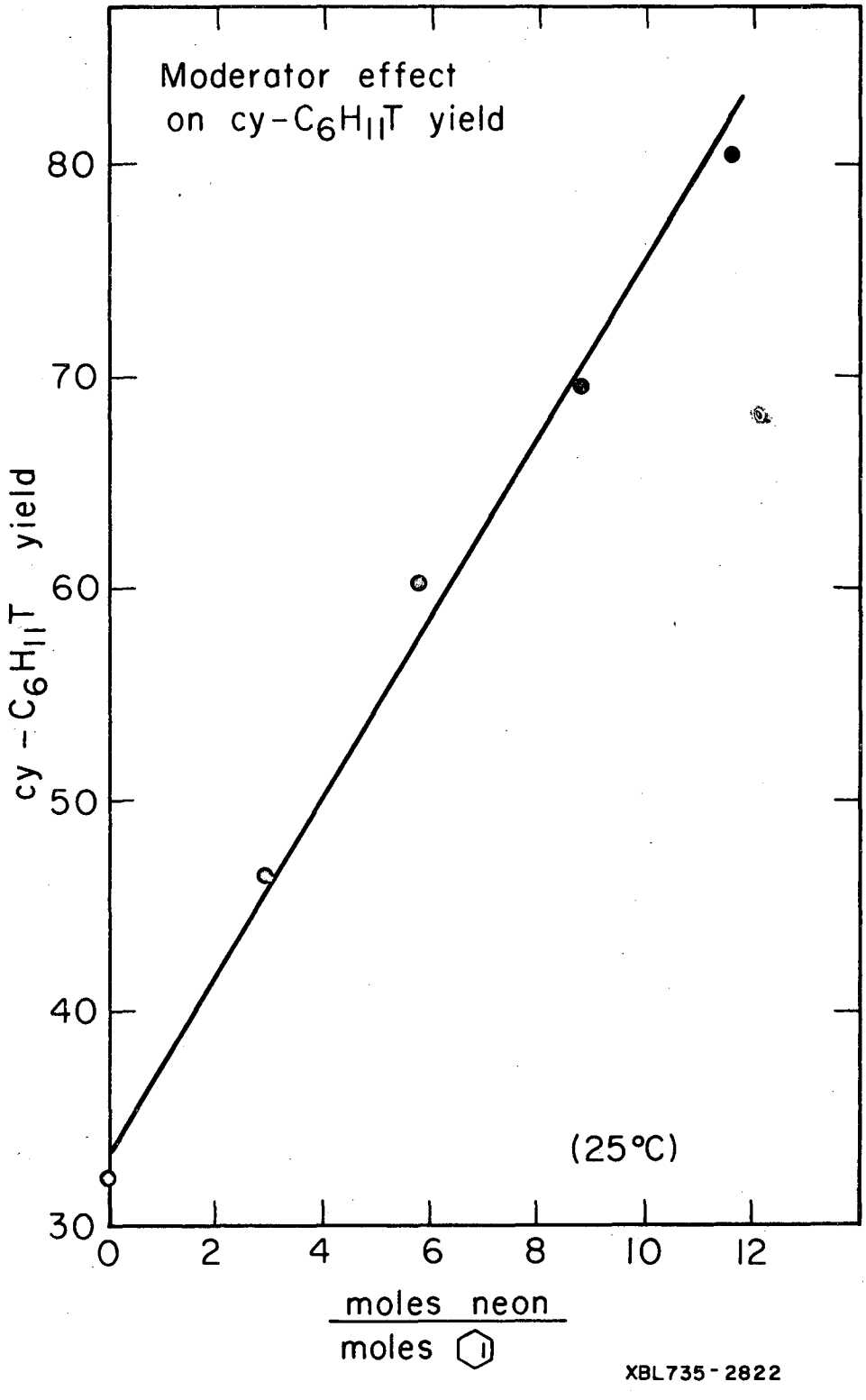

Fig. 9.3. Moderator effect on cyclohexane-t yield at 25°C. The ordinate lists the cyclohexane-t yield relative to the cyclohexene-t yield as 100. (Data in Appendix, Table A-9-2.)

possible reactions of cyclohexyl-t radicals other than with scavenger are: (a) Abstraction of a hydrogen atom from the bulk system to form cyclohexane-t as discussed.[171] (b) Addition to the double bond of cyclohexene to initiate a radical chain.[172,173] These tritiated products would be monitored as polymer-t. (c) Decomposition or isomerization.[174-176] The isomerization of cyclohexyl radicals to straight chain alkenyl radicals has been postulated as the first step of a unimolecular decomposition process which leads to a complex series of products including methane, ethane, ethylene, propane, propylene, butenes, and methylcyclopentane.[174-176]

The formation of n-hexenyl radicals without a cyclohexyl radical precursor results in: (a) n-hexene via H-atom abstraction, (b) methylcyclopentane via an isomerization reaction.[177] This is shown in Eq. (9-3).

$$CH_2{=}CHCH_2CH_2CH_2CH_2 \xrightarrow{H^{\bullet}} CH_2{=}CHCH_2CH_2CH_2CH_3 \qquad 9\text{-}3$$

or 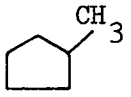

The decomposition (isomerization) of cyclohexyl-t radicals from T + cyclohexene reactions may result in any or all of the aforementioned products from cyclohexyl radicals being tritium labeled.

Many of the species which may result from the decomposition/isomerization of cyclohexyl-t radicals are observed as tritiated products in T + cyclohexene reactions. This list includes methane-t, ethane-t, ethylene-t, propane-t, propylene-t, 1-butene-t, trans-2-butene-t,

cis-2-butene-t, n-hexene-t/methylcyclopentane-t*, cyclohexane-t, and "polymer-t". The scavenger dependence of the ethylene-t yield and the scavenger and moderator dependence of "polymer-t" have been discussed. Some of the remaining tritiated products show the same scavenger dependence as the cyclohexane-t yield. The yields of methane-t, ethane-t, 1-butene-t and n-hexene-t decrease to nearly zero with O_2 or SO_2 scavenging and increase with H_2S scavenging, indicating a radical precursor. I propose the following reaction scheme for excited cyclohexyl-t radicals formed by the addition of a tritium atom to cyclohexene.

---

*The n-hexene radio-gas-chromatographic peak was neither resolved into 1-, 2-, and 3-hexene-t components nor resolved from methyl-cyclopentane-t. Only the sum of these tritiated yields was monitored. This sum of products is referred to as n-hexene-t. The major component of the n-hexene-t yield is probably 1-hexene-t. A strong preference for C-C cleavage β to the radical site has been observed in other studies.[178,179]

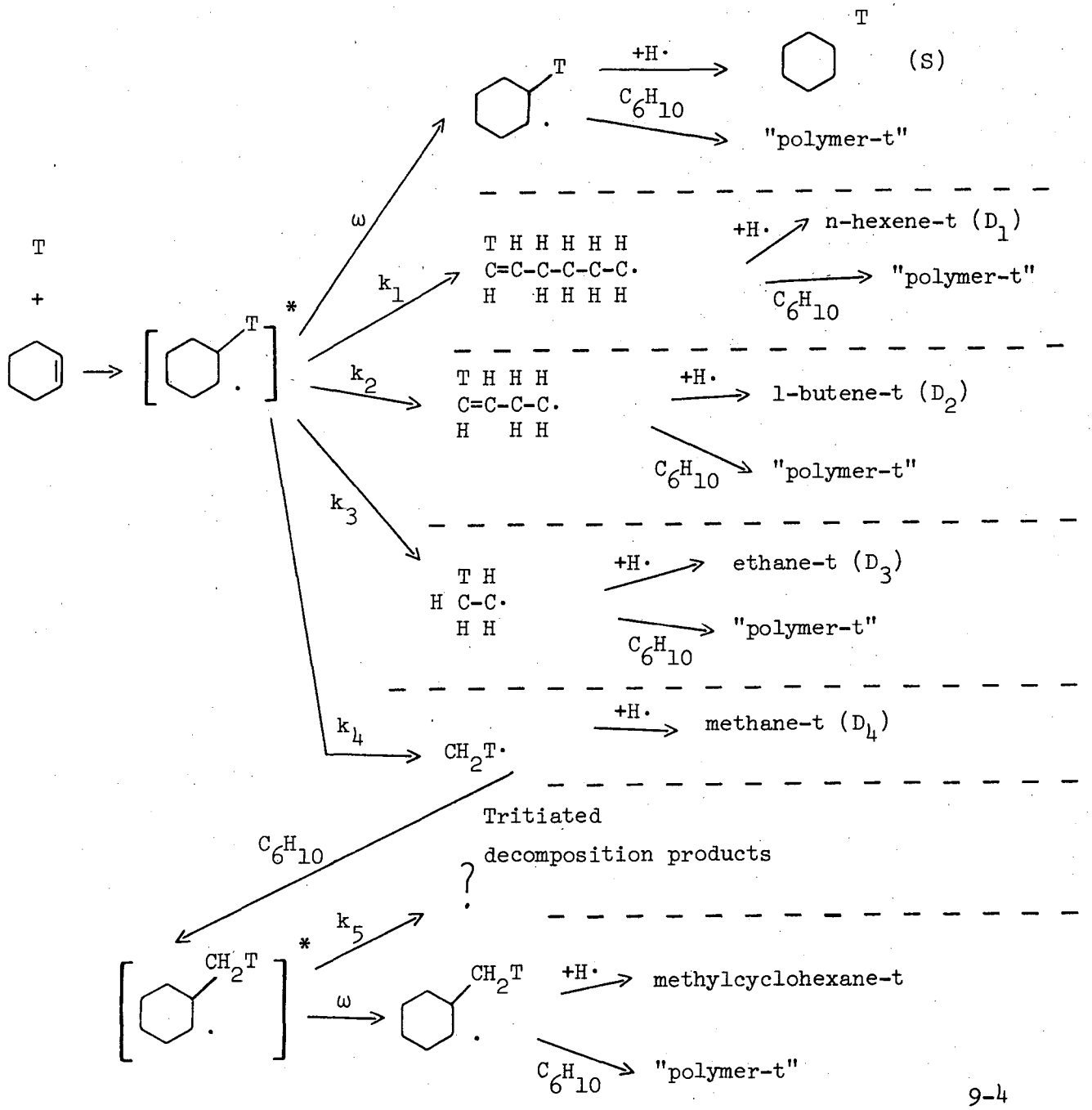

9-4

In Eq. (9-4), the +H· over the reaction arrow signifies that the radical abstracts a hydrogen atom from the bulk hydrocarbon system. The site of the tritium label in the n-hexenyl-t radical and the butenyl-t radical shown in Eq. (9-4) is purely arbitrary and is shown only for the sake of material balance along the reaction path.

With H_2S scavenging, all the radicals are intercepted before they add to cyclohexene (C_6H_{10}) to eventually form "polymer-t". For example, all n-hexenyl-radicals formed by channel 1 (with rate constant k_1) are monitored as n-hexene-t when H_2S is employed as a scavenger. The pressure dependence of the S/D ratio for reaction channel 1, 2 and 4 (with rate constants k_1, k_2 and k_4) are shown in Figs. 9.4, 9.5 and 9.6, respectively.

The pressure dependence of the S/D_1 and S/D_2 ratio may be well represented by a line for the unimolecular decomposition/isomerization of cyclohexyl-t radicals to give n-hexenyl-t and 1-butenyl-t radicals, respectively. The increased scatter in the pressure dependence of the S/D_4 ratio for the unimolecular decomposition of cyclohexyl-t to give methyl-t radicals results from the small yield of methane-t. A small uncertainty in the methane-t yield is reflected in a large uncertainty in the S/D_4 ratio. In this respect the yield of ethane-t is so small that the resultant uncertainty in the S/D_3 ratio makes observation of a pressure dependence of the S/D_3 ratio impossible.

The rate constants k_1 and k_2 were determined from extrapolation of the S/D versus effective pressure line in a manner similar to that described in Sec. 9.1. In this case the effective pressure was

$$P_{effective} = P_{C_6H_{10}} + 0.2\ P_{^3He} + 0.5\ P_{H_2S} \qquad 9\text{-}5$$

using relative collisional deactivation efficiencies estimated from published sources.[71] The calculation of Z (Eq. (2-3)) was made with $\sigma_d = 5.67 \times 10^{-8}$ cm for cyclohexyl-t radicals. This value was estimated from tabulated values in Ref. 71. The pressures at which S/D = 1.0 and

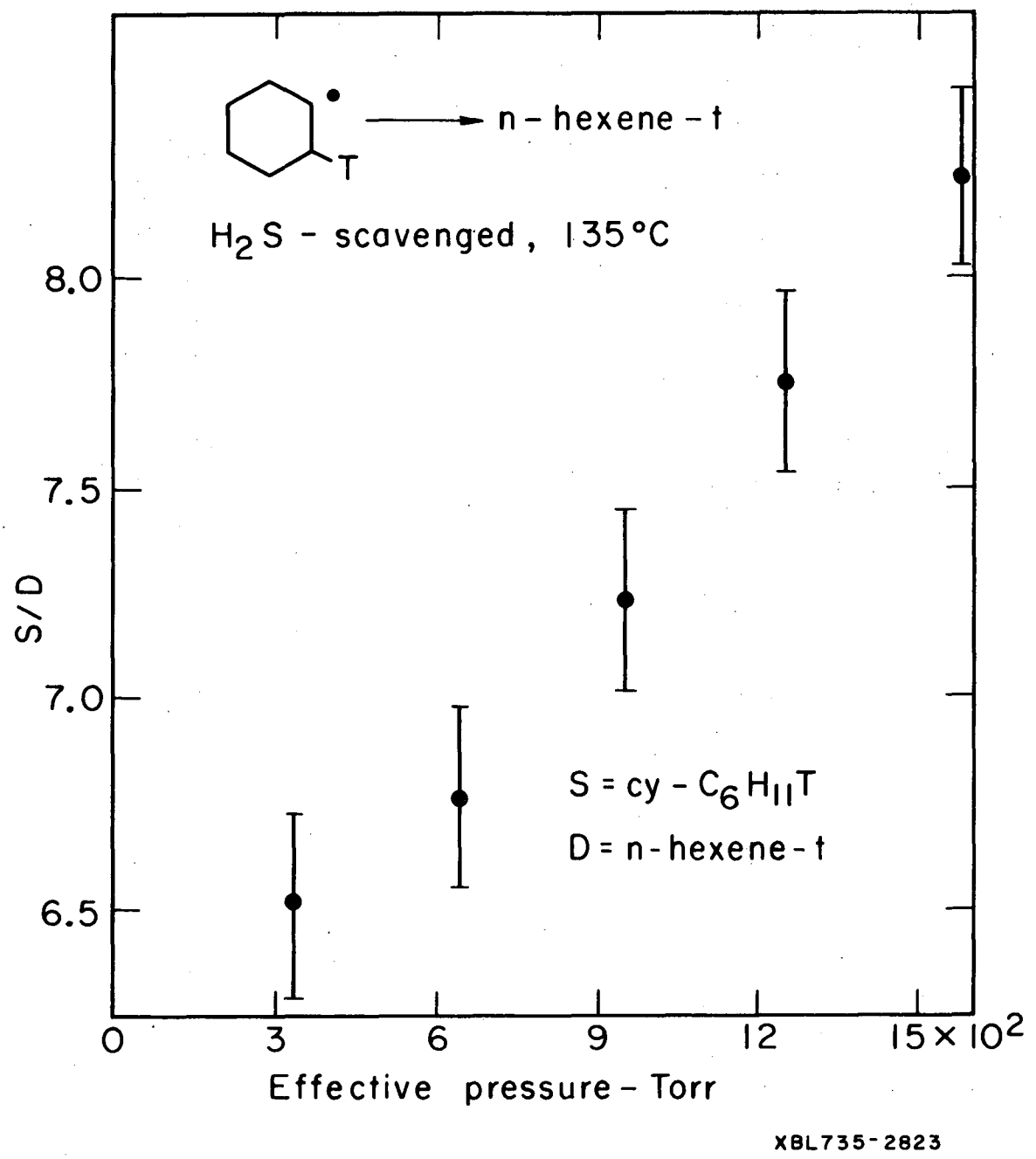

Fig. 9.4. The unimolecular decomposition of cyclohexyl-t radicals to n-hexene-t; H_2S scavenged data at 135°C. Activated cyclohexyl-t radicals are formed by recoil T atom addition to cyclohexene. The abscissa is the effective collisional deactivation pressure (in the sample capsule) defined as: effective pressure = cyclohexene pressure + 0.2 (helium-3 pressure) + 0.5 (hydrogen sulfide pressure). (Data in Appendix, Table A-9-3.)

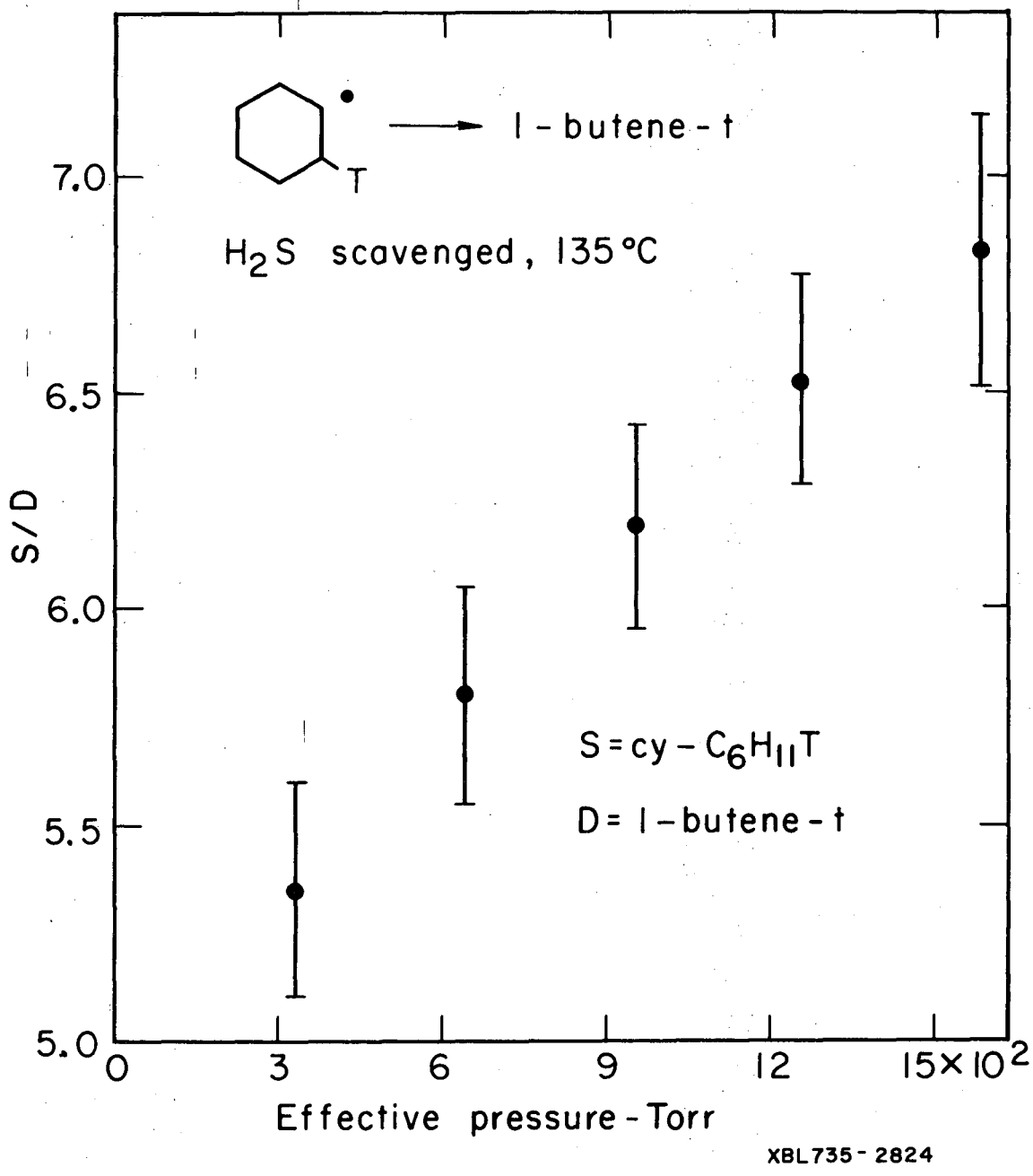

Fig. 9.5. The unimolecular decomposition of cyclohexyl-t radicals to 1-butene-t; H_2S scavenged data at 135°C. Activated cyclohexyl-t radicals are formed by recoil T atom addition to cyclohexene. The abscissa is the effective collisional deactivation pressure (in the sample capsule) defined as: effective pressure = cyclohexene pressure + 0.2 (helium-3 pressure) + 0.5 (hydrogen sulfide pressure). (Data in Appendix, Table A-9-3.)

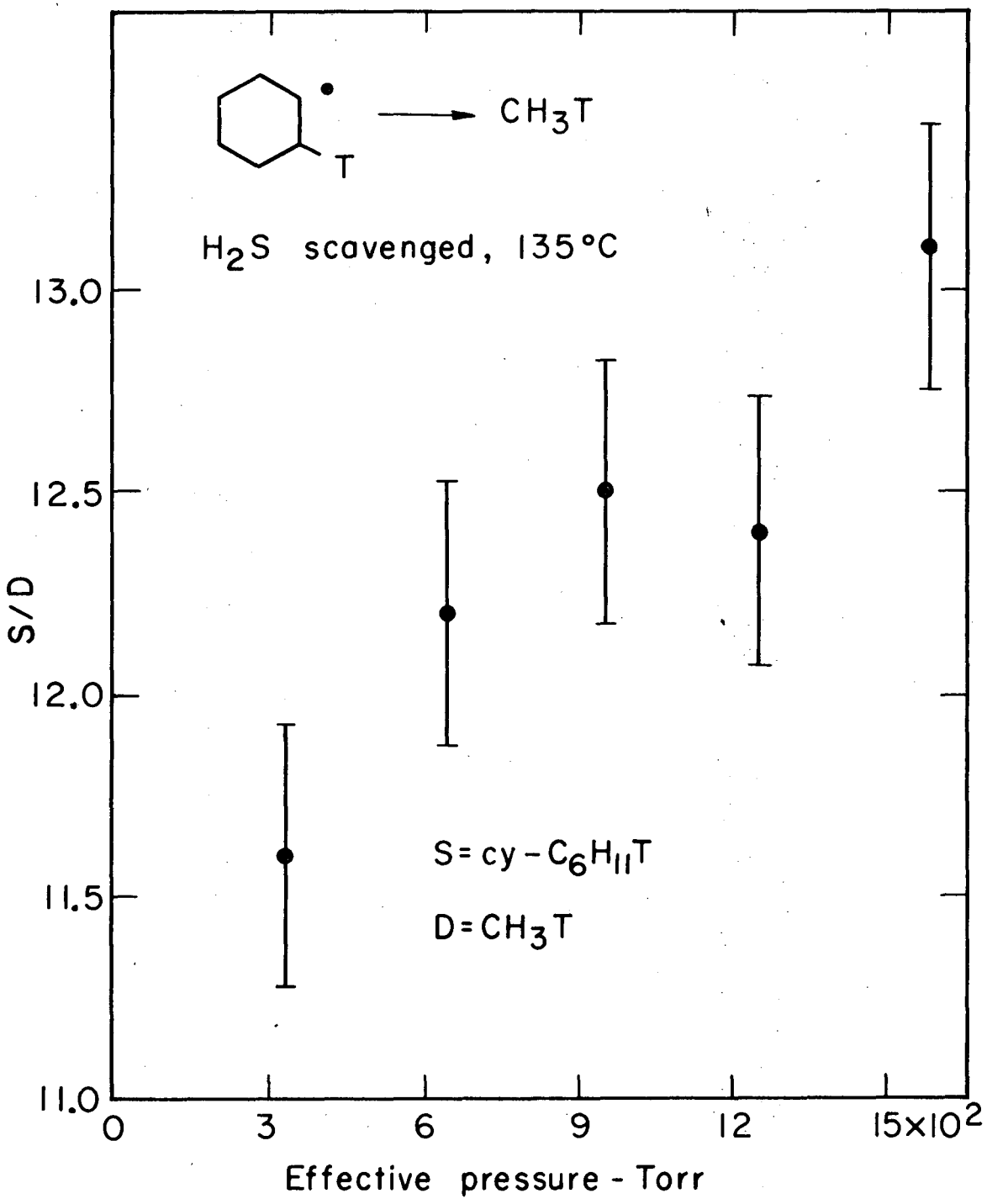

Fig. 9.6. The unimolecular decomposition of cyclohexyl-t radicals to methane-t; H_2S scavenged data at 135°C. Activated cyclohexyl-t radicals are formed by recoil T atom addition to cyclohexene. The abscissa is the effective collisional deactivation pressure (in the sample capsule) defined as: effective pressure = cyclohexene pressure + 0.2 (helium-3 pressure) + 0.5 (hydrogen sulfide pressure). (Data in Appendix, Table A-9-3.)

the values of the rate constants at 135°C computed from $k = \omega = Z\ P$ at this pressure were: $k_1 = 8.4 \times 10^3\ sec^{-1}$ (7.9×10^{-4} Torr), $k_2 = 3.4 \times 10^4\ sec^{-1}$ (3.2×10^{-3} Torr). Using Eq. (2-26) to determine k_4 and comparing k_4 with k_1 and k_2 values similarly derived allowed k_4 to be estimated as $5 \times 10^2\ sec^{-1}$. The large uncertainty in the cyclohexane-t/methane-t ratio, as indicated by the large error bars in Fig. 9.6, prevented meaningful extrapolation over a large pressure range to the pressure of which S/D = 1.

A previous determination by Weeks and Garland of k_1 in a recoil tritium-cyclohexene system showed that S/D = 1.0 at 26 torr. As discussed before, the temperature control employed by Weeks and Garland was inadequate.[143] It is interesting to note that the effect of inadequate temperature control in determining the pressure at which S/D = 1.0 was larger for cyclohexyl-t radical unimolecular decomposition/isomerization than for the unimolecular decomposition of cyclohexene-t. This is consistent with cyclohexene-t decomposition being a higher energy process.

9.3 Determination of the Relative Rate of Abstraction Versus Addition of Radicals in Alkenes

As shown in Eq. (9-4), the addition of a tritium atom to an alkene produces an alkyl-t radical. The alkyl-t radical either undergoes unimolecular decomposition/isomerization or is stabilized by collision. Stabilized alkyl-t radicals can either abstract a hydrogen atom to form an alkane-t species or add to the double bond to initiate a radical chain. As shown by reaction channel k_4, the addition of the tritiated alkyl

radical to the alkene may sufficiently energize the newly formed alkyl radical to cause it to also undergo unimolecular decomposition/isomerization.

Methylcyclohexane-t has been observed in unscavenged T + cyclohexene systems. In O_2 and SO_2 scavenged systems, the yield of methylcyclohexane-t was zero. Either the CH_2T radical or the methylcyclohexyl-t radical could be scavenged by O_2 or SO_2. In neon moderated systems, the yield of methylcyclohexane-t increased with increasing moderation. This is consistent with increased stabilization of the new methylcyclohexyl-t radical formed from CH_2T addition to cyclohexene.

In H_2S scavenged T + cyclohexene systems, the yield of methylcyclohexane-t was also zero. A precursor to the methylcyclohexyl-t radical was being intercepted by H_2S. If methylcyclohexyl-t radicals were formed directly from T + cyclohexene reactions, H_2S would readily donate a hydrogen atom to the methylcyclohexyl-t radical and the yield of methylcyclohexane-t would increase with H_2S scavenging. The yield of methane-t increased with H_2S scavenging. As shown by the data in Table 8-2, H_2S would intercept the CH_2T radical (to form methane-t) before the CH_2T radical could add to the parent alkene, cyclohexene.

I propose that: (a) The increase in the methane-t yield with H_2S scavenging represents that portion of the total CH_2T radicals formed by T + alkene reactions that add to the parent alkene in unscavenged systems. (b) The decrease in the methane-t yield with O_2 or SO_2 scavenging represents that portion of the total CH_2T radical formed from T + alkene reactions that abstract a hydrogen atom from the parent alkene in unscavenged systems. This is shown in Eqs. (9-6) and (9-7).

$$CH_3T(H_2S) - CH_3T(\text{unscavenged}) = \text{addition} \qquad 9\text{-}6$$

$$CH_3T(\text{unscavenged}) - CH_3T(O_2) = \text{abstraction} \qquad 9\text{-}7$$

The subtraction of the O_2 scavenged methane-t yield value removes that portion of the methane-t yield which is formed by an unscavengeable, non-radical reaction path. This non-scavengeable methane-t yield may result from a direct T-for-alkyl substitution process on the terminal carbon in the carbon chain,[6,7] or a similar, but undefined high energy process.

$$T + R\text{-}CH_3 \longrightarrow R\cdot + CH_3T \qquad 9\text{-}8$$

The implicit assumption in this determination of the abstraction/addition ratio of CH_2T radicals (or other tritiated radicals) in T + alkene systems is that the added scavenger does not affect the production of CH_2T radicals. The added scavenger has two effects:

(a) <u>Increased pressure</u>. Increasing the pressure of the system may increase the stabilization of the alkyl-t radical (cyclohexyl-t radical) formed from tritium atom addition to the alkene (cyclohexene). With increased stabilization there is less unimolecular decomposition of the alkyl-t radical to form CH_2T radicals. The increase in the effective pressure is small, however. The scavenger pressure is usually only 5 to 10% of the hydrocarbon pressure. In addition, the scavenger is usually less efficient as a collisional de-activator than the parent alkene. The effect of increased effective pressure on CH_2T radical production is very probably less than the experimental error.

(b) Removal of thermal tritium atoms. Scavenging of the thermal tritium atoms (which constitutes the majority of tritium atoms which undergo addition (Sec. 1.2.1)) before they add to the alkene reduces the number of excited alkyl-t radical precursors to the CH_2T yield. From the data in Table 8-1, oxygen is obviously capable of removing all thermalized tritium atoms. This does not affect the proposed determination of the abstraction/addition ratio. Oxygen scavenging of thermalized tritium atoms means that oxygen has two chances (thermal T atom and CH_2T radical) to eliminate a radical contribution to the methane-t yield. The methane-t yield which remains with oxygen scavenging is truly the result of a high energy, non-scavengeable process.

The data in Table 8-1 also shows that H_2S is not too efficient in removing H atoms. In fact, the rate constant of tritium atom addition to the alkene (k_1) may be slightly larger than the rate constant for tritium atom to abstract a hydrogen atom from H_2S to form HT (k_2).

$$T + \text{alkene} \xrightarrow{k_1} \text{alkyl-t radical} \qquad 9\text{-}9$$

$$T + H_2S \xrightarrow{k_2} HT + HS\cdot \qquad 9\text{-}10$$

$$\frac{-d[T]}{dt} = k_1[T][\text{alkene}] + k_2[T][H_2S] \qquad 9\text{-}11$$

$$\text{fraction of thermalized tritium atoms scavenged by } H_2S = \frac{k_2[H_2S]}{k_1[\text{alkene}] + k_2[H_2S]} \qquad 9\text{-}12$$

For $k_1 = k_2$, Eq. (9-12) becomes

$$\frac{[H_2S]}{[\text{alkene}] + [H_2S]} = \text{mole \% } H_2S \text{ scavenger} \qquad 9\text{-}13$$

The fraction of thermalized tritium atoms scavenged by H_2S may be: (a) lessened by using a low mole % scavenger. (b) corrected for if k_1 and k_2 are known. Addition as defined in Eq. (9-6) when corrected for tritium atom scavenging by H_2S becomes (to 1st order)

$$\text{addition} = CH_3T(H_2S) - CH_3T(\text{unscavenged}) +$$

$$\frac{k_2[H_2S]}{k_1[\text{alkene}] + k_2[H_2S]} \left(CH_3T(H_2S) - CH_3T(O_2)\right) \qquad 9\text{-}14$$

The quantity $(CH_3T(H_2S) - CH_3T(O_2))$ represents the total CH_3T yield from a radical precursor formed by the addition of a tritium atom to the alkene parent. Without the correction factor in Eq. (9-14) the abstraction/addition ratio from Eq. (9-6) and (9-7) would be overestimated.

The abstraction/addition ratio calculated from Eq. (9-7) and (9-14) is really the ratio of the rate constants of the abstraction and addition reactions of CH_2T radicals in the unscavenged parent alkene.

$$\text{Abstraction Rx:} \quad CH_2T + \text{alkene} \xrightarrow{k_3} CH_3T(\text{unscavenged}) + \text{unlabeled radical} \qquad 9\text{-}15$$

$$\text{Addition Rx:} \quad CH_2T + \text{alkene} \xrightarrow{k_4} \text{alkyl-}CH_2T \text{ radical} \qquad 9\text{-}16$$

$$\frac{d[CH_3T(\text{unscavenged})]}{dt} = k_3[CH_2T][\text{alkene}] \qquad 9\text{-}17$$

$$\frac{d[\text{alkyl-}CH_2T\text{ radical}]}{dt} = k_4[CH_2T][\text{alkene}] \qquad 9\text{-}18$$

$$\frac{-\,d[CH_2T]}{dt} = (k_3 + k_4)\,[CH_2T][\text{alkene}] \qquad 9\text{-}19$$

Addition and abstraction as defined by Eq. (9-14) and (9-6), respectively, are related to the integrated rate expressions by

$$\text{addition + abstraction} \approx \int -\,d[CH_2T] = (k_3 + k_4) \int_0^t [CH_2][\text{alkene}]dt \qquad 9\text{-}20$$

$$\text{addition} \approx \int d[CH_3T(\text{unscavenged})] = k_3 \int_0^t [CH_2T][\text{alkene}]dt \qquad 9\text{-}21$$

$$\text{abstraction} \approx \int d[\text{alkyl-}CH_2T] = k_4 \int_0^t [CH_2T][\text{alkene}]dt \qquad 9\text{-}22$$

$$\frac{\text{abstraction}}{\text{addition}} = \frac{k_4}{k_3} \qquad 9\text{-}23$$

The abstraction/addition ratio using the uncorrected form for addition (Eq. (9-6)) are found in Table 9-1. In Table 9-1, the abstraction/addition rate constant ratio for methylcyclohexyl-t radicals was calculated using

$$\text{abstraction} = C_7H_{13}T(\text{unscavenged}) - C_7H_{13}(O_2) \qquad 9\text{-}24$$

$$\text{addition} = (CH_3T(H_2S) - CH_3T(\text{unscavenged})) - C_7H_{13}T(\text{unscavenged}) \qquad 9\text{-}25$$

Table 9-1. Abstraction/Addition Rate Constant Ratio of Tritiated Radicals at 25°C

Radical	Parent Alkene	$(k_4/k_3)^*$	Literature value of k_4/k_3
CH_2T	ethylene	0.0028	0.015
	1-butene	0.075	0.37
	butadiene	0.0019	
	cyclohexene	0.36	
ethyl-t	ethylene	0.091	
	cyclohexene	0.37	
butyl-t	1-butene	0.16	
1-butenyl	cyclohexene	0.35	
n-hexenyl		0.29	
cyclohexyl-t		0.32	
methylcyclohexyl-t		1.2	

*From recoil tritium reaction data.

where

$$(CH_3T(H_2S) - CH_3T(\text{unscavenged})) = \text{total amount of } CH_2T \text{ radicals which add to cyclohexene in unscavenged systems} \qquad 9\text{-}26$$

The determination of relative rate constants may be extended to a two alkene system. The relative rate constants for the addition of CH_2T radicals to the two alkenes may be determined with two sets of yield and pressure (of each parent alkene) values plugged into two equations with two unknowns. If for one of the alkenes $k_3/k_4 \cong 0$ (as is the case for butadiene) the simpler set of equations does not require simultaneous solution. For the butadiene-d_6/cyclohexene system, k_4(butadiene-d_6)/ k_4(cyclohexene) wad determined as 7.5 and 5.0 for two sets of yield and pressure values. Although there is a large spread in the data, the determination that k_4 for butadiene is larger than k_4 for cyclohexene is consistent with the trend of rate constants in Table 8-2. Similarly for the butadiene/1-butene system, k_4(butadiene)/k_4(1-butene) was determined as 76 and 309 for two sets of yield and pressure values. The literature value of k_3/k_4 for 1-butene of 0.37 (Table 9-1) was used. The reported value of k_4(butadiene)/k_4(1-butene) from Table 8-2 is 160. Once again the determination that k_4 for butadiene is larger than k_4 for 1-butene is qualitatively correct. The large spread in the values is inherent in the extention of the determination of relative rate constants to a two alkene system. Determination of relative k_4 values depends on taking the difference of two yield values which are nearly equal. This small difference between two large numbers is often only a factor of two or

three larger than the uncertainty of each of the large yield values. The resultant spread in the data is obvious. This effect is also inherent in determining k_3/k_4 but is not as serious.

9.4 Summary and Conclusions

Recoil tritium studies often are limited by the lack of knowledge of the energy of the tritium atom when it reacts. This often precludes determining kinetic parameters from hot atom studies. More frequently kinetic parameters from other chemical methods are used with recoil tritium reaction yields to further the study of recoil tritium reactions. In this section I have tried to reverse the direction of data flow and use recoil tritium reactions to determine kinetic parameters. First, the pressure dependence of the unimolecular decomposition of cyclohexene-t to ethylene-t and butadiene or ethylene and butadiene-t was determined. The apparent rate constant of cyclohexene unimolecular decomposition at 135°C and the s parameter in the RRK treatment of the unimolecular decomposition of cyclohexene were calculated from this data. Second, the unimolecular decomposition/isomerization of cyclohexyl-t radicals to give n-hexene-t, 1-butene-t, and methane-t was established and the individual rate constants for these processes were determined. Finally, the scavenger dependence of yields with an obvious radical precursor was used to determine the relative rate constants of abstraction versus addition of that radical in the alkene parent compound. This area looks promising. Further comparisons of abstraction/addition ratios from recoil tritium experiments with conventional kinetic determinations are necessary.

10. RECOIL TRITIUM REACTIONS WITH METHYLCYCLOHEXENE: INCLUDING A TEST OF THE RRK-RRKM ASSUMPTION OF ENERGY RANDOMIZATION PRIOR TO UNIMOLECULAR DECOMPOSITION

10.1 General Considerations in the T + Methylcyclohexene System

The reactions of recoil tritium atoms with gas phase 1-methylcyclohexene, 3-methylcyclohexene, and 4-methylcyclohexene have been studied at 135°C. The major gas phase products observed from each methylcyclohexene isomer were: (a) HT formed by hydrogen atom abstraction reaction. (b) Tritiated parent compound formed by a T-for-H substitution reaction. (c) Methylcyclohexane-t formed by tritium atom addition to the double bond on methylcyclohexene to form a methylcyclohexyl-t radical. The methylcyclohexyl-t radical then abstracts a hydrogen atom from the bulk hydrocarbon system to form methylcyclohexane-t. These three products compose 90% of the total observed gas phase tritiated product yield.

The proposed methylcyclohexyl-t radicals were intercepted by 9 mole % nitric oxide (NO) scavenger. With nitric oxide scavenging, the methylcyclohexane-t yield decreased to 1 to 4% of the unscavenged yield value. Similar concentrations of H_2S, O_2, and SO_2 scavenger did not affect the methylcyclohexane-t yield. This may indicate bulk chemical reactions between the parent hydrocarbon and the scavenger. The methylcyclohexane-t yields from T + 3-methylcyclohexene reactions and T + 4-methylcyclohexene reactions were nearly equal. The yield of methylcyclohexane-t from T + 1-methylcyclohexene reactions was only about one-half that from T + 3- and 4-methylcyclohexene reactions. This is consistent with the methylcyclohexyl-t radical formed by tritium atom

addition to 1-methylcyclohexene being less reactive via H-atom abstraction than the methylcyclohexyl-t radicals formed by tritium atom addition to 3- and 4-methylcyclohexene. In tritium atom addition to 1-methylcyclohexene, the formation of a 1-methylcyclohexyl-2-t radical (a in Eq. (10-1)) is highly favored. The study of H-atom addition to other alkenes shows that tertiary radicals are favored over secondary radicals by 20 to 1.[3] The adjacent methyl

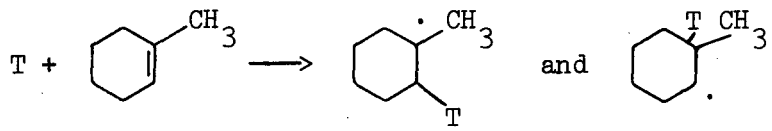

(a) (b) 10-1

group probably hinders H-atom abstraction by the tertiary methylcyclohexyl-t radicals from T + 1-methylcyclohexene reactions compared to H-atom abstraction by the secondary methylcyclohexyl-t radicals from T + 3- and 4-methylcyclohexene reactions.

Several of the tritiated products present in small yield showed interesting pressure or scavenger effects: (a) <u>methane-t</u>. The yield of methane-t in nitric oxide scavenged systems is roughly the same from tritium atom reactions with 3- and 4-methylcyclohexene. The yield of methane-t in nitric oxide scavenged T + 1-methylcyclohexene systems is only about one-half the yield of methane-t from nitric oxide scavenged T + 3- and 4-methylcyclohexene reactions. The methane-t yield in nitric oxide scavenged methylcyclohexene systems probably results from a direct T-for-cyclohexene substitution process as shown in Eq. (9-8). In this case R· is the 1-cyclohexenyl, 3-cyclohexenyl, and 4-cyclohexenyl radical

from T + 1-, 3-, and 4-methylcyclohexene, respectively. This trend of the methane-t yields is consistent with decreased probability for T-for-cyclohexene substitution to give methane-t when the cyclohexene-CH_3 bond strength is increased (see Eq. (3-12) and (3-13)).

(b) Methylcyclohexene-t isomers other than the parent. The parent isomers were API Standard Reference Materials certified at greater than 99.8% chemically and isomerically pure. The radio-gas-chromatographic system employed for analysis (Sec. 6) would not resolve small amounts of 3-methylcyclohexene from a larger 4-methylcyclohexene peak and vice-versa. The 1-methylcyclohexene peak was well resolved from the 3-/4-methylcyclohexene peak. The mass tracing during the radio-gas-chromatographic analysis did not reveal the presence of any methylcyclohexene isomers other than the parent compound. However, tritiated methylcyclohexene isomers other than the parent compound were observed in greater than 0.2% abundance compared to the tritiated parent compound.

For example, T + 4-methylcyclohexene reactions gave 1-methylcyclohexene in both unscavenged and nitric oxide scavenged samples. The 1-methylcyclohexene-t yield from T + 4-methylcyclohexene reactions was: (a) 4.8% as large as the 4-methylcyclohexene yield in unscavenged samples. (b) decreased by 60% with nitric oxide scavenging. This is consistent with a high energy and a thermal route to 1-methylcyclohexene formation from T + 4-methylcyclohexene reactions. The high energy (unscavengeable) route is probably hydrogen atom "scrambling" following a high energy T-for-H substitution reaction. The low energy (scavengeable) route is probably via a methylcyclohexyl-t radical formed by tritium atom

addition to 4-methylcyclohexene. Some examples of double-bond-shifting via a methylcyclohexyl-t radical intermediate are shown in Eqs. (10-2) to (10-5). The -H over the reaction arrow signifies loss of a hydrogen atom to the hydrocarbon system (see Ref. 180). Methylcyclohexyl-t radical mechanisms with more complex H-atom migration sequences can be postulated to give 1-methylcyclohexene-t from T + 4-methylcyclohexene reactions (and 4-methylcyclohexene-t from T + 1-methylcyclohexene reactions).

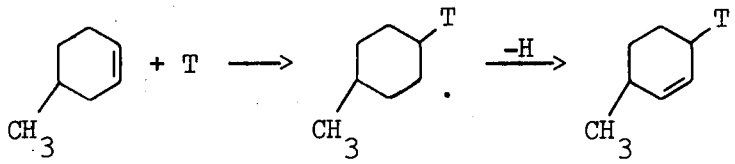

10-2

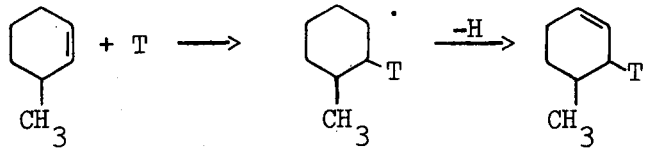

10-3

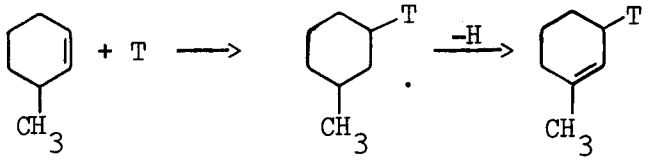

10-4

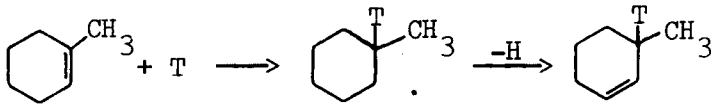

10-5

In unscavenged T + 1-methylcyclohexene reactions, the combined 3- and 4-methylcyclohexene-t yield was 9% as large as the 1-methylcyclohexene-t yield. In unscavenged T + 3-methylcyclohexene

reactions, the 1-methylcyclohexene-t yield was only 3% as large as the 3-methylcyclohexene yield. In both T + 3-methylcyclohexene and T + 1-methylcyclohexene reactions the yield of the non-parent methylcyclohexene-t isomer(s) doubled with nitrix oxide scavenging. Similar anomalous increases with nitric oxide scavenging[138] have been discussed in Sec. 7.1.

(c) Unimolecular decomposition products. The retro-Diels-Alder cleavage of the isomeric methylcyclohexenes has been shown in Eqs. (3-7) to (3-9). The unimolecular decomposition of the methylcyclohexene isomers following a T-for-H substitution reaction is shown in Eqs. (10-6) to (10-8).

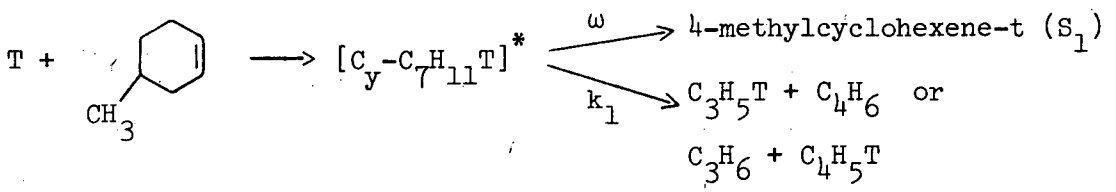

$D_1 = C_3H_5T$ (propylene-t) + C_4H_5T (butadiene-t)

10-6

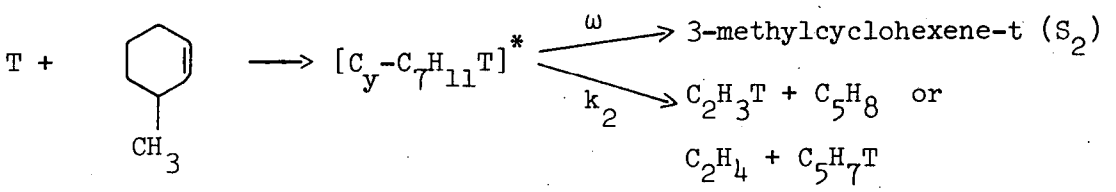

$D_2 = C_2H_3T$ (ethylene-t) + C_5H_7T (1,3-pentadiene-t)

10-7

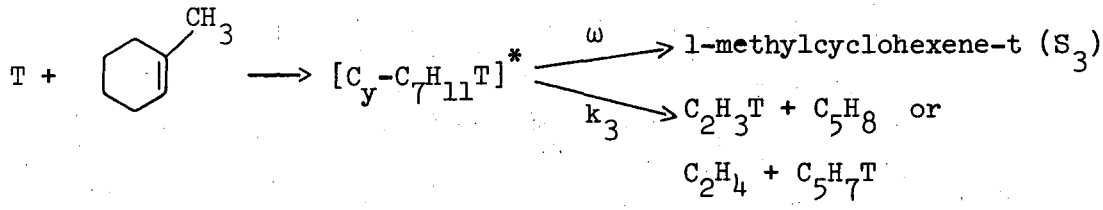

$$D_3 = C_2H_3T \text{ (ethylene-t)} + C_5H_7T \text{ (isoprene-t)}$$

10-8

The pressure dependence of the S/D ratios from the recoil tritium reactions shown in Eqs. (10-6) and (10-7) are displayed in Figs. 10.1 and 10.2, respectively. The data are from unscavenged samples. In the data in Figs. 10.1 and 10.2 scavenging with nitric oxide and butadiene-d_6 revealed that the butadiene-t yield was not depleted by reactions with radiolysis produced H-atoms. Nitric oxide scavenging showed no radical contribution to the 1,3-pentadiene-t yield but a 14% radical contribution to the ethylene-t yield and a 15% radical contribution to the propylene-t yield. The data in Figs. 10.1 and 10.2 were corrected to remove the thermal contribution to the ethylene-t and propylene-t yields in a manner to that described in Sec. 9.1. The resultant "scavenged" S/D ratios are shown in Figs. 10.3 and 10.4.

The pressure dependence of the unimolecular decomposition of 4-methylcyclohexene-t (Fig. 10.1) and 3-methylcyclohexene-t (Fig. 10.2) may be well represented by a line. The rate parameters shown in Table 10.1 were determined by extrapolation to S/D = 1.0 in a manner similar to that previously described. The effective pressure was defined as

$$P_{effective} = 1.0\ P_{C_7H_{12}} + 0.17\ P_{^3He} \qquad 10\text{-}9$$

using relative collisional deactivation efficiencies from published sources.[71]

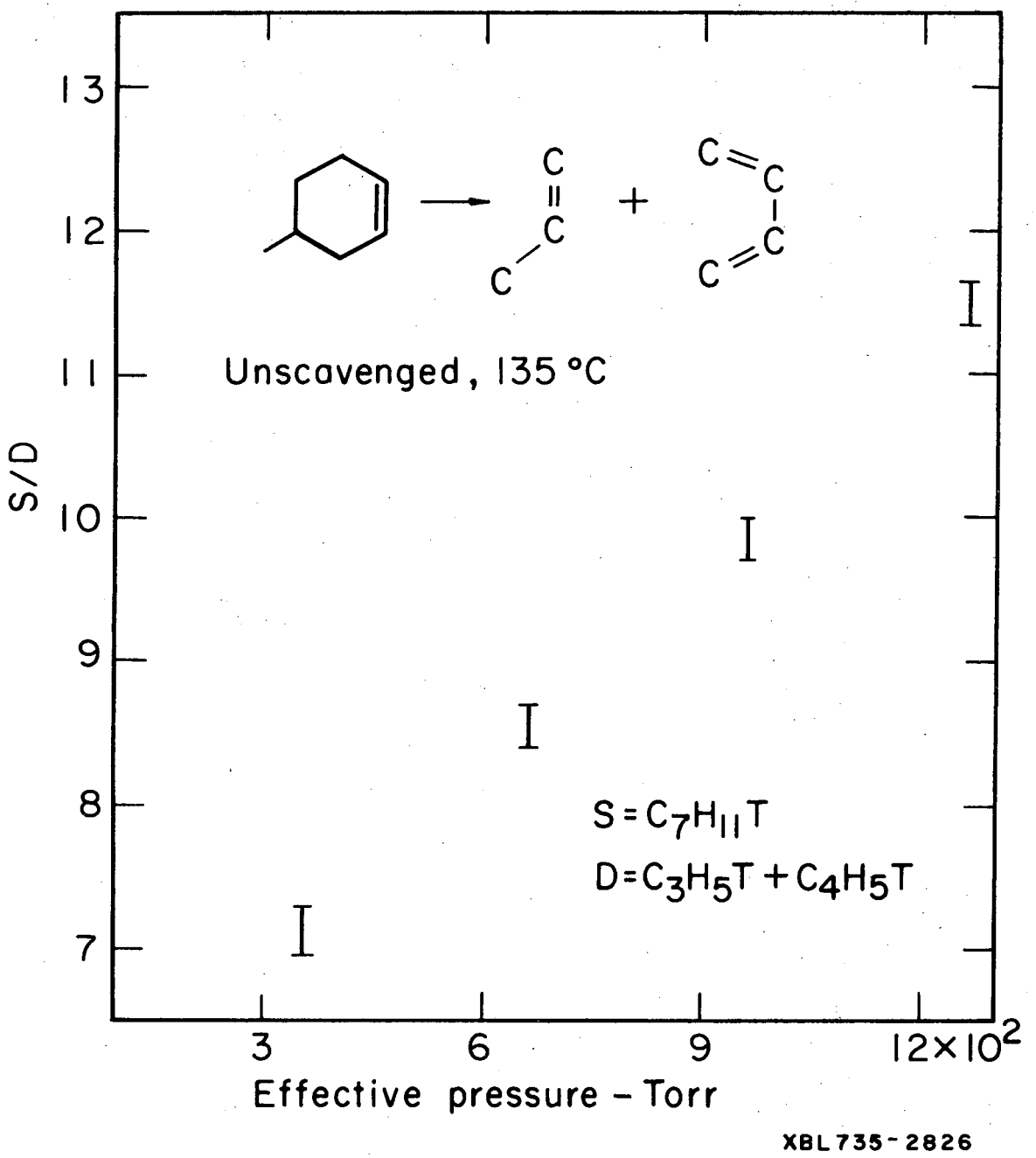

Fig. 10.1. The unimolecular decomposition of 4-methylcyclohexene-t to give propylene-t or butadiene-t; unscavenged data at 135°C. Activated 4-methylcyclohexene-t molecules are formed by recoil T-for-H substitution. The abscissa is the effective collisional deactivation pressure (in the sample capsule) defined as: effective pressure = 4-methylcyclohexene pressure + 0.17 (helium-3 pressure). (Data in Appendix, Table A-10-1.)

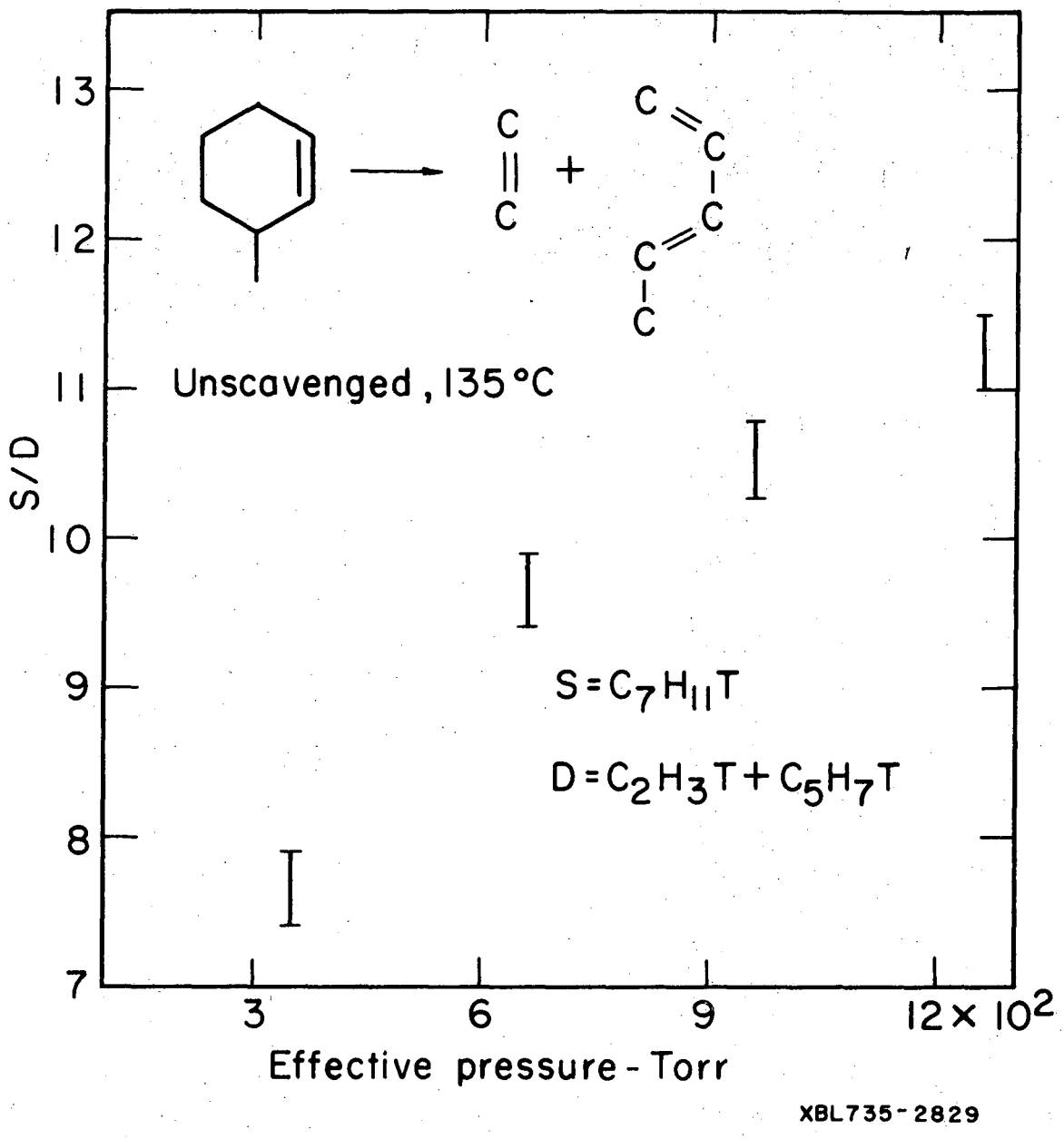

Fig. 10.2. The unimolecular decomposition of 3-methylcyclohexene-t to give ethylene-t or pentadiene-t; unscavenged data of 135°C. Activated 3-methylcyclohexene-t molecules are formed by recoil T-for-H substitution. The abscissa is the effective collisional deactivation pressure (in the sample capsule) defined as: effective pressure = 3-methylcyclohexene pressure + 0.17 (helium-3 pressure). (Data in Appendix, Table A-10-2.)

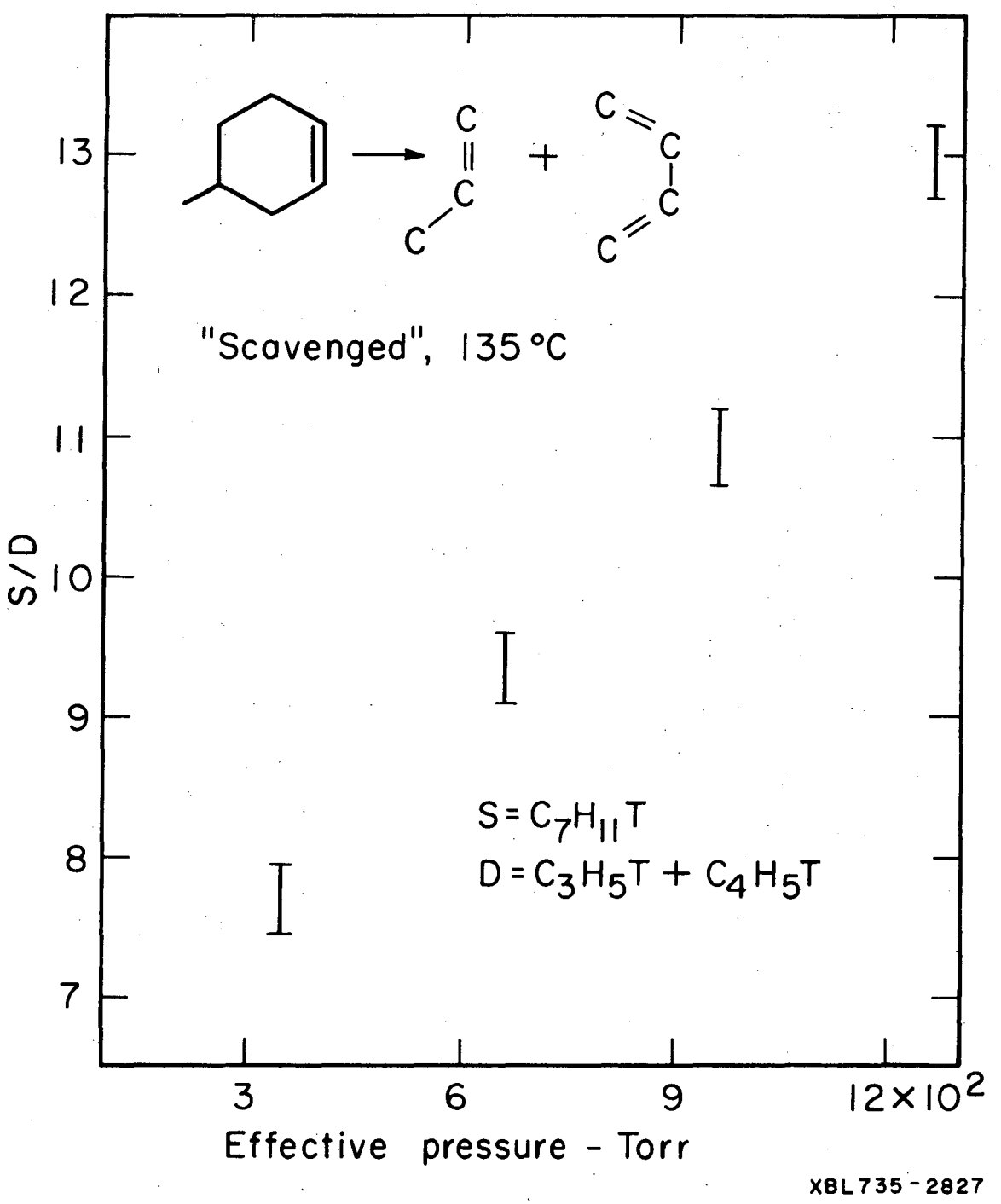

Fig. 10.3. The unimolecular decomposition of 4-methylcyclohexene-t to give propylene-t or butadiene-t; "scavenged" data at 135°. Activated 4-methylcyclohexene-t molecules are formed by recoil T-for-H substitution. The abscissa is the effective collisional deactivation pressure (in the sample capsule) defined as: effective pressure = 4-methylcyclohexene pressure + 0.17 (helium-3 pressure). The "scavenged" data represents the unscavenged experimental data in Fig. 10.1 from which a 15% radical contribution to the propylene-t yield has been subtracted. (Data in Appendix, Table A-10-1.)

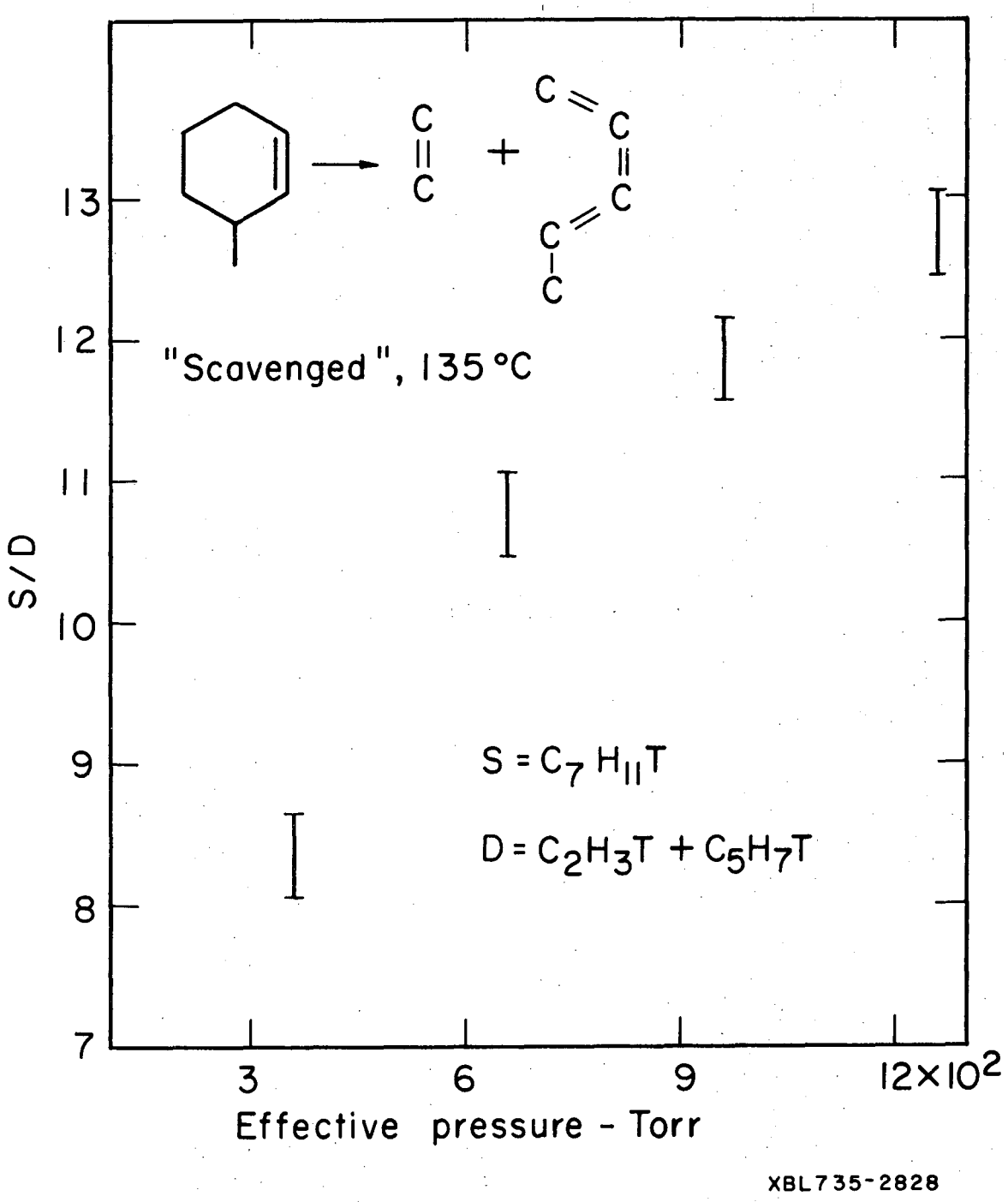

Fig. 10.4. The unimolecular decomposition of 3-methylcyclohexene-t to give ethylene-t or pentadiene-t; "scavenged" data of 135°C. Activated 3-methylcyclohexene-t molecules are formed by recoil T-for-H substitution. The abscissa is the effective collisional deactivation pressure (in the sample capsule) defined as: effective pressure = 3-methylcyclohexene pressure + 0.17 (helium-3 pressure). The "scavenged" data represents the unscavenged experimental data in Fig. 10.2 from which a 14% radical contribution to the ethylene-t yield has been subtracted. (Data in Appendix, Table A-10-2.)

Table 10-1. Rate Parameters from the Unimolecular Decomposition of Methylcyclohexene-t

parent compound	"scavenged"	Pressure at S/D = 1.0, Torr	k_a sec^{-1}	E in eV for s=22	25[a]	34[b]	38[c]
4-methylcyclohexene	no	1.3	1.5×10^7	5.0	5.4	6.8	7.4
	yes	42	5.0×10^8				
3-methylcyclohexene	no	0.29	3.4×10^6				
	yes	0.48	5.7×10^6				

Calculated with σ_d(methylcyclohexene) = 6.12×10^{-8} cm,[71] $A = 1.35 \times 10^{15}$ sec^{-1},[81] $E_o = 2.89$ eV,[81] and

$$k_a = A\left[\frac{E - E_o}{E}\right]^{s-1}$$

(a) $25 \approx \frac{1}{2}(3N-6)$, (b) $34 \approx \frac{2}{3}(3N-6)$, (c) $38 \approx \frac{3}{4}(3N-6)$

The data for the unimolecular decomposition of 1-methylcyclohexene-t to ethylene-t or isoprene-t are not shown. The data points were widely scattered and a pressure effect was not observed. The lack of a linear dependence of S/D on pressure may result from the extreme reactivity of isoprene-t. Isoprene-t polymerization[181] may prevent an accurate determination of the isoprene-t yield from the unimolecular decomposition of 1-methylcyclohexene-t.

10.2 A Test of the RRK-RRKM Assumption of Energy Randomization Prior to Unimolecular Decomposition

The formation of cyclohexene-t (S) and butadiene-t (D) by the reaction pathways shown in Eqs. (3-1) and (3-2) was a small reaction channel (less than 3% of the gas phase tritiated products) in the recoil tritium reactions with 1- and 3-methylcyclohexene. The pressure dependence of the S/D ratio in Eqs. (3-1) and (3-2) could not be determined in high pressure unscavenged T + 1-methylcyclohexene and T + 3-methylcyclohexene systems, respectively. The methylcyclohexane-t peak was broadened by column overloading in the high pressure samples. Consequently, the cyclohexene-t peak could not be resolved from the methylcyclohexane-t peak. Good resolution of the cyclohexene-t peak and the methylcyclohexane-t peak was obtained at the lowest pressure samples. A comparison of unscavenged and nitric oxide scavenged samples at the lowest pressure showed that the yield of cyclohexene-t and butadiene-t was unaffected by scavenger.

A small difference in the D/S ratio from Eq. (3-1) versus (3-2) was observed. The average energy of excitation deposited in

cyclohexene-t by a T-for-methyl substitution was estimated from the nitric oxide scavenger data using the previously described techniques, namely:

$$k_a = (D/S)\ \omega \qquad \omega = Z\ P \qquad 10\text{-}10$$

$$P_{effective} = 1.0\ P_{C_7H_{12}} + 0.17\ P_{^3He} + 0.24\ P_{NO} \quad [71] \qquad 10\text{-}11$$

In calculating Z, σ_d was estimated as 5.47×10^{-8} cm for cyclohexene and 6.12×10^{-8} cm for methylcyclohexene.[71]

$$k_a = A \left[\frac{E - E_o}{E}\right]^{s-1}, \qquad A = 2 \times 10^{15},^{82} \quad E_o = 2.90\ eV^{82}$$

$$s = 24\ (\text{Sec. } 9.1) \qquad 10\text{-}12$$

For Eq. (3-1), $D/S = 0.36$, $k_{1c} = 1.6 \times 10^9\ sec^{-1}$, $E = 6.4$ eV

10-13

For Eq. (3-2), $D/S = 0.59$, $k_{3c} = 2.6 \times 10^9\ sec^{-1}$, $E = 6.5$ eV

10-14

The near equivalence of the average energy of excitation in cyclohexene-1-t and cyclohexene-3-t (from T-for-methyl substitutions on 1-methylcyclohexene and 3-methylcyclohexene, respectively) shows: (a) The RRK-RRKM assumption of energy randomization prior to unimolecular decomposition is valid for the recoil tritium initiated unimolecular decomposition of cyclohexene.

(b) A T-for-methyl substitution reaction leaves an average energy of excitation of about 6.5 eV in the resultant tritiated molecule. The

energy of the C-CH_3 bond broken in the T-for-methyl substitution process apparently has little effect on the average energy deposited in the resultant tritiated molecule.

The proven RRK-RRKM assumption of energy randomization prior to unimolecular decomposition can now be put to use. There are ten possible T-for-H substitution sites in cyclohexene. Assuming retro-Diels-Alder cleavage of cyclohexene, T-for-H substitution at four of the sites results in ethylene-t; at six of the sites in butadiene-t.

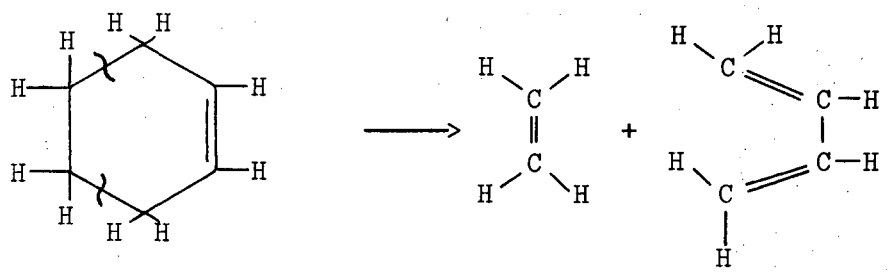

10-15

By analogy to T-for-methyl substitution in methylcyclohexenes, the average energy of excitation in cyclohexene-t following T-for-H substitution is probably independent of the strength of the C-H bond that was broken. This means that the cyclohexene-t molecule formed by T-for-H substitution has the same average energy of excitation, regardless of the site of the T label. Because all cyclohexene-t molecules have the same average excitation energy and energy is randomized in cyclohexene prior to unimolecular decomposition, cyclohexene-t molecules decompose with equal probability regardless of the site of the T label. Consequently, the 1,3-butadiene-t/ethylene-t ratio should be 1.5 to 1.0 from the retro-Diels-Alder cleavage of cyclohexene-t formed in T + cyclohexene reactions.

The butadiene-t/ethylene-t ratio from scavenged T + cyclohexene systems was 1.00 at 25°C and 1.05 at 135°C. Similarly the 1,3-pentadiene-t/ethylene-t ratio at 135°C is scavenged T + 3-methylcyclohexene reactions (see Eq. (10-7)) was 0.68. However, the butadiene-t/propylene-t ratio at 135°C in scavenged T + 4-methylcyclohexene reactions was 1.20. The further reactions of butadiene-t (see Sec. 3.2) are presumably the same for butadiene-t from T + cyclohexene reactions as from T + 4-methylcyclohexene reactions. Hence the further reactions of butadiene-t (or pentadiene-t) cannot be used to explain the low butadiene-t/ethylene-t ratio. Only when ethylene-t is not the smaller of the assumed retro-Diels-Alder cleavage products does the ratio of the tritiated products approach the statistical prediction based of equal unimolecular decomposition per T-for-H substitution site. An explanation consistent with this observation is the production of ethylene-t from a non-retro-Diels-Alder reaction. The postulated non-retro-Diels-Alder path to ethylene-t formation in recoil tritium systems is shown in Eqs. (10-16) and (10-17).

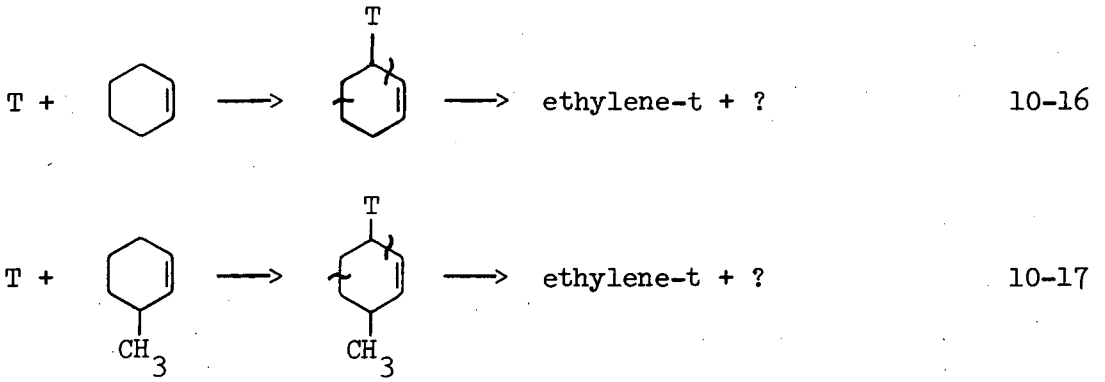

Ethylene-t from a non-retro-Diels-Alder-cleavage pathway has been observed in cyclohexene-3,3,6,6-d_4 decompositions[85] (see Eq. (3-6)). The

postulated non-retro-Diels-Alder cleavage of methylcyclohexene-t is supported by the observation of a 1,3-pentadiene-t peak 14% as large as the butadiene-t peak in scavenged T + 4-methylcyclohexene reactions.

10.3 Summary and Conclusions

In the reactions of recoil tritium atoms with the three methylcyclohexene isomers ninety per cent of the reactions which gave gas phase products can be attributed to: (a) abstraction to form HT. (b) Addition to form a methylcyclohexyl-t radical which may abstract a hydrogen atom to form methylcyclohexane-t.
(c) Substitution of T-for-H to form the tritiated parent isomer. Small yield reaction channels have also been observed: (i) Unimolecular Decomposition. The unimolecular decomposition of 4-methylcyclohexene-t to give propylene-t or butadiene-t; and the unimolecular decomposition of 3-methylcyclohexene-t to give ethylene-t or 1,3-pentadiene-t has been well established from the pressure dependence of the tritiated products. The apparent rate constants for these unimolecular decomposition processes are 1×10^7 sec^{-1} and 3×10^6 sec^{-1}, respectively. (ii) T-for-Methyl Substitutions. The average energy of excitation following T-for-methyl substitution is the same for cyclohexene-1-t and cyclohexene-3-t, namely 6.5 eV. From this I concluded that the energy of the $C-CH_3$ bond broken in T-for-methyl substitution has little effect on the average energy deposited in the resultant molecule.

I therefore conclude that the RRK-RRKM assumption of energy randomization prior to unimolecular decomposition is valid for the recoil tritium initiated unimolecular decomposition of cyclohexene.

11. SUMMARY AND CONCLUSIONS

Nearly three and one-half years ago I started out to test the RRK-RRKM assumption of energy randomization prior to unimolecular decomposition. I planned to study the reactions of recoil tritium atoms with methylcyclohexene. If the assumption of energy randomization was valid, cyclohexene-t molecules (from T-for-methyl substitution reactions with methylcyclohexene) should decompose unimolecularly at the same rate regardless of the site of the tritium label. This is true, of course, provided that the cyclohexene-t molecules possessed the same average energy of excitation following T-for-methyl substitution.

The experimental plan was simple: Place ^{3}He and gaseous methylcyclohexene in a sample capsule, irradiate with neutrons to form recoil tritium atoms from $^{3}He(n,p)T$ reactions, separate and analyze the radioactive tritium labeled products by radio-gas-chromatography. I immediately designed and constructed a vacuum line for sample preparation (Sec. 5). I also designed and constructed a radio-gas-chromatography system that was to grow to that described in Sec. 6.

In the beginning I had three immediate goals: (a) to test the reliability of my new sample filling and analysis systems. This could best be accomplished with simple parent hydrocarbons where the tritiated products are not numerous. (b) to try to reproduce published results. (c) to work toward a study of T + cyclohexene reactions as a prelude to studying T + methylcyclohexene reactions. Preliminary studies of T + cyclohexene reactions showed problems with oxygen scavenging. I decided that all three goals could be neatly met by trying to develop

sulfur dioxide as a new scavenger for the T + cyclohexene system. I would determine the effects of added sulfur dioxide in T + n-butane and T + trans-2-butene systems where the effects of added oxygen scavenger were well established.

Sulfur dioxide was not as efficient as scavenger as oxygen in T + n-butane systems. Unlike oxygen, sulfur dioxide could not remove all the thermalized tritium atoms before the tritium atoms abstracted a hydrogen atom from n-butane to form HT. In T + trans-2-butene systems, sulfur dioxide was as efficient as oxygen in removing thermalized alkyl-t radicals (formed by tritium atom addition to trans-2-butene) before the alkyl-t radical abstracted a hydrogen from the bulk system to form butane-t. Similarly in the T + cyclohexene system, sulfur dioxide and oxygen were equally efficient in: (a) scavenging cyclohexyl-t radicals before the cyclohexyl-t radicals abstracted in hydrogen atom to form cyclohexane-t.

(b) scavenging a small radical contribution to the ethylene-t yield.

However, while the butadiene-t yield from T + cyclohexene reactions was constant with sulfur dioxide scavenging, the butadiene-t yield increased with oxygen scavenging. The anomalous oxygen scavenging effect in T + cyclohexene reactions was clarified by H_2S and butadiene-d_6 scavenging. The "hot" butadiene-t yield could only be determined with oxygen or butadiene-t scavenging. In the absence of oxygen or butadiene-d_6 scavenging, the butadiene-t yield was selectively depleted by reactions with radiolysis produced hydrogen atoms.

The pressure dependence (in the 300 to 1500 torr pressure range) of the products of recoil tritium reactions with cyclohexene was

determined at 135°C. Neutron irradiations at 135°C were performed in a specially designed irradiation container (Sec. 5). Both at 135°C and at 25°C roughly 85% of the T + cyclohexene reactions which gave gas phase products resulted from tritium atom: abstraction to form HT, addition to form cyclohexyl-t radicals, or T-for-H substitution to form cyclohexene-t. The dependence of product yield on pressure showed that ethylene-t and butadiene-t resulted from the unimolecular decomposition of excited cyclohexene-t (formed by T-for-H substitution). The apparent rate constant of cyclohexene-t unimolecular decomposition was determined as 5.1×10^6 sec^{-1}. The s parameter in the RRK treatment of the unimolecular decomposition of cyclohexene was determined as s = 24. Similarly the dependence of product yield on pressure showed that n-hexene-t, 1-butene-t and methane-t resulted from the unimolecular decomposition of cyclohexyl-t radicals (formed by T addition to cyclohexene) with rate constants 8×10^3 sec^{-1}, 3×10^4 sec^{-1} and 5×10^2 sec^{-1}, respectively. The relative rate of abstraction versus addition of radicals in alkenes was determined from the scavenger dependence of the yield of products with a radical precursor.

The reactions of recoil tritium atoms with methylcyclohexene were also studied at 135°C. Roughly 90% of the T + methylcyclohexene reactions which gave gas phase products resulted from tritium atom: abstraction to form HT, addition to form methylcyclohexyl-t radicals, or T-for-H substitution to form methylcyclohexene-t. The dependence of product yield on pressure (in the 300 - 1200 torr pressure range) showed that excited 4-methylcyclohexene-t (formed by T-for-H substitution)

decomposed unimolecularly to give propylene-t or butadiene-t with a rate constant of 1×10^7 sec^{-1} and that similarly excited 3-methylcyclohexene-t decomposed unimolecularly to give ethylene-t or pentadiene-t with a rate constant of 3×10^6 sec^{-1}.

Finally there came that long awaited moment when the rates of unimolecular decomposition of cyclohexene-1-t and cyclohexene-3-t (from T-for-methyl substitution reactions with 1-methylcyclohexene and 3-methylcyclohexene, respectively) could be compared. The rates of unimolecular decomposition of cyclohexene-1-t and cyclohexene-3-t were similar. Using the previously determined RRK parameter (s = 24) for the unimolecular decomposition of cyclohexene, the average energy of excitation deposited in cyclohexene-t by T-for-methyl substitution reactions with methylcyclohexene was estimated at 6.5 eV for both cyclohexene-1-t and cyclohexene-3-t.

I concluded that the RRK-RRKM assumption of energy randomization prior to unimolecular decomposition is valid for the recoil tritium initiated unimolecular decomposition of cyclohexene.

I further concluded that although recoil tritium studies are often limited by the lack of knowledge of the energy of the tritium atom when it reacts, kinetic parameters and fundamental contributions to gas kinetics can come from carefully designed recoil tritium experiments.

ACKNOWLEDGEMENTS

I would like to acknowledge the support and encouragement of a great teacher and research director, Sam Markowitz.

I would like to thank:

Drs. John K. Garland, Robert W. Weeks, and Kent I. Mahan for getting me started in recoil tritium chemistry.

Dr. F. S. Rowland for a series of stimulating discussions on hot atom chemistry.

Dr. Amos Newton and Al Sciamanna for a series of tips on gas chromatography.

Fred Vogelsberg for his excellent work in designing and maintaining the electronics upon which all of this work depended.

Irwin Binder, a fellow graduate student, for sharing his great insights on the recoil tritium methylcyclohexene system.

I would like to thank the staff of the Lawrence Berkeley Laboratory for their support in the areas of:

electronics - Milt Firth, George Kilian and Frank Belden

mechanical design - Doug MacDonald, Don Malone, and Warren Harnden

Mechanical construction - G. G. Young, Hardy Wandesforde, Larry Ornelas, and Bert Watkins

purchasing - Dan Westfall and Crystall Llewellyn

irradiations - Bob McCracken and Eldred Calhoun

gas regulators - Walt Niemi

glass blowing - Paul Henrickson and Dane Anderberg

technical illustration - Evelyn Grant

I would like to thank Don Eliot, Dick Curtis, Harry Braun, and Tekhanian Lim of The Berkeley Campus Research Reactor.

I would like to acknowledge a nearly infinite series of Coke drinking and world problem solving sessions with other members of the Markowitz group: Norm Jacob, Tom Campbell, Bahman Parsa, Don Murphy, Man King Go, Diana Lee, and John Lee.

I would like to acknowledge the support of the Graduate Fellowships Division of the National Science Foundation and the Atomic Energy Commission.

APPENDIX

This appendix will be composed mainly of tables of tritiated product yields. The yields will be listed relative to the yield of tritiated parent compound as 100. The column in the tables which corresponds to the yield of tritiated parent is not repeatedly listed as 100, however. The tritiated parent yield column lists the net counts of tritiated parent recovered and counted in the radio-gas-chromatographic analysis.

The tables of relative yields will be placed in roughly the same order as the data therein is discussed in the text. This will be indicated by the table number. For example, Table A-7-1 is a table in the appendix (A) containing the first (1) data discussed in section seven (7).

Table A-6-1. Calibrated Retention Data Using the Sequence of Operations Given in Table 6-1.

Compound	Retention Time, Min.	Compound	Retention Time, Min.
^{3}He	52	cis-pentadiene	417
air	59	n-hexenes	454
methane	86	cyclohexane	487
ethylene	137	cyclohexene	540
ethane	149	methylcyclohexane	580
propane	170	3-methylcyclohexene	725
propylene	178	4-methylcyclohexene	770
isobutane	181	1-methylcyclohexene	840
acetylene	188		
butane	195		
1-butene	214		
isobutene	217		
trans-2-butene	232		
cis-2-butene	245		
3-methyl-1-butene	259		
1,3-butadiene	281		
1,2-butadiene	342		
pentene	389		
isoprene	403		
trans-pentadiene	411		

Table A-7-1. T + Cyclohexene Reaction Data (25°C)

Sample Filling Conditions Pressures, cm Hg			Vol.	Yields Relative to Cyclohexene-t as 100																		
												2-butene								"Polymer-t"		
^3He	O_2	SO_2	ml	HT	CH_3T	C=C	C-C					trans/cis			pen-tene	hex-ene		10^3 cts		L	M	H
1.75			13.89	260	3.15	21.9	1.4	1.8	1.3	2.0	5.7	0.5	0.2	13.9	1.1	4.7	32.4	70.9	4.5	7.4	6.5	56.7
1.75			13.81	271	3.06	22.9	1.6	2.2	1.7	2.3	6.3	0.5	0.5	15.2	0.7	4.0	32.0	66.1	4.2	8.7	9.5	60.9
1.64	0.29		14.28	270	0.27	20.6	0	1.1	1.2	3.0	1.5	0.2	0.1	20.8	0	0.4	0.6	90.7	0	6.8	9.7	47.3
1.64	0.29		15.26	279	0.32	21.1	0.1	1.1	1.4	2.4	1.8	0.4	0.2	20.8	0	0	0.1	92.3	0	5.6	17.	47.8
1.64	0.98		15.42	273	0.28	20.5	0	1.3	1.2	2.2	1.5	0.1	0	19.7	0	0.8	0.7	91.7	0	4.8	8.6	41.5
1.64	0.98		14.05	273	0.30	21.2	0	1.3	1.2	2.2	1.4	0.1	0	20.4	0	0	0.2	87.6	0	11.	13.	48.0
1.64		0.29	14.00	279	0.28	21.4	0.2	1.2	1.7	2.2	2.0	0.4	0.2	14.6	0	0.2	0.9	88.5	0	2.2	3.0	152.
1.64		0.29	13.65	274	0.32	20.0	0	1.2	1.6	2.4	2.0	0.6	0.4	14.1	0	0.8	1.0	91.0	0	1.9	3.4	151.
1.75		0.90	14.00	270	0.27	19.7	0.2	1.6	1.7	3.5	2.0	0.5	0.3	14.6	0	0.1	0.5	95.2	0	1.9	1.9	121.
1.75		0.90	13.62	276	0.30	19.6	0.1	1.6	1.8	1.8	1.8	0.4	0.2	13.0	0	0.5	0.8	96.5	0	2.2	3.5	164.

Cyclohexene pressure in all samples - 5.64 cm Hg

Table A-7-2. T + Trans-2-butene Reaction Data (25°C)

Sample Filling Conditions Pressures, cm Hg			Vol.	Yields Relative to Trans-2-butene-t as 100									2-butene			"Polymer-t"		
^3He	O_2	SO_2	ml	HT	CH_3T	C=C	C-C				C≡C		trans/cis		L	M	H
1.69			13.94	162	6.1	3.2	0.8	0.9	57.7	22.8	2.0	19.2	176	9.7	1.7	49.	3.	11.
1.69			13.99	156	4.2	3.4	0.9	0.7	56.1	22.0	1.7	18.4	198	9.4	1.7	49.	3.9	13.4
1.64	0.28		14.04	166	4.4	3.3	0.1	0.5	57.6	0.27	1.9	8.5	175	6.7	2.9	3.3	3.5	5.2
1.64	0.28		14.06	165	4.3	3.2	0.1	0.4	57.8	0.19	1.9	8.5	178	7.1	3.0	15.5	5.6	8.6
1.69	1.20		14.65	162	4.0	3.1	0.1	0.5	56.3	0.23	1.9	8.4	206	6.8	2.9	27.7	5.7	7.5
1.69	1.20		14.23	163	3.8	3.1	0.1	0.4	56.7	0.27	1.8	8.4	191	7.0	2.9	23.6	4.6	6.1
1.69	3.32		15.10	159	5.6	3.0	0.1	0.5	57.2	0.22	1.8	8.6	202	7.1	2.8	38.3	6.1	9.8
1.69	3.32		15.25	165	2.7	3.1	0.1	0.4	58.5	0.24	1.9	8.7	201	6.9	2.8	14.1	4.6	8.3
1.58	6.52		15.25	149	3.0	2.9	0.1	0.5	56.8	0.25	1.7	8.4	200	6.7	2.7	20.0	3.5	2.6
1.58	6.52		14.87	155	8.4	3.0	0.1	0.5	57.4	0.21	1.9	8.4	177	6.8	2.7	38.0	6.5	7.3
1.80		0.28	14.75	166	5.5	3.0	0.1	0.6	58.8	0.43	2.6	8.9	195	7.7	1.1	2.3	0.6	76.8
1.80		0.28	15.11	162	4.3	3.0	0.1	0.5	57.1	0.53	2.6	8.9	202	8.0	1.2	2.3	0.7	69.2
1.80		1.19	13.95	162	4.7	2.9	0.1	0.5	57.6	0.39	1.8	8.6	184	7.3	1.2	3.1	0.6	92.8
1.80		1.19	14.12	165	3.9	2.9	0.1	0.5	58.1	0.96	2.1	8.6	185	7.6	1.3	1.5	0.7	76.4
1.69		3.39	14.28	160	5.6	2.9	0.1	0.5	56.6	0.29	1.8	8.7	200	7.9	1.3	3.8	0.8	85.5
1.69		3.39	14.31	160	4.3	2.9	0.1	0.5	56.9	0.25	1.9	8.5	187	7.5	1.5	4.4	0.7	91.8
1.80		7.00	15.21	159	4.8	2.9	0.1	0.1	58.0	0.33	1.9	8.6	210	7.9	1.4	2.0	1.5	89.0
1.80		7.00	15.44	157	8.6	3.0	0.1	0.5	57.4	0.25	2.0	8.7	192	7.8	1.3	2.5	1.2	75.2
1.69		6.95*	14.50	146	5.4	2.8	0.1	0.5	51.8	0.27	1.2	35.6	219	10.	2.5	13.3	3.1	24.2
1.69		6.95	14.56	149	5.1	2.7	0.5	0.5	50.8	0.50	1.5	38.9	218	11.	2.0	12.7	2.7	17.5

Trans-2-butene pressure in each sample - 67.4 cm Hg

10^3 cts

*Nitric Oxide, NO

Table A-7-3. Neon Moderated T + n-Butane Reaction Data (25°C)

Sample Filling Conditions Pressures, cm Hg				Vol.	Yields Relative to n-Butane-t as 100								2-butene		"Polymer-t"		
^3He		O_2	SO_2	ml	HT	CH_3T	C=C	C-C					trans/cis		L	M	H
1.53	11.3			14.00	347	7.0	5.7	9.5	12.0	3.7	130.	1.5	-	-	17.8	2.3	3.4
1.53	11.3			13.55	361	3.3	5.4	9.7	10.4	3.6	122.	1.3	-	-	18.7	2.9	4.8
1.25	11.1	0.28		13.86	207	6.5	6.9	4.8	4.6	1.8	77.6	0.8	0.4	0.4	6.0	3.0	1.0
1.25	11.1	0.28		13.67	208	6.9	6.9	4.5	4.1	1.7	75.9	0.9	0.3	-	6.6	8.5	0.8
1.15	10.3	1.14		13.83	170	8.2	7.1	3.5	4.3	1.8	103.	0.8	0.3	0.2	4.5	6.3	0.7
1.15	10.3	1.14		14.11	175	9.3	7.1	3.4	4.0	1.8	112.	0.9	0.4	0.2	4.1	7.0	1.6
1.25	8.97	2.17		14.54	162	10.1	7.0	3.3	4.1	1.9	73.2	0.9	0.3	0.3	1.0	5.1	0.5
1.25	8.97	2.17		13.22	166	12.1	7.1	3.5	4.4	1.7	77.9	0.7	0.3	0.1	7.3	8.8	0.7
1.30	5.37	5.38		13.41	155	10.4	7.3	3.5	4.7	2.3	58.8	0.3	0.2	0.1	5.3	10.1	0.4
1.30	5.37	5.38		-	156	7.9	7.2	3.3	4.0	1.6	59.2	0.7	0.2	0.2	7.4	2.1	0.6
1.15	10.0		1.19	13.85	307	10.4	6.1	3.7	4.2	1.5	69.2	2.1	0.5	0.3	5.7	2.4	-
1.15	10.0		1.19	14.05	300	12.0	5.8	3.4	4.0	1.5	66.5	2.5	0.5	0.3	6.8	6.5	33.1
1.25	9.20		2.32	14.00	258	13.6	7.9	3.5	4.1	1.5	70.2	3.1	0.6	0.3	5.4	7.5	25.6
1.25	9.20		2.32	13.85	260	13.4	6.3	3.4	4.1	1.5	70.2	2.5	0.5	0.2	3.9	3.8	25.0
1.25	5.70		5.75	13.41	225	8.8	6.8	3.6	4.2	1.7	49.1	1.5	0.4	0.4	14.9	12.0	25.4
1.25	5.70		5.75	13.65	223	8.7	7.1	3.3	4.0	1.5	50.6	1.6	0.4	0.2	10.5	7.6	25.6
											10^3 cts						

Neon pressure in each sample - 66.3 cm Hg

Table A-7-4. T + n-Butane Data (25°C)

Sample Filling Conditions				Yields Relative to n-Butane-t as 100												
Pressures, cm Hg			Vol.									2-butene		"Polymer-t"		
^3He	O_2	SO_2	ml	HT	CH_3T	C=C	C-C	C_CC	C_CC	C_CC_C	C_CC_C	trans/cis		L	M	H
1.69			14.15	292	7.2	5.3	6.9	7.4	1.8	201	1.0	-	-	4.1	1.3	1.6
1.69			13.88	298	7.6	5.2	6.7	7.2	2.0	198	1.0	-	-	6.8	4.5	1.1
1.69		1.13	13.96	286	8.3	5.5	4.0	4.3	1.6	197	0.6	0.3	0.2	1.4	2.5	9.8
1.69		1.13	13.73	289	5.9	5.4	3.9	4.2	1.5	185	0.5	0.3	0.1	1.1	1.1	5.7
1.69		2.38	14.37	267	5.8	5.8	4.0	4.0	1.6	191	0.7	0.4	0.1	3.0	1.4	9.2
1.69		2.38	14.46	271	5.8	5.8	4.0	4.0	1.6	196	0.8	0.4	0.1	1.8	1.5	12.1
1.69		5.47	14.21	244	9.4	6.0	3.8	4.2	2.2	191	0.8	0.3	0.1	1.1	2.7	12.4
1.69		5.47	14.89	245	5.5	5.8	3.9	3.9	1.6	200	0.8	0.3	0.1	2.3	1.8	12.5
1.80		11.3	13.86	226	6.7	6.1	4.0	4.5	1.8	181	0.4	0.3	0.2	6.4	3.5	7.4
1.80		11.3	13.74	224	3.9	6.0	3.9	3.8	1.6	182	1.2	0.4	0.2	9.0	3.0	11.6
1.80	5.55		15.15	184	9.9	6.5	3.9	3.9	2.0	208	0.7	0.5	0.2	1.1	3.2	0.6
1.80	5.55		13.67	188	8.5	6.5	4.0	3.8	1.9	220	0.7	0.4	0.2	2.1	6.4	0.3
n-Butane pressure in each sample - 45.2 cm Hg										10^3 cts						

Table A-8-1. T + Cyclohexene Reaction Data (25°C)

Sample Filling Conditions Pressures, cm Hg			Vol.	Yields Relative to Cyclohexene-t as 100																		
^3He	H_2S	C_4D_6	ml	HT	CH_3T	C=C	C-C					2-butene trans/cis		C_4D_5T	C_4H_5T	hex-ene				"Polymer-t" L	M	H
1.64	0.30		14.45	302	11.2	25.2	5.4	1.4	1.6	2.2	22.1	0	0	0	6.2	13.8	114	81.9	0	2.6	2.0	35.8
1.64	0.30		14.38	288	10.4	24.3	5.2	1.9	1.6	2.5	21.6	0	0	0	5.8	14.0	113	83.8	0	2.1	2.0	35.4
1.64	1.03		14.03	304	10.9	25.2	5.3	0.1	1.6	2.1	22.6	0	0	0	5.7	13.7	107	80.1	0	1.9	2.1	32.6
1.64	1.03		14.33	316	11.4	27.2	5.8	1.4	1.8	2.1	23.0	0	0	0	6.5	15.5	111	74.9	0	0.8	2.1	34.7
1.64		0.30	14.36	277	2.4	24.0	1.1	1.2	1.5	1.9	5.2	0.8	0.4	2.7	19.3	3.6	19	76.8	2.9	8.5	13.0	39.1
1.64		0.30	14.22	276	2.7	23.2	0.9	1.8	1.6	2.2	5.4	0.6	1.0	3.5	19.7	3.6	20	76.9	2.9	4.9	8.7	75.2
1.64		1.07	14.38	268	1.7	24.4	0.5	1.1	1.4	2.0	4.1	0.8	0.5	11.7	20.8	2.9	9	90.5	1.0	20.8	15.2	95.0
1.64		1.07	14.38	272	1.7	24.3	0.7	2.0	1.7	2.4	4.3	0.6	1.5	12.8	20.6	3.5	8	95.8	1.2	15.3	7.1	92.3
																		10^3 cts				

Cyclohexene pressure in each sample - 5.76 cm Hg

Table A-8-2. T + Cyclohexene Dual Scavenged Reaction Data (25°C)

Sample Filling Conditions Pressures, cm Hg					Vol.	Yields Relative to Cyclohexene-t as 100																		
														2-butene									"Polymer-t"	
^3He	H_2S	O_2	SO_2	C_4D_6	ml	HT	CH_3T	C=C	C-C					trans/ cis		C_4D_5T	C_4H_5T	hex-ene				L	M	H
1.64		0.28		1.03	13.22	276	0.3	27.2	0.1	0.3	1.3	2.5	1.8	0	0	24.9	22.5	0.5	1.1	82.2	0	9.6	9.7	71.5
1.64		0.28		1.03	14.13	272	0.4	26.6	0.2	1.5	1.5	3.2	1.8	0	0	25.0	22.1	1.0	1.1	70.5	0	14.5	9.6	63.3
1.64		0.98		1.03	14.47	272	0.3	28.7	0.2	0.5	1.5	2.6	1.8	0	0	25.4	22.8	1.0	1.6	73.8	0	9.2	10.2	68.3
1.64		0.98		1.03	14.27	272	0.5	28.2	0.1	0.7	1.8	2.9	1.9	0	0	25.4	23.4	1.5	1.2	64.7	0	11.7	11.2	69.6
1.69			0.30	0.96	14.13	270	0.4	27.2	0.3	0.6	1.7	2.7	2.7	3.2	1.3	23.0	22.2	0.4	0.8	73.1	0	17.6	8.3	133.
1.69			0.30	0.96	14.36	282	0.2	28.3	0.2	0.7	1.7	2.8	2.6	3.4	1.4	25.6	23.6	1.9	1.1	70.1	0	19.3	5.6	137.
1.64			1.03	1.07	14.33	276	0.3	27.3	0.1	0.6	1.7	2.5	1.3	2.8	1.1	25.6	21.4	0.5	0.6	80.1	0	12.9	4.2	119.
1.64			1.03	1.07	14.09	283	0.3	28.5	0.1	0.6	1.6	2.8	1.7	2.8	2.4	25.6	23.2	1.8	0.8	73.4	0	13.1	5.3	-
1.64	0.30			1.07	13.71	288	9.9	30.9	4.5	1.2	1.4	2.9	25.0	1.1	0.6	21.0	21.7	15.2	71.2	76.2	0	26.5	5.1	47.6
1.64	0.30			1.07	13.75	270	9.7	30.2	4.0	1.4	1.4	2.8	24.2	1.3	0.7	20.8	21.7	13.2	68.0	79.0	0	19.8	5.9	46.6
1.64	1.03			1.07	14.00	301	11.9	32.0	5.3	0.8	1.5	3.0	27.2	2.5	0.6	24.8	22.7	13.4	67.2	78.6	0	21.2	6.0	47.1
1.64	1.03			1.07	14.31	310	11.9	33.8	6.0	0.4	1.9	3.1	28.3	2.4	0.8	24.5	21.6	13.0	73.6	79.2	0	21.0	9.6	45.1

Cyclohexene pressure in each sample - 5.65 cm Hg

Table A-9-1. T + Cyclohexene Reaction Data (unscavenged, 135°C)

Sample Filling Conditions Pressures, cm Hg$^{\phi}$			Yields Relative to Cyclohexene-t as 100														"Polymer-t"		
^{3}He	scavenger	⬡	ml	HT	CH_3T	C=C	C-C				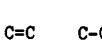	C_4D_5T		hexene	⬡	10^3 cts		L	M	H
9.52		30.0	13.75	216	6.39	13.1	3.07	0.65	1.69	1.86	13.3		13.4	13.7	60.9	32.1	0	9.5	26.9	3.2
9.52		30.0	14.17	223	6.87	13.1	3.05	1.20	1.01	1.62	15.5		13.6	11.7	63.0	34.0	0	17.0	-	1.6
9.52		60.3	13.56	230	6.60	12.0	3.33	0.67	1.48	1.77	14.3		12.3	11.9	65.2	35.4	0	16.0	32.5	2.3
9.52		60.3	13.31	225	6.42	11.7	3.20	1.23	1.75	1.55	13.0		11.2	12.0	69.2	33.0	0	20.2	51.4	1.0
9.30		90.5	13.67	251	7.48	11.9	3.79	1.02	1.81	1.60	12.6		10.4	10.4	73.5	29.3	0	20.2	46.8	2.1
9.41		90.5	14.06	249	6.86	11.4	3.59	0.92	1.82	1.45	13.2		8.79	11.6	79.6	30.6	0	16.6	25.3	1.4
9.52		120.	13.37	247	6.71	11.2	3.62	0.28	1.69	1.45	12.7		9.40	9.13	69.0	30.2	0	13.1	42.2	2.0
9.52		120.	13.97	248	6.71	10.7	3.60	0.67	1.71	1.67	12.2		9.91	11.0	74.3	28.5	0	15.8	30.8	1.9
9.52		152.	14.85	230	6.90	9.75	3.34	0.59	1.53	1.46	11.4		8.23	7.57	73.8	35.2	0	19.8	43.1	1.2
9.52		152.	14.41	247	7.03	10.8	3.82	0.62	1.43	2.41	12.0		8.83	7.67	77.3	31.0	0	17.1	42.7	1.7
35.7		7.80	14.55	322	8.78	22.8	3.46	0.58	1.56	2.51	16.3		20.4	10.9	137.	43.6	1.92	3.5	55.9	25.1
34.4		7.80	13.86	297	7.67	21.5	3.13	1.63	2.02	2.50	14.0		20.2	9.95	121.	39.4	3.07	15.3	82.8	17.9
34.9	1.26*	7.80	14.16	332	0.08	20.3	0.04	0.53	1.41	2.22	1.37		21.8	9.01	1.93	39.7	0	10.9	68.8	11.2
35.6	1.26	7.80	14.12	326	0.34	19.3	0.01	2.15	1.84	2.42	1.62		19.8	8.85	1.37	37.9	0	38.8	73.5	47.5
34.4	1.47‡	7.63	14.18	316	2.61	25.5	0.52	1.11	1.45	2.65	3.74	13.7	21.1	8.50	11.2	35.0	3.80	14.5	203	76.6
34.7	1.47	7.63	14.32	317	2.40	25.4	0.42	0.65	1.44	2.37	4.42	14.3	19.8	8.37	4.0	31.0	1.61	17.8	24.1	183

*O_2 ‡C_4D_6 $^{\phi}$at 135°C

Table A-9-2. Neon Moderated T + Cyclohexene Reaction Data (25°C)

Sample Conditions Pressures, cm Hg		Vol. ml	Yields Relative to Cyclohexene-t as 100																	
											2-butene							"Polymer-t"		
^{3}He	Neon		HT	CH_3T	C=C	C-C					trans/cis		hex-ene		10^3 cts		L	M	H
1.64	16.4	13.84	259	2.74	21.0	1.33	1.46	1.45	2.06	5.48	0.35	0.23	13.0	4.96	45.2	123.	5.65	5.9	8.2	76.7
1.64	16.4	13.62	268	2.81	23.0	1.59	1.10	1.64	2.28	6.41	0.45	0.35	13.0	4.50	47.6	105.	5.50	4.5	8.7	76.8
1.64	32.7	14.05	255	2.69	21.0	1.52	1.21	1.45	2.04	5.85	0.42	0.29	12.8	5.02	58.6	112.	7.70	5.3	10.8	86.4
1.64	32.7	13.96	283	2.95	22.7	1.60	1.52	1.67	2.00	6.64	0.47	0.31	13.4	5.45	62.2	101.	7.13	3.5	9.5	91.3
1.64	48.2	14.62	253	2.60	19.7	1.59	1.30	1.56	2.08	5.73	0.51	0.35	11.6	4.71	71.4	111.	8.53	8.9	12.1	73.1
1.64	48.2	14.79	-	2.41	18.4	1.31	0.88	1.35	1.80	5.39	0.46	0.24	10.2	4.50	67.5	121.	9.29	5.0	9.0	86.2
1.64	65.5	14.34	244	2.49	17.7	1.47	1.58	1.81	2.00	5.27	0.43	0.54	8.75	4.01	79.8	114.	11.4	7.1	13.3	106.
1.64	65.5	13.95	231	2.30	17.2	1.33	0.99	1.38	1.87	4.84	0.38	0.28	8.82	3.41	80.9	106.	10.8	6.3	9.1	99.5

Table A-9-3. T + Cyclohexene Reaction Data (H_2S scavenged, 135°C)

Sample Filling Conditions Pressures, cm Hg‡			Vol.	Yields Relative to Cyclohexene-t as 100													"Polymer-t"		
^3He	H_2S	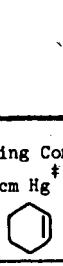	ml	HT	CH_3T	C=C	C-C	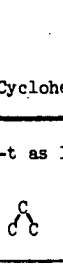	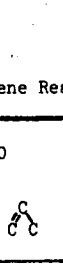	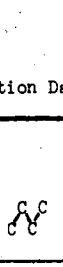	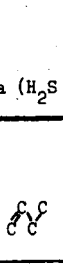		hex-ene	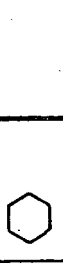	10^3 cts	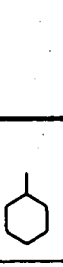	L	M	H
9.82	3.10	30.0	14.27	227	7.32	13.9	2.89	0.95	1.83	2.14	15.2	12.2	13.1	82.5	31.4	0	11.1	31.0	0.9
9.82	3.10	30.0	14.01	236	7.46	14.8	4.01	1.53	2.13	1.48	16.8	13.3	13.2	89.0	29.2	0	16.4	42.4	2.2
9.82	5.45	60.3	14.15	245	7.68	14.3	4.47	1.13	2.73	1.46	16.6	13.1	14.3	98.0	28.0	0	18.2	20.3	2.0
9.82	5.45	60.3	14.22	237	8.03	13.1	4.14	1.43	2.70	2.97	16.5	11.8	14.1	94.2	32.3	0	23.0	24.1	0.5
9.82	7.75	90.5	14.26	253	7.81	12.9	4.28	0.76	2.65	1.86	15.1	10.8	12.7	100.	28.8	0	10.7	25.6	1.1
9.82	7.75	90.5	14.08	254	8.20	12.8	4.43	0.85	2.74	1.65	17.3	11.0	15.1	99.7	30.6	0	12.7	22.3	0.9
9.82	10.2	120.	14.20	261	8.36	13.0	5.02	0.44	3.19	2.60	16.1	10.5	12.2	103.	34.8	0	10.4	23.8	0.4
9.82	10.2	120.	14.59	259	8.28	12.5	4.92	0.43	2.35	1.70	15.6	10.6	14.7	104.	32.2	0	8.4	16.7	0.2
9.82	12.6	152.	13.48	273	8.23	12.6	4.74	1.07	2.68	1.84	15.2	10.1	12.2	111.	35.2	0	15.4	41.8	0.3
9.82	12.6	152.	13.62	244	8.38	10.1	3.95	1.66	2.87	1.73	16.7	8.38	14.4	106.	31.0	0	10.9	15.8	0.2

‡ at 135°C

Table A-9-4. Abstraction/Addition Ratio Data (25°C)

Sample Filling Conditions Pressures, cm Hg			Vol.	Yields Relative to Parent-t as 100								2-butene				"Polymer-t"		
^3He	H_2S	O_2	ml	HT	CH_3T	C=C	C-C					trans/cis				L	M	H
1.64	1.07		14.08	44.8	5.89	24.5	1.11	0.51	0.32	2.76	11.9	1.70	0.90	249.	3.87	47.9	4.7	32.3
1.64	1.07		14.17	44.0	5.82	24.2	1.16	0.39	0.31	2.62	11.6	1.64	0.85	241.	4.50	40.0	5.6	33.0
1.64			14.51	33.6	0.17	21.4	0.04	0.40	0.25	2.50	0.97	0.43	0.46	257.	7.89	48.2	7.0	-
1.64			14.75	33.4	0.17	21.8	0.01	0.26	0.26	2.49	0.91	0.42	0.22	255.	4.15	44.2	5.1	31.8
1.64		1.14	14.36	30.7	0.16	22.2	0.06	0.23	0.27	2.61	0.84	0.16	0.01	230.	4.02	8.2	1.5	32.6
1.64		1.14	13.99	31.2	0.16	22.2	0.09	0.26	0.30	2.59	0.95	0.12	0.01	211.	4.08	6.8	2.0	22.3
All samples - 11.3 cm Hg butadiene																		
1.69	1.07		14.39	198.	29.2	55.6	5.56	0.57	68.6	135.	141.	6.87	2.17	0.28		12.4	2.5	10.5
1.69	1.07		14.58	200.	29.5	54.2	5.57	1.52	69.3	135.	143.	6.76	2.12	0.24		4.0	4.1	10.7
1.69			14.33	144.	7.95	47.4	6.76	2.60	63.0	20.8	151.	32.1	5.93	2.15		-	7.2	15.7
1.69			14.18	148.	8.21	48.9	6.64	2.24	63.2	20.9	162.	31.6	6.49	2.02		34.0	7.3	12.6
1.69		1.15	13.71	157.	6.58	52.1	2.13	2.05	69.9	2.96	128.	5.36	3.72	2.78		28.4	5.3	17.1
1.69		1.15	14.37	156.	6.38	52.9	1.98	1.71	70.6	2.74	131.	5.40	3.67	2.64		15.0	4.7	18.9
All samples - 11.3 cm Hg 1-butene																		
1.69	1.13		14.55	27.4	3.07	221.	44.8	1.03	-	-	-					0.5	0.4	0.8
1.69	1.13		14.46	27.1	3.13	216.	48.1	1.03	0.27	3.88	0.13					0.7	0.4	1.2
1.69			14.20	22.6	0.19	249.	5.02	6.12	0.34	33.8	0.47					1.4	0.9	7.3
1.69			14.13	22.3	0.23	230.	4.43	5.92	0.35	32.9	0.36					0.9	0.7	5.4
1.69		1.09	13.45	21.2	0.14	221.	0.76	0.91	0.19	4.06	0					2.2	0.9	2.1
1.69		1.09	13.90	21.4	0.16	244.	1.41	0.22	0.18	4.07	0					2.4	0.9	1.7
All samples - 11.3 cm Hg ethylene																		

Underlined values are 10^3 cts in parent peak

Table A-9-5. Abstraction/Addition Ratio Data (25°C)

Sample Filling Conditions Pressures, cm Hg			Vol.	Yields Relative to 1-butene-t as 100										
H_2S	O_2	C_4H_6	ml	HT	CH_3T	C=C	C-C					2-butene trans/cis		
4.57		1.07	14.23	156	20.6	43.2	4.35	0.73	46.6	125.	255.	4.60	2.83	4.66
		1.07	14.96	139	7.36	41.5	2.65	1.02	46.4	9.13	281.	-	3.58	4.85
		1.07	14.19	139	7.38	41.0	2.68	1.66	46.0	9.09	298.	-	3.71	4.97
	4.41	1.07	14.43	139	5.84	42.2	2.10	0.48	47.0	2.35	301.	4.51	3.27	6.12
	4.41	1.07	14.50	142	6.04	43.4	2.13	0.27	47.4	2.23	270.	4.45	3.26	6.08
4.57		0.33	14.93	156	20.6	42.3	4.26	1.01	47.4	132.	252.	4.61	3.07	2.08
		0.33	14.22	138	7.92	40.8	3.12	1.08	45.4	15.1	272.	-	4.11	2.63
		0.33	14.03	137	7.89	40.3	3.05	1.31	46.0	15.4	297.	-	4.13	2.61

All samples contained 75.6 cm Hg 1-butene and 1.69 cm Hg ^3He

C_4H_6 = butadiene

Table A-10-1. T + 4-Methylcyclohexene Reaction Data (135°C)

Sample Filling Conditions Pressures, cm Hg			Vol.	Yields Relative to 4-methylcyclohexene as 100															"Polymer-t"		
^{3}He	scavenger		ml	HT	CH_3T	C=C	C-C						pentene						L	M	H
																	10^3 cts				
31.4	3.05$^\phi$	30.	14.32	245	4.26	6.91	0.01	0.69	5.74	1.14	1.29	6.89	0.34	1.10	1.64	1.68	154.	1.94	7.1	49.8	2.0
31.4	3.05	30.	14.41	243	4.17	6.16	0.05	0.61	5.96	1.14	1.30	7.14	0.61	1.04	0.83	2.18	167.	1.31	14.9	24.7	1.8
31.4		30.	14.86	251	10.2	7.67	1.48	1.34	6.87	1.32	8.08	7.04	1.95	1.12	0.91	89.6	375.	4.88	9.2	20.8	2.9
31.4		30.	14.24	249	10.3	7.35	1.43	1.81	7.02	1.31	8.21	7.14	1.64	1.17	1.58	85.7	358.	4.93	8.7	22.1	2.0
31.4		60.	14.00	247	10.1	6.63	1.37	1.10	5.99	1.32	6.86	5.80	1.69	1.04	1.95	83.9	348.	2.64	7.3	20.0	1.6
31.4		60.	14.09	249	10.5	6.55	1.41	1.75	5.83	1.37	7.05	5.80	1.25	0.88	2.13	82.0	405.	1.31	6.7	22.3	1.5
31.4		90.	15.27	229	9.19	5.85	1.30	1.76	4.78	1.28	6.26	5.19	1.88	0.78	2.00	75.4	179.	1.68	8.0	18.9	1.3
31.4		90.	14.52	238	9.65	6.17	1.39	1.48	4.96	1.21	5.16	5.39	2.20	0.83	1.78	76.6	195.	3.64	8.6	22.5	0.4
31.4		120.	14.10	219	5.90	5.49	1.33	1.38	4.48	1.13	5.74	4.50	1.87	0.63	1.97	72.8	397.	-	5.7	29.9	0.6
31.4		120.	14.34	204	8.25	5.06	1.19	1.46	4.31	1.09	5.29	4.13	1.38	0.43	1.72	63.5	451.	-	6.2	21.2	0.4
													C_4D_5T								
33.6		8.9	-	←	316.			→	8.53	1.32	7.16	8.71	0	2.35	1.28	145.	209.	-	14.3	51.0	15.1
33.6		8.9	13.86	294	12.3	9.85	1.76	1.41	8.49	1.73	9.25	7.80	0	1.63	2.11	140.	218.	2.15	-	33.6	6.5
33.6	1.47*	8.9	-	261	7.17	10.6	0.31	0.61	7.92	1.47	4.32	8.34	-	1.77	2.11	20.2	230.	1.79	6.0	113	33.9
33.6	1.47	8.9	14.19	261	7.58	10.8	0.70	1.49	7.71	1.89	4.49	8.39	5.90	1.40	2.30	19.9	56.3	-	5.4	100	49.2

‡at 135°C $^\phi$nitric oxide *butadiene-d_6

Table A-10-2. T + 3-Methylcyclohexene Reaction Data (135°C)

Sample Conditions			Yields Relative to 3-methylcyclohexene-t as 100															"Polymer-t"		
Pressures‡, cm Hg		Vol.																		
NO		ml	HT	CH_3T	C=C	C-C						pen-tene				10^3 cts		L	M	H
3.05	30.	14.45	264	5.21	7.18	0.01	0.90	2.37	1.50	0.75	5.21	0.86	4.96	8.96	4.69	149.	5.36	11.6	59.3	1.8
3.05	30.	14.21	256	5.10	6.77	0.01	0.63	2.56	1.38	0.93	5.16	0.76	4.56	8.52	3.18	150.	4.20	10.7	49.7	3.2
	30.	14.51	268	13.7	8.39	3.27	1.99	3.06	1.62	5.70	5.36	6.22	4.86	9.30	98.5	313.	2.67	8.2	14.1	1.2
	30.	14.25	252	13.2	7.95	3.02	1.29	3.81	1.47	5.32	5.28	4.29	4.73	9.16	104.	333.	3.08	6.1	-	1.5
	60.	15.50	235	11.8	6.51	2.96	0.89	2.22	1.23	4.30	4.36	3.53	3.64	7.08	85.1	364.	2.68	4.5	12.6	0.8
	60.	14.90	240	12.2	6.78	2.97	1.45	2.54	1.33	4.34	4.33	4.58	3.86	7.66	89.7	358.	2.66	3.8	12.2	1.1
	90.	14.47	237	11.2	6.15	2.81	1.24	2.17	1.18	3.97	3.79	3.15	3.08	4.49	93.7	364.	2.18	1.5	18.6	0.3
	90.	14.28	235	11.6	6.36	2.94	0.84	2.14	1.20	4.20	4.05	3.79	3.44	5.21	88.0	373.	3.99	4.6	16.5	0.5
7.75	90.	14.28	259	5.35	6.25	0.23	1.04	2.38	1.39	0.85	4.38	0.68	3.90	6.96	2.79	158.	5.77	9.1	27.2	2.2
7.75	90.	14.26	259	5.35	6.13	0.05	0.73	2.20	1.25	0.80	4.35	0.57	3.41	7.03	2.61	155.	5.21	11.2	35.8	2.1
	120.	14.71	225	11.2	5.81	2.72	1.01	2.15	1.22	3.94	4.07	1.66	2.96	3.58	78.8	458.	2.30	0.7	19.1	0.3
	120.	14.32	219	11.1	5.74	2.66	1.21	2.36	1.16	3.85	3.62	3.76	3.32	1.91	89.1	426.	-	4.8	14.1	0.4

‡at 135°C 31.4 cm Hg ^{3}He in each sample

Table A-10-3. T + 1-Methylcyclohexene Reaction Data (135°C)

Sample Conditions Pressures*, cm Hg NO		Vol. ml	Yields Relative to 1-methylcyclohexene-t as 100 HT	CH_3T	C=C	C-C						pen-tene				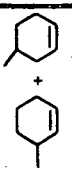	10^3 cts	"Polymer-t" L	M	H
3.05	30.	14.47	257	2.42	5.90	0.03	0.40	1.58	1.02	0.93	1.90	0.21	5.51	5.44	2.37	18.7	165.	11.8	30.4	1.5
3.05	30.	14.81	261	2.52	6.06	0.14	0.49	1.71	1.10	1.07	1.94	0.24	6.01	5.16	9.16	18.2	161.	11.1	30.9	3.8
	30.	14.52	213	6.83	4.78	2.33	0.79	1.92	0.78	1.12	1.52	4.23	3.75	4.50	45.7	8.84	444.	4.5	12.0	0.6
	30.	14.64	220	6.92	5.07	2.44	0.82	2.22	0.99	1.29	1.69	4.68	4.25	5.19	47.9	10.2	429.	4.5	11.6	1.0
	60.	14.55	190	6.90	4.02	2.08	0.73	1.67	0.72	1.10	1.32	3.49	3.34	2.90	32.2	4.82	552.	1.1	-	0.4
	60.	14.12	182	5.65	3.91	2.05	0.52	1.65	0.75	1.03	1.30	3.50	3.04	3.15	34.0	5.40	611.	3.0	7.9	0.2
	90.	15.00	177	5.46	4.27	1.93	0.40	1.44	0.71	0.86	1.22	2.55	3.36	2.56	36.3	-	542.	2.6	9.0	0.2
	90.	14.75	170	5.27	3.57	1.91	0.60	1.43	0.67	0.95	1.21	2.95	3.13	2.45	34.8	-	581.	3.3	11.1	0.2
7.75	90.	13.94	216	1.56	4.30	0.11	0.62	1.33	0.70	0.81	1.38	0.22	4.04	4.47	2.72	12.8	199.	8.6	26.2	1.9
7.75	90.	14.27	215	2.09	4.31	0.05	0.73	1.29	0.58	0.73	1.30	0.20	3.82	4.07	1.61	9.32	201.	8.1	25.0	1.9
	120.	14.29	193	5.81	3.97	2.13	0.51	1.51	1.49	1.20	1.26	2.49	4.40	1.94	32.6	2.90	542.	1.5	-	0.2
	120.	14.34	159	4.86	3.40	1.78	0.20	1.31	0.63	0.83	1.07	2.99	2.67	1.65	31.0	-	691.	1.9	8.2	0.2

*at 135°C each sample contains 31.4 cm Hg ^3He

REFERENCES

1. M. Menzinger and R. Wolfgang, J. Chem. Phys. 50, 2991 (1969).

2. S. Wexler and J. W. Beatty, J. Phys. Chem. 75, 2417 (1971).

3. W. M. Ollison and J. Dubrin, Radiochimica Acta 14, 111 (1970).

4. C. C. Chou and F. S. Rowland, J. Phys. Chem. 75, 1283 (1971).

5. R. G. Gann, W. M. Ollison, and J. Dubrin, J. Chem. Phys. 54, 2304 (1971).

6. R. Wolfgang, Progress in Reaction Kinetics 3, 97 (1965).

7. D. S. Urch, MTP International Review of Science, Inorg. Chem. Ser. 8, 149 (1972).

8. F. S. Rowland, N. Turton, and R. Wolfgang, J. Am. Chem. Soc. 78, 2354 (1956).

9. F. S. Rowland and R. Wolfgang, Nucleonics 14, 58 (1956).

10. The amount of radiation damage may be estimated by approximating one ion pair produced in the hydrocarbon per 30 eV of recoil energy deposited.

11. M. A. El-Sayed, P. Estrup, and R. Wolfgang, J. Phys. Chem. 62, 1356 (1958).

12. D. Seewald and R. Wolfgang, J. Chem. Phys. 52, 1120 (1969).

13. F. S. Rowland, Proc. Int. School of Physics "Enrico Fermi", Academic Press, New York (1970), p. 108.

14. E. W. R. Steacie, Atomic and Free Radical Reactions, 2nd Edition, Rheinhold Publishing Co., New York (1954), p. 508.

15. K. R. Jennings and R. J. Cvetanovic, J. Chem. Phys. 35, 1233 (1961).

16. R. Kushner and F. S. Rowland, J. Phys. Chem. 75, 3771 (1971).

17. K. I. Mahan and J. K. Garland, J. Phys. Chem. 75, 1031 (1971).

18. J. K. Garland, Anal. Lett. 1, 273 (1968).

19. R. Kushner and F. S. Rowland, J. Phys. Chem. 76, 190 (1972).

20. H. A. Kazmi and D. J. LeRoy, Can. J. Chem. 42, 1145 (1964).

21. See the bond dissociation data in the Handbook of Chemistry and Physics, 53rd Edition, Chemical Rubber Co., Cleveland (1972), p. F-189 ff.

22. E. Tachikawa and F. S. Rowland, J. Am. Chem. Soc. 90, 4767 (1968).

23. T. Smail and F. S. Rowland, J. Phys. Chem. 74, 456 (1970).

24. C. Chou and F. S. Rowland, J. Chem. Phys. 50, 2763 (1969).

25. E. K. C. Lee and F. S. Rowland, J. Am. Chem. Soc. 85, 897 (1963).

26. A. Hosaka and F. S. Rowland, J. Phys. Chem. 75, 3781 (1971).

27. C. T. Ting and F. S. Rowland, J. Phys. Chem. 74, 445 (1970).

28. F. S. Rowland and G. F. Palino, J. Phys. Chem. 75, 1299 (1971).

29. D. S. Urch and R. Wolfgang, J. Am. Chem. Soc. 83, 4668 (1961).

30. D. L. Bunker and M. D. Pattengill, J. Chem. Phys. 53, 3041 (1970).

31. K. Morokuma and R. Davis, J. Am. Chem. Soc. 94, 1060 (1972).

32. F. S. Rowland, Y.-N. Tang, E. K. C. Lee, and E. Tachikawa, J. Phys. Chem. 75, 1290 (1971).

33. E. K. C. Lee, Y.-N. Tang, and F. S. Rowland, J. Phys. Chem. 73, 4024 (1969).

34. J. W. Root, J. Phys. Chem. 73, 3174 (1969).

35. T. Smail, B. Arezzo, and F. S. Rowland, J. Phys. Chem. 76, 187 (1972).

36. R. M. White and F. S. Rowland, J. Am. Chem. Soc. 82, 4713 (1960).

37. P. J. Estrup and R. Wolfgang, J. Am. Chem. Soc. 82, 2665 (1960).

38. R. Wolfgang, J. Chem. Phys. 39, 2983 (1963).

39. A. H. Rosenberg and R. Wolfgang, J. Chem. Phys. 41, 2159 (1964).

40. D. S. Urch, Radiochimica Acta 14, 10 (1970).

41. M. Baer, Chem. Phys. Letters 11, 229 (1971).

42. D. J. Malcolme-Lawes, J. Chem. Phys. 56, 3442 (1972).

43. N. E. Holden and F. W. Walker, Chart of the Nuclides, General Electric Co., New York (1968).

44. J. W. Root and F. S. Rowland, Radiochimica Acta 10, 104 (1968).

45. P. J. Robinson and K. A. Holbrook, Unimolecular Reactions, Wiley-Interscience, New York (1972).

46. L. D. Spicer and B. S. Rabinovitch, Ann. Rev. Phys. Chem. 21, 349 (1970).

47. D. L. Bunker, Theory of Elementary Gas Reactions, Chap. 3, Pergamon Press, New York (1966).

48. F. A. Lindemann, Trans. Faraday Soc. 17, 598 (1922).

49. C. N. Hinshelwood, Proc. Roy. Soc. (A) 113, 230 (1927).

50. Reference 45, p. 164.

51. O. K. Rice and H. C. Ramsperger, J. Am. Chem. Soc. 49, 1617 (1927).

52. O. K. Rice and H. C. Ramsperger, J. Am. Chem. Soc. 50, 617 (1928).

53. L. S. Kassel, J. Phys. Chem. 32, 225 (1928).

54. L. S. Kassel, J. Phys. Chem. 32, 1065 (1928).

55. H. S. Johnston, Gas Phase Reaction Rate Theory, Ronald Press Co., New York (1966), p. 32.

56. G. Emanuel, Int. J. Chem. Kinetics 4, 591 (1972).

57. R. A. Marcus and O. K. Rice, J. Phys. and Colloid. Chem. 55, 894 (1951).

58. R. A. Marcus, J. Chem. Phys. 20, 359 (1952).

59. N. B. Slater, Proc. Camb. Phil. Soc. 35, 56 (1939).

60. N. B. Slater, Theory of Unimolecular Reactions, Metheun Press, London (1959).

61. T. S. Chambers and G. B. Kistiakowsky, J. Am. Chem. Soc. 56, 399 (1934).

62. H. O. Prichard, R. G. Snowden, and A. F. Trotman-Dichenson, Proc. Roy. Soc. (A) 217, 563 (1953).

63. N. B. Slater, Proc. Roy. Soc. (A) 218, 224 (1953).

64. G. M. Wieder and R. A. Marcus, J. Chem. Phys. 37, 1835 (1962).

65. E. W. Schlag and B. S. Rabinovitch, J. Am. Chem. Soc. 82, 5996 (1960).

66. Reference 45, p. 59.

67. J. N. Butler and G. B. Kistiakowsky, J. Am. Chem. Soc. 82, 759 (1960).

68. J. D. Rynbrandt and B. S. Rabinovitch, J. Chem. Phys. 75, 2164 (1971).

69. R. E. Harrington, B. S. Rabinovitch, and H. M. Frey, J. Chem. Phys. 33, 1271 (1960).

70. Reference 45, p. 103.

71. S. C. Chan, B. S. Rabinovitch, J. T. Bryant, L. D. Spicer, T. Fujimoto, Y. N. Lin, and S. P. Pavlou, J. Phys. Chem. 74, 3160 (1970).

72. D. C. Tardy and B. S. Rabinovitch, J. Chem. Phys. 45, 3720 (1966).

73. H. Budzikiewicz, J. I. Brauman, and C. Djerassi, Tetrahedron 21, 1855 (1965).

74. R. F. Nystrom, S. S. Rajan, N. H. Nam, and D. Gurne, Proc. Int. Conf. Method Prep. Storage Labeled Compds. 2, 407 (1966).

75. H. Beiler, F. Battig, and P. Jordan, Zeitschrift fur Physikalishe Chemie Neue Folge 72, 1 (1970).

76. N. D. Zelinskii, B. M. Mikhailov, and Y. A. Arbuzov, J. Gen. Chem. (USSR) 4, 856 (1934).

77. L. Kuchler, Trans. Faraday Soc. 35, 874 (1939).

78. S. R. Smith and A. S. Gordon, J. Phys. Chem. 65, 1124 (1961).

79. M. Uchiyama, T. Tomioka, and A. Amano, J. Phys. Chem. 68, 1178 (1964).

80. T. Sakai, T. Nakatani, T. Takahashi, and T. Kungi, Ind. Eng. Chem. Fundam. 11, 529 (1972).

81. W. Tsang, J. Chem. Phys. 42, 1805 (1965).

82. W. Tsang, Int. J. Chem. Kinetics 2, 311 (1970).

83. W. Tsang, J. Phys. Chem. 76, 143 (1972).

84. R. D. Doepker and P. Ausloos, J. Chem. Phys. 42, 3746 (1965).

85. R. Lesclaux, S. Searles, L. W. Sieck, and P. Ausloos, J. Chem. Phys. 53, 336 (1970).

86. G. R. DeMare, O. P. Strausz, and H. E. Gunning, Can. J. Chem. 43, 1329 (1965).

87. F. O. Rice and M. T. Murphy, J. Am. Chem. Soc. 66, 765 (1944).

88. M. Kraus and V. Bazant, Collection Czech. Chem. Comm. 25, 2695 (1960).

89. G. R. DeMare, Bull. Soc. Chim. Belges 81, 459 (1972).

90. M. Amagasa, Y. Saito, and Y. Kasuga, Japanese Patent #72-13,252 April 1972. Chem. Abstracts 77: 49788s.

91. J. A. Takacs and G. R. Freeman, Nature 208, 996 (1965).

92. R. E. Winters and J. H. Collins, Org. Mass. Spec. 2, 299 (1969).

93. E. P. Smith and E. R. Thornton, J. Am. Chem. Soc. 89, 5079 (1967).

94. T. H. Kinstle and R. E. Stark, J. Org. Chem. 32, 1318 (1967).

95. E. F. H. Brittain, C. H. J. Wells, and H. M. Paisley, J. Chem. Soc. (B) 304 (1968).

96. E. F. H. Brittain, C. H. J. Wells, and H. M. Paisley, J. Chem. Soc. (B) 503 (1969).

97. M. Uchiyama and A. Amano, Kogyo Kagaku Zasshi 69, 71 (1966). Chem. Abstracts 65: 3723d.

98. J. K. Garland and J. W. Schroeder, J. Phys. Chem. 72, 2277 (1969).

99. Reference 21, p. C-259 ff.

100. G. R. Freeman, Radiation Research Reviews 1, 1 (1968).

101. D. Brune, Anal. Chim. Acta 44, 15 (1969).

102. G. Glanz, N. Dutescu, and A. Georgescu, Rev. Romaine. Phys. 9, 137 (1964).

103. A. C. Klank, T. H. Blewitt, J. J. Minarik, and T. L. Scott, Bull. Inst. Int. Froid. Annexe 5, 373 (1966).

104. W. Decker, J. Diehl, K. Hain, H. Katheder, and C. Leitz, Kerntechnik 8, 257 (1966).

105. N. Berglund, D. Brune, and B. Schuberg, Nucl. Instr. Methods 75, 103 (1969).

106. J. Ahlf and G. A. Melkonian, Atomkernenergie 10, 459 (1965).

107. J. H. O'Donnell, Chem. Ind. 15, 481 (1968).

108. J. Ahlf, D. Anders, and R. Benefeld, Kerntechnik 8, 173 (1966).

109. T. Hayashi and M. Kudoh, J. Nucl. Sci. Technol. 6, 390 (1969).

110. R. Wolfgang and F. S. Rowland, Anal. Chem. 30, 903 (1958).

111. E. Gil-Av, J. Herling, and J. Shabtai, J. Chromatography 1, 508 (1958).

112. M. E. Bednas and D. S. Russell, Can. J. Chem. 36, 1272 (1958).

113. J. K. Lee, E. K. C. Lee, B. Musgrave, Y.-N. Tang, J. W. Root, and F. S. Rowland, Anal. Chem. 34, 741 (1962).

114. L. Mikkelsen, Adv. in Chromatography 2, 337 (1966).

115. L. S. Ettre, L. Mazor, and J. Takacs, Adv. in Chromatography 8, 271 (1969).

116. J. Takacs and L. Mazor, J. Chromatography 38, 317 (1968).

117. B. M. Mitzner and W. V. Jones, Anal. Chem. 37, 447 (1965).

118. J. H. Purnell, Ann. Rev. Phys. Chem. 18, 81 (1967).

119. G. Eppert, J. Gas Chromatography 6, 361 (1968).

120. J. Kwok, L. R. Snyder, and J. C. Sternberg, Anal. Chem. 40, 118 (1968).

121. F. Willeboordse, Q. Quick, and E. T. Bishop, Anal. Chem. 40, 1455 (1968).

122. J. D. Rynbrandt, D. F. Ring, and B. S. Rabinovitch, J. Gas Chromatography 6, 531 (1968).

123. J. W. Root, W. Breckenridge, and F. S. Rowland, J. Chem. Phys. 43, 3694 (1965).

124. J. W. Root, E. K. C. Lee, and F. S. Rowland, Science 143, 676 (1964).

125. H. Borfitz, Anal. Chem. 33, 1632 (1961).

126. K. J. Bombaugh, B. J. Hayes, and W. R. Shaw, J. Gas Chromatography 3, 373 (1965).

127. V. J. Dardin, J. Gas Chromatography 5, 556 (1967).

128. R. L. Burnett, Anal. Chem. 41, 606 (1969).

129. E. K. C. Lee and F. S. Rowland, Anal. Chem. 36, 2181 (1964).

130. T. A. McKenna and J. A. Idleman, Anal. Chem. 32, 1299 (1960).

131. R. Feinland, A. J. Andreatch, and D. P. Cotrupe, Anal. Chem. 33, 991 (1961).

132. D. E. Matire and L. Z. Pollara, J. Chem. Eng. Data 10, 40 (1965).

133. D. S. Glass, Int. J. Appl. Radiation and Isotopes 21, 531 (1970).

134. D. S. Urch and M. J. Welch, Trans. Faraday Soc. 62, 388 (1966).

135. R. T. K. Baker and R. L. Wolfgang, Trans. Faraday Soc. 65, 1842 (1969).

136. J. K. Lee, B. Musgrave, and F. S. Rowland, Can. J. Chem. 38, 1756 (1960).

137. J. Hawke and R. Wolfgang, Radiochimica Acta 14, 116 (1970).

138. F. S. Rowland, J. K. Lee, B. Musgrave, and R. M. White, Chemical Effects of Nuclear Transformations, IAEA, Vienna, Vol. 1 (1960), p. 67.

139. A. Henglein, H. Url, and W. Hoffmeister, Z. Physik. Chem. 18, 26 (1958).

140. D. S. Urch and M. J. Welch, Chem. Comm. 1, 129 (1965).

141. D. J. Malcolme-Lawes, S. S. Urch, and M. J. Welch, Radiochimica Acta 6, 184 (1966).

142. R. W. Weeks and J. K. Garland, J. Phys. Chem. 73, 2508 (1969).

143. R. W. Weeks and J. K. Garland, J. Am. Chem. Soc. 93, 2380 (1971).

144. D. C. Fee and J. K. Garland, Trans. Mo. Acad. Sci. 3, 46 (1969).

145. In the absence of good kinetic data for the addition of a hydrogen atom to cyclohexene, assume a maximum 10^2 to 1 ratio of rate constants for addition to butadiene versus cyclohexene, respectively. The concentration effects alone favor addition to cyclohexene 10^7 (to 10^8) to 1 over butadiene. This should result in a large preference for addition to cyclohexene.

146. A. T. Touma and F. H. Verhoek, Fifth Symposium on Combustion, Pittsburgh (1954), p. 741.

147. Reference 21, p. D-171.

148. R. W. Getzinger and G. L. Schott, J. Chem. Phys. 43, 3237 (1965).

149. P. Riesz and E. J. Hart, J. Phys. Chem. 63, 858 (1959).

150. R. W. Fair and B. A. Thrush, Trans. Faraday Soc. 65, 1550 (1969).

151. G. R. Wolley and R. J. Cvetanovic, J. Chem. Phys. 50, 4697 (1969).

152. R. J. Cvetanovic and L. C. Doyle, J. Chem. Phys. 50, 4705 (1969).

153. Less than 3% of the gamma radiolysis products of cyclohexene result from ring fission. See G. R. Freeman, Can. J. Chem. 38, 1043 (1960).

154. H. W. Melville and J. C. Robb, Proc. Roy. Soc. (A) 202, 181 (1950).

155. Z. B. Alfassi and S. Amiel, Radiochimica Acta 15, 201 (1971).

156. C. M. Wai and F. S. Rowland, J. Phys. Chem. 74, 434 (1970).

157. W. A. Pryor and U. Tonellato, J. Phys. Chem. 73, 850 (1969).

158. N. Basco, D. G. L. James, and F. C. James, Int. J. Chem. Kinetics 4, 129 (1972).

159. A. Good and J. C. J. Thynne, Trans. Faraday Soc. 63, 2708 (1967).

160. N. Imai and O. Toyama, Bull. Chem. Soc. Japan 33, 652 (1960).

161. R. J. Cvetanovic and R. S. Irwin, J. Chem. Phys. 46, 1694 (1967).

162. W. M. Jackson, J. R. McNesby, and B. de B. Darwent, J. Chem. Phys. 37, 1610 (1962).

163. N. Imai and O. Toyama, Bull. Chem. Soc. Japan 38, 224 (1965).

164. W. Ando, K. Sugimoto, and S. Oae, Bull. Chem. Soc. Japan 38, 226 (1965).

165. K. Sugimoto, W. Ando, and S. Oae, Bull. Chem. Soc. Japan 38, 221 (1965).

166. K. Sugimoto, W. Ando, and S. Oae, Bull. Chem. Soc. Japan 37, 365 (1964).

167. Reference 21, p. D-171, D-154 ff.

168. G. Meissner and A. Henglein, Z. Naturforschung 20b, 1005 (1965).

169. D. B. Hartly and B. A. Thrush, Proc. Roy. Soc. (A) 297, 520 (1967).

170. N. Basco, D. G. L. James, and R. D. Stuart, Int. J. Chem. Kinetics 2, 215 (1970).

171. M. Cher, C. S. Hollingsworth, and B. Browning, J. Chem. Phys. 41, 2270 (1964).

172. S. K. Ho and G. R. Freeman, J. Phys. Chem. 68, 2189 (1964).

173. W. A. Cramer, J. Phys. Chem. 71, 1112 (1967).

174. S. Aria, S. Sato, and S. Shida, J. Chem. Phys. 33, 1277 (1960).

175. A. S. Gordon and S. R. Smith, J. Phys. Chem. 66, 521 (1962).

176. A. S. Gordon, Pure and Applied Chem. 5, 441 (1962).

177. R. A. Sheldon and J. K. Kochi, J. Am. Chem. Soc. 92, 4395 (1970).

178. H. M. Frey and R. Walsh, Chem. Rev. 69, 103 (1969).

179. E. K. C. Lee and F. S. Rowland, J. Phys. Chem. 74, 439 (1970).

180. K. I. Mahan and J. K. Garland, J. Phys. Chem. 73, 1247 (1969).

181. Y. Tabata, R. Shimazawa, and H. Sobue, J. Polymer Sci. 54, 201 (1961).

LEGAL NOTICE

This report was prepared as an account of work sponsored by the United States Government. Neither the United States nor the United States Atomic Energy Commission, nor any of their employees, nor any of their contractors, subcontractors, or their employees, makes any warranty, express or implied, or assumes any legal liability or responsibility for the accuracy, completeness or usefulness of any information, apparatus, product or process disclosed, or represents that its use would not infringe privately owned rights.

TECHNICAL INFORMATION DIVISION
LAWRENCE BERKELEY LABORATORY
UNIVERSITY OF CALIFORNIA
BERKELEY, CALIFORNIA 94720